(2)

CHEMICAL
RESEARCH,
DEVELOPMENT &
ENGINEERING
CENTER

CRDEC-SP-046

SPECIALTY SYMPOSIUM - PARTICLE PRODUCTION, CHARACTERIZATION, AND APPLICATIONS

Madhav B. Ranade

PARTICLE TECHNOLOGY, INC.
College Park, MD 20742

Erica R. Petersen

RESEARCH DIRECTORATE

March 1992

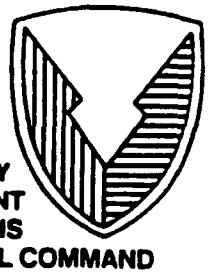

U.S. ARMY
ARMAMENT
MUNITIONS
CHEMICAL COMMAND

Aberdeen Proving Ground, Maryland 21010-5423

Disclaimer

The findings in this report are not to be construed as an official Department of the Army position unless so designated by other authorizing documents.

REPORT DOCUMENTATION PAGE

Form Approved
OMB No 0704-0188

1. AGENCY USE ONLY (Leave blank)	2. REPORT DATE	3. REPORT TYPE AND DATES COVERED
	1992 March	Final, 88 Apr - 88 Oct

4. TITLE AND SUBTITLE
Specialty Symposium - Particle Production, Characterization, and Applications

5. FUNDING NUMBERS
PR-88266
(Delivery
Order No. 0977)

6. AUTHOR(S)
Ranade, Madhav B. (Particle Technology, Inc.), and Petersen, Erica R. (CRDEC)

7. PERFORMING ORGANIZATION NAME(S) AND ADDRESS(ES)
Particle Technology, Inc.
Building 335
Technology Advancement Program
College Park, MD 20742

8. PERFORMING ORGANIZATION REPORT NUMBER
CRDEC-SP-046

9. SPONSORING/MONITORING AGENCY NAME(S) AND ADDRESS(ES)
CDR, CRDEC, ATTN: SMCCR-RSP-B,
APG, MD 21010-5423

10. SPONSORING/MONITORING AGENCY REPORT NUMBER

11. SUPPLEMENTARY NOTES
Task was performed under a Scientific Services Agreement issued by Battelle, Research Triangle Park Office, 200 Park Drive, P.O. Box 12297, Research Triangle Park, NC 27709.

12a. DISTRIBUTION/AVAILABILITY STATEMENT
Approved for public release; distribution is unlimited.

12b. DISTRIBUTION CODE

13. ABSTRACT (Maximum 200 words)

A Specialty Symposium was held at Hunt Valley Marriott near Baltimore, MD on May 16-18, 1988. Participants were invited from industry, academic institutions, and government agencies engaged in particle technology-related work. A total of 20 presentations were made on several topics which included particle production, aerosol characterization, and applications. The final report contains summaries of the presentations and discussions. Recommendations for future conferences with joint participation by industry and government are made to facilitate technology transfer from various disciplines.

14. SUBJECT TERMS
Fine particles
Particle technology
Powders
Aerosols
Size measurement

15. NUMBER OF PAGES
133

16. PRICE CODE

17. SECURITY CLASSIFICATION OF REPORT	18. SECURITY CLASSIFICATION OF THIS PAGE	19. SECURITY CLASSIFICATION OF ABSTRACT	20. LIMITATION OF ABSTRACT
UNCLASSIFIED	UNCLASSIFIED	UNCLASSIFIED	UL

Blank

PREFACE

The work described in this report was authorized under Project No. 88266 (Delivery Order No. 0977). This work was started in April 1988 and completed in October 1988.

The use of trade names or manufacturers' names in this report does not constitute an official endorsement of any commercial products. This report may not be cited for purposes of advertisement.

This report has been approved for release to the public.

Acknowledgments

Valeric Ford (Particle Technology, Inc.) provided secretarial support and was responsible for a smooth running Symposium Program.

Blank

CONTENTS

SPECIALTY SYMPOSIUM - PARTICLE PRODUCTION, CHARACTERIZATION, AND APPLICATIONS

INTRODUCTION

In recent years, the science and technology of fine particles has become a crucial factor in many fields, both in government and in industry. Fine particles differ from bulk materials, exhibiting properties that make them critical components in many products and processes. These differences necessitate specialized approaches to research and development efforts associated with fine particles.

Applications of fine particles span a range covering ceramics and composites processing, pigment and pharmaceutical components, military smokes and obscurants, military protection systems, and powder metallurgy. Subjects of concern to these fields include particle generation, control of morphology and homogeneity, filtering, measurement and characterization, particle capture, handling and contamination control.

Because of the breadth of concerns about fine particles the information available on the subject is scattered throughout the literature of numerous fields. Treatment of particle technology as a significant discipline independent of application is a relatively new effort, requiring expertise in numerous fields of applications as well as in the particle-specific technologies. In many instances the concerns of Department of Defense scientists and contractors are unique and are not well addressed by the general scientific community. This fact led us to the organization of a meeting of particle specialists from a broad spectrum of applications specifically suited to addressing some of the current military concerns.

A major goal of the Symposium was to identify overlap of technical issues in defense and other communities. For example particle removal from air or gases is of importance for chemical defense, microcontamination control, and air pollution control and the basic mechanisms of filtration are common to all. Other examples include powder flow and dispersion problems in industry as well as in developing smoke munitions.

The technical areas we were able to cover in the rather short time for preparation of the Program and for the Symposium were of areas of direct interest to the Army. The Sections were arranged to permit natural flow of topics from particle production, their characterization, and uses and applications in other technological areas.

In the next Section the papers are arranged according to the major topical areas and not necessarily in the order of their presentation. The Symposium Program is included in the Appendix. The details and the length of the written papers were not uniformly specified to facilitate publication in a timely manner without causing a burden to the participants.

Blank

SECTION I: SPECIAL TOPIC - PLENARY LECTURE

Blank

ADVANCES IN AEROSOL FILTRATION

Benjamin Y.H. Liu
Professor and Director, Particle Technology Laboratory,
Mechanical Engineering Department, University of Minnesota
Minneapolis, MN 55455

Introduction

Fibrous and membrane filters are widely used for the removal of particulate contaminants from air or gas streams. As such, they are important in various applicationa requiring purfied streams for health or equipment protection or for manufacturing processes.

Advances in filtration technology in recent years have proceeded along two fronts. On the one hand, there are significant advances in the theory of air and gas filtration. The theoretical understanding of filtration mechanisms and the theory of fibrous and membrane filters have progressed to the point where many filters can now be designed theoretically. Further, there is a concomitant advance in manufacturing technology. Filter media and filtration devices with varying characteristics can now be manufactured, often with high and consistent quality. As a result, numerous filtration products are available commercially and they can be used to meet the diverse filtration needs of industry.

The purpose of this paper is to provide an overview of air and gas filtration with the major emphasis on the mechanism and the theory of filtration. The influence of filter fiber or pore size, filter structure and other important filtration parameters on filter performance will be discussed. The method of tests of air and gas filters will then be described along with the performance characteristics of some commercially available filters.

Types of Filters and Their Physical Characteristics

Fibrous and membrane filters are both used for high purity air or gas filtration. Fibrous filters are more commonly used where a large volume of air or gas must be processed. Membrane filters, on the other hand, because of their higher cost and absolute particle retention characteristics, are more often used where the purity requirement is high and the volume of gas to be processed is comparatively small. Major application of fibrous filters include ventilation and clean room air filtration and industrial air or gas cleaning for pollution and contamination control and product recovery. Major applications of membrane filters include process gas and liquid filtration in the pharmaceutical, semiconductor and biomedical industries and their applications as sampling filter media for analytical purposes.

Fibrous filters are made of glass or polymer fibers. The fiber diameter may range from as small as 0.1 to tens of micrometers. They are usually made through a wet, paper making process in which the fibers are first made into a wet slurry and formed into mats which are subsequently dewatered and pressed. In the case of fibrous filters made of polymeric fibers, the fibers may be spun and formed into the final filter sheet directly.

In the case of the membrane filter, the desired membrane material is usually first dissolved in a suitable solvent and cast into a thin film from

which the solvent is removed, usually by evaporation, forming a porous structure. Membrane materials may include cellulose ester, polyvinyl chloride, nylon, polypropylene, polyvinylidene fluoride (PVDF), polytetrafluorethylene, polycarbonate, among others. Membrane filters made by this process usually have uniform pore like structures and are usually rated by the size of the filter pores. Other membrane manufacturing technique includes sintering--for making metal membranes--and track-etching, in which the polymer film is exposed to nuclear radiation and subsequently etched to form uniform sized holes. Another membrane filter manufactured technique suitable for making PVDF membranes is the stretching technique in which the PVDF membrane is stretched to form fiber like structures.

Filter Pressure Drop

Filter pressure drop is an important parameter that must be controlled in the design of filters. The pressure drop at a given flow rate determines the resistance of the filter to the fluid flow. As such, it is important in determining the fluid pumping power required, or the amount of fluid that can be processed at a specific pressure drop.

The pressure drop of a filter is usually proportional to the surperficial face velocity of the fluid passing through the filter. At high filtration velocities, the pressure drop may increase more rapidly with increasing flow rate due to fluid inertial and turbulent effects. This is illustrated in Figure 1. However, most filters do operate in the linear pressure drop regime, which is also referred to as the Darcy law regime.

Theory of pressure drop for fibrous filters usually begins by considering the drag force exerted by the flowing fluid on the individual fibers in the filter. The specific fiber drag, F_d, i.e. the drag force per unit fiber length, can then be related to the total pressure drop of the fluid through the filter,

$$\Delta P = l_f F_d \qquad (1)$$

where l_f is the total length of fibers in a unit filter area. In the Darcy law regime, ΔP is proportional to the fluid velocity, u, and viscosity, m. Consequently, F_d is also proportional to these quantities,

$$F_d = F^* \mu u \qquad (2)$$

where F^* is a dimensionless constant of proportionality known as the dimensionless fiber drag parameter.

The mathematical theory of fibrous filtration shows that the dimensionless fiber drag parameter, F^*, is a function of the packing density, α, of the fibers in the filter. The widely used Kuwabara theory of filter pressure drop predicts the following functional dependence of F^* on α,

$$F^* = \frac{4\pi}{K} \tag{3}$$

where K is the hydrodynamic factor

$$K = \frac{1}{2}\ln\alpha + \alpha - \frac{1}{4}\alpha^2 - \frac{3}{4} \tag{4}$$

The actual pressure drop through a filter is usually smaller than that predicted by theory due to the fact that some part of the fiber in a filter is located in the wake region of another fiber and these fibers do not experience the full hydrodynamic drag. The ratio of the theoretical to actual filter pressure drop is usually in the vicinity of 1.6 according to the measurement of Yeh and Liu [1] and Lee and Liu [2,3] among others. A comprehensive measurement of the relationship between F^* and α has been made by Shaefer and Liu [4] and by Monson [5] over a wide range of values of α . The results are shown in Figure 2.

Filter Efficiency

For air or gas filtration, the efficiency of the filter for particle capture is due to the mechanisms of diffusion, interception and inertial impaction. Diffusion refers to the random Brownian motion of the particles resulting from molecular impact by the surrounding gas molecules. Interception refers to the capture of a particle as a result of the finite size of the particle when it is brought to the vicinity of the fiber by the flowing gas stream. Capture by inertial impaction is a consequence of the finite mass and momentum of the particle causing the particle to deviate from the streamline and impact on the collecting fiber. These mechanisms are illustrated in Figure 3. For high efficiency filters, diffusion is usually dominant for small particles below 0.1 μm and interception, for particles larger than 1 μm. In the size range between 0.1 and 1.0 μm, both diffusion and interception are important and must be considered. Inertial impaction may become important for large particles or when the filtration velocity is high.

The operation of the diffusion, interception and inertial mechanisms of filtration generally leads to a filter efficiency characteristics as shown in Figure 4. In the small particle size range where diffusion dominants, the filter efficiency would decrease with increasing particle size, because the particle diffusion coefficient generally decreases with increasing particle size. On the other hand, in the large particle size range where interception and inertial impaction dominate, increasing particle size generally leads to an increase in filter efficiency. The combination of these mechanisms would lead to the existence of a minimum in the filter efficiency in some intermediate particle size range as shown in Figure 4. The existence of a minimum in the filter efficiency versus particle size curve in air and gas filtration is well documented both theoretically and experimentally.

In contrast to gas filtration, liquid filtration by fibrous or membrane media generally does not involve capture by diffusion or inertial impaction as these effects are usually negligible in liquids. Consequently, filtration of particles by liquids often involves pure interception only, and particle capture is reduced to a screening effect. Particles smaller than the pore openings in the filter usually will pass through the filter while those larger than the pore opening will be retained.

The mathematical theory of gas filtration by fibrous filters usually begins by defining a single fiber efficiency, η_s, the fraction of particles collected by a fiber from a volume of air geometrically swept out by the fiber. The single fiber efficiency is related to the overall efficiency of the filter, η, by the simple exponential relationship,

$$\eta = 1 - e^{-\eta_s l_f D_f} \qquad (5)$$

An extensive series of measurements on single fiber efficiencies has been reported by Lee and Liu [2,3] who varied the filter packing density, filtration velocity and particle size over a wide range of values. Their results can be correlated by a dimensionless plot involving the Peclet number,

$$Pe = \frac{U D_f}{D} \qquad (6)$$

and the interception parameter

$$R = \frac{D_p}{D_f} \qquad (7)$$

where D is the particle diffusion coefficient and D_p and D_f are respectively the particle and fiber diameters. Their results are shown in Figure 5.

The theoretical dependence of the single fiber efficiency on fiber and particle size is shown in Figure 6. It is interesting to note the existence of the minimum in filter efficiency and that the single fiber efficiency generally increases with decreasing fiber size. This underscores the advantage of using small fibers in making filters.

Performance of Filters and Filter Testing

The performance of an actual filter usually must be determined by testing. To measure the efficiency of a filter as a function of particle size, it is usually necessary to generate a monodisperse test aerosol and measuring the concentration of the aerosol upstream and downstream of the filter to determine the aerosol penetration, P, through the filter. The collection efficiency is then equal to 1 - P.

Figure 7 shows a system developed at the University of Minnesota for measuring filter efficiency by means of monodisperse test aerosols. The aerosol is usually generated by an electrostatic classification method and the particle size can be varied systematically over a range of particle sizes, usually between 0.03 and 1.3 μm. The concentration of the aerosol upstream and downstream of the filter is usually measured with a condensation nucleus counter.

Figure 8 shows the measured penetration through a commercially available high-efficiency particulate air (HEPA) filter. It is interesting to note that the filter penetration first increases with increasing particle size, reaching a peak at a particle size of approximately 0.1 to 0.2 μm, after which the penetration decreases with further increase in particle size. This is completely in accord with the theoretical predictions as discussed above.

Measurement of the efficiency of membrane filters shows that the performance of the membrane filter is quite analogous to that of fibrous filters. Indeed the study of membrane filter by Rubow [6] shows that the performance of the membrane filter can best be correlated with the fibrous filtration theory and that the equivalent fiber size for a membrane filter is quite close to the size of the structural elements in the membrane media. Figure 9 shows a comparison of the theoretically calculated filter penetration with the measured value for a Millipore SC membrane filter with a nominal pore size of 8.0 μm. The equivalent "fiber size" used in the

calculation is 0.87 μm which is close to the size of the structural element in this particular membrane.

For the filtration of high purity gases used in semiconductor manufacturing, it is necessary to provide a high degree of filtration and to make use of a filter media that is non-shedding. For this purpose membrane filters are commonly used. One widely used filter is the Millipore 0.2 μm PVDF Durapore filter. Testing of this filter by Rubow and Liu [7] and Accomazzo et al [8] show a filter penetration of less than 1×10^{-9}, which is limited by the sensitivity of the test method used.

Summary

This paper has provided a summary of the mechanisms and theory of filtration as they relate to high purity air or gas filtration. The major capture mechanisms for particles in a filter are diffusion, interception and inertial impaction. These mechanisms have led to the existence of a most penetrating particle size for filters, which for fibrous media is usually in the vicinity of 0.1 to 0.2 μm. The use of monodisperse aerosols for filter testing is then discussed and the performance characteristics of some commercially available filter is then described.

References

1. Yeh, H. C. and Liu, B. Y. H., "Aerosol Filtration by Fibrous Filters--Part II. Experimental," J. Aerosol Sci.5:205-217, 1973.

2. Lee, K.W. and Liu, B. Y. H., "Experimental Study of Aerosol Filtration by Fibrous Filters," Aerosol Sci. Technol. 1:35-46, 1982.

3. Lee, K. W. and Liu, B. Y. H., "Theoretical Study of Aerosol Filtration by Fibrous Filters," Aerosol Sci. Technol. 1:147-162, 1982.

4. Schaefer, J. W. and Liu, B. Y. H. , "An Investigation of Pressure Loss Across Fibrous Filter Media," Aerosols: Science, Technology and Industrial Applications (B. Y. H. Liu, D. Y. H. Pui and H. Fissan, Editors), pp. 555-558, Elsevior Science Publishing Co., New York, 1984.

5. Monson, D. R., "A Filter Pressure Loss Model for Uniform Fibers," Aerosols: Science, Technology and Industrial Applications (B. Y. H. Liu, D. Y. H. Pui and H. Fissan, Editors), pp. 551-554, Elsevior Science Publishing Co., New York, 1984.

6. Rubow, K. L., "Submicron Aerosol Filtration Characteristics of Membrane Filters," Ph.D. Thesis, Mechanical Engineering Department, University of Minnesota, Minneapolis, Minnesota, 1981.

7. Rubow, K. L. and Liu, B. Y. H., "Evaluation of Ultra-high Efficiency Membrane Filters," Proceedings of the 30th Annual Technical Meeting of the Institute of Environmental Sciences, pp. 64-68, 1984.

8. Accomazzo, M. A., Rubow, K. L. and Liu, B. Y. H., "Ultrahigh Efficiency Membrane Filters for Semiconductor Process Gases," Solid State Technology, pp. 141-146, March, 1984.

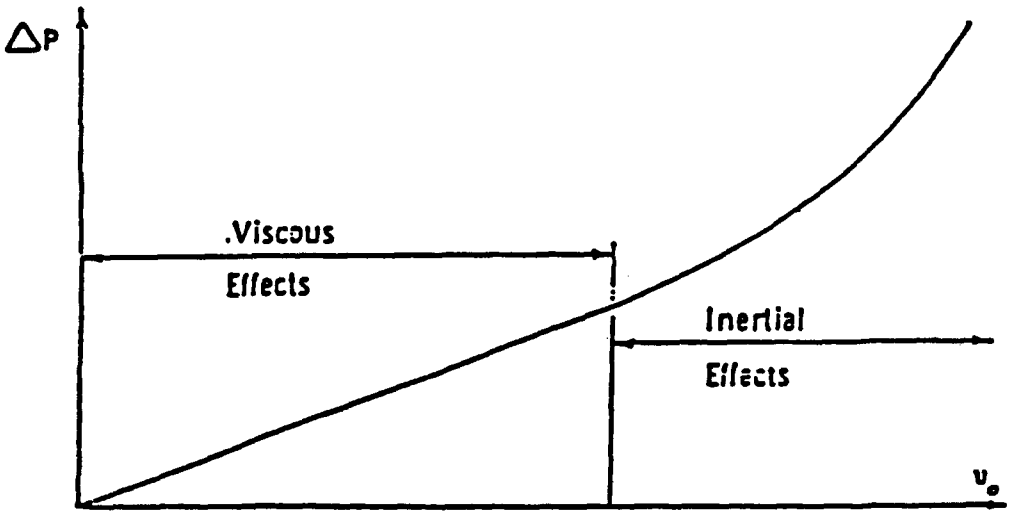

Figure 1. Schematic diagram showing pressure drop of a filter as a function of filtration velocity

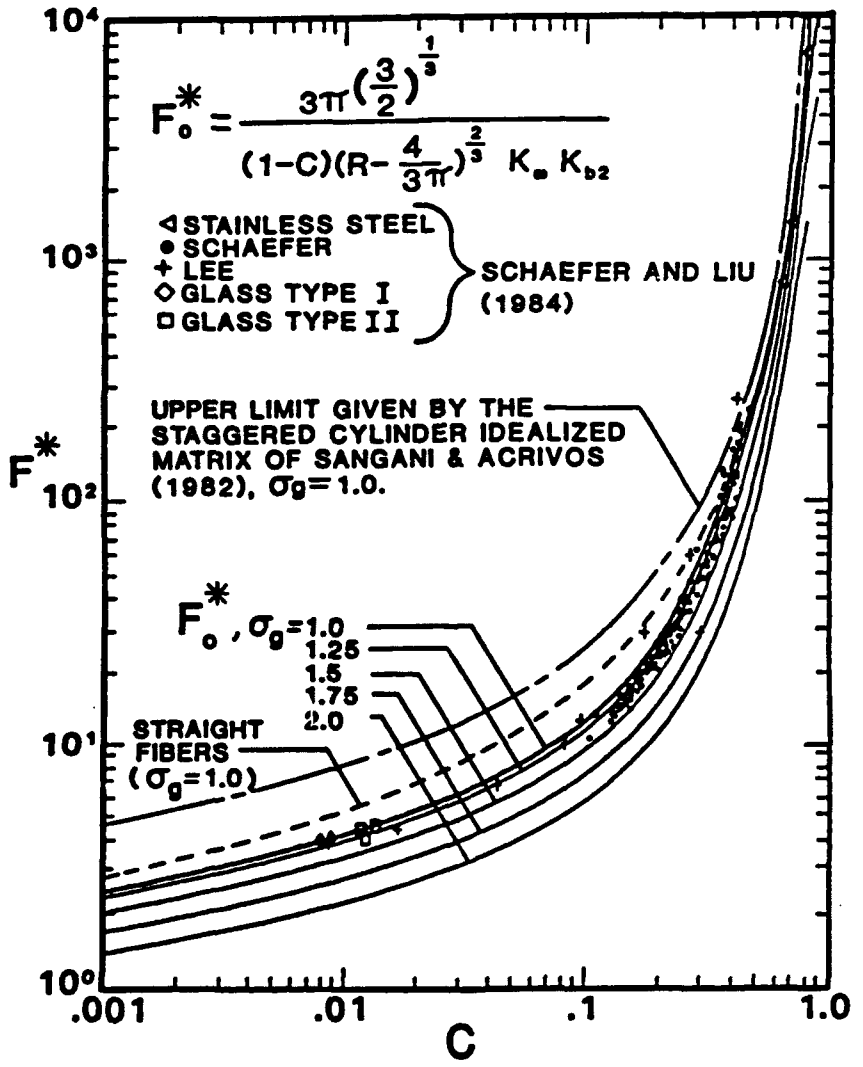

Figure 2. Dimensionless fiber drag parameter as a function of packing density

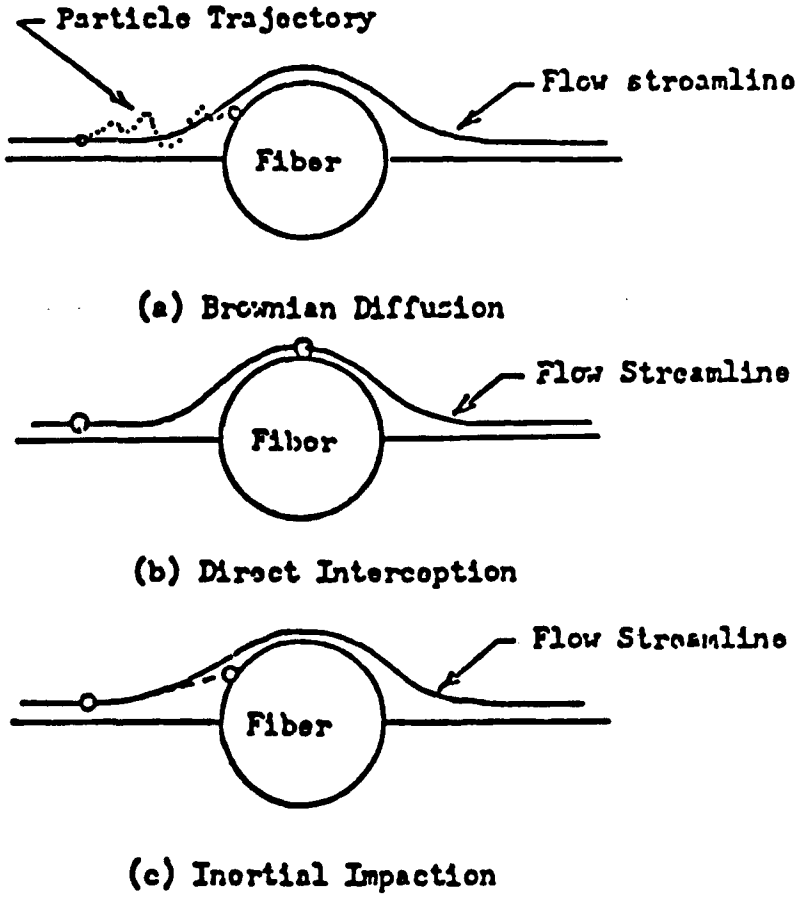

Figure 3. Schematic diagram of filtration mechanisms

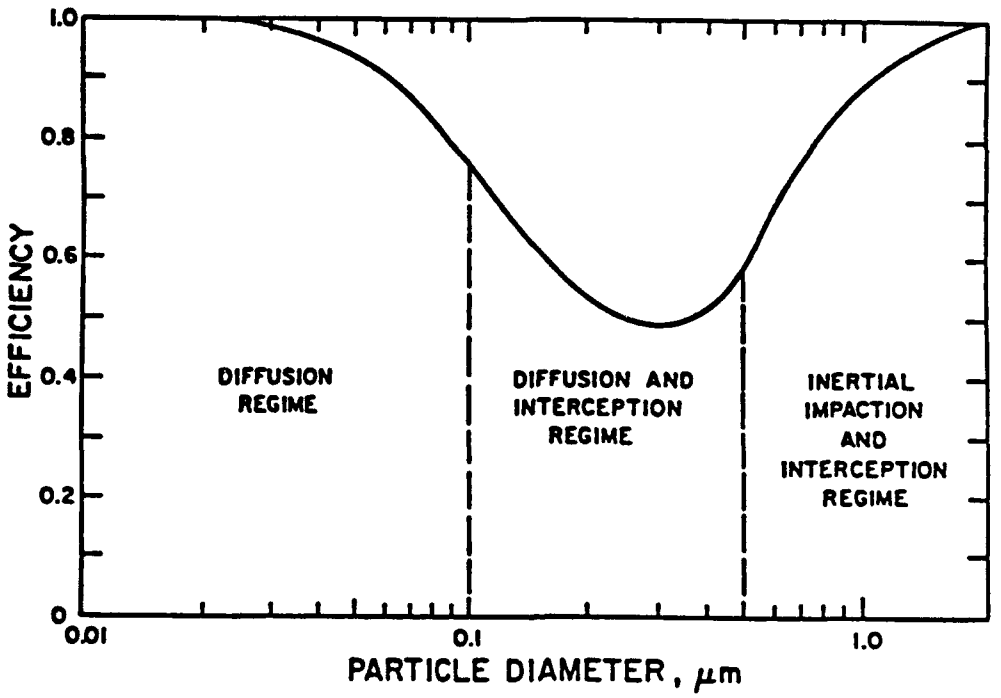

Figure 4. Schematic diagram of filter efficiency as a function of particle size

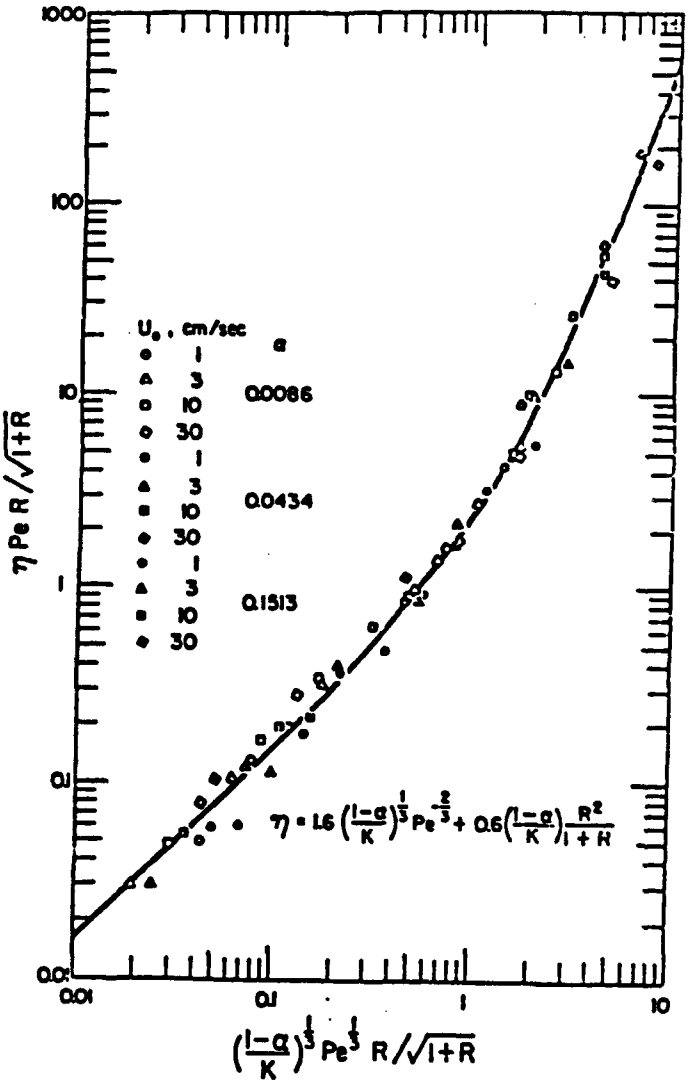

Figure 5. Dimensionless correlation of Lee and Liu for single fiber effieincy

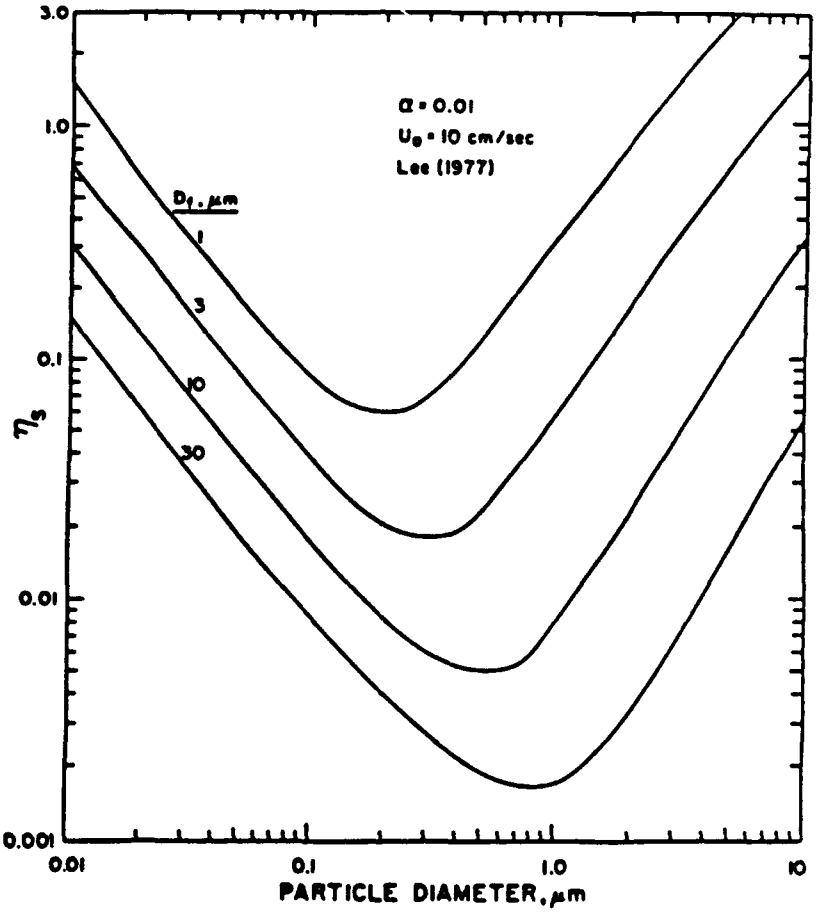

Figure 6. Single fiber efficiency as a function of particle and fiber size

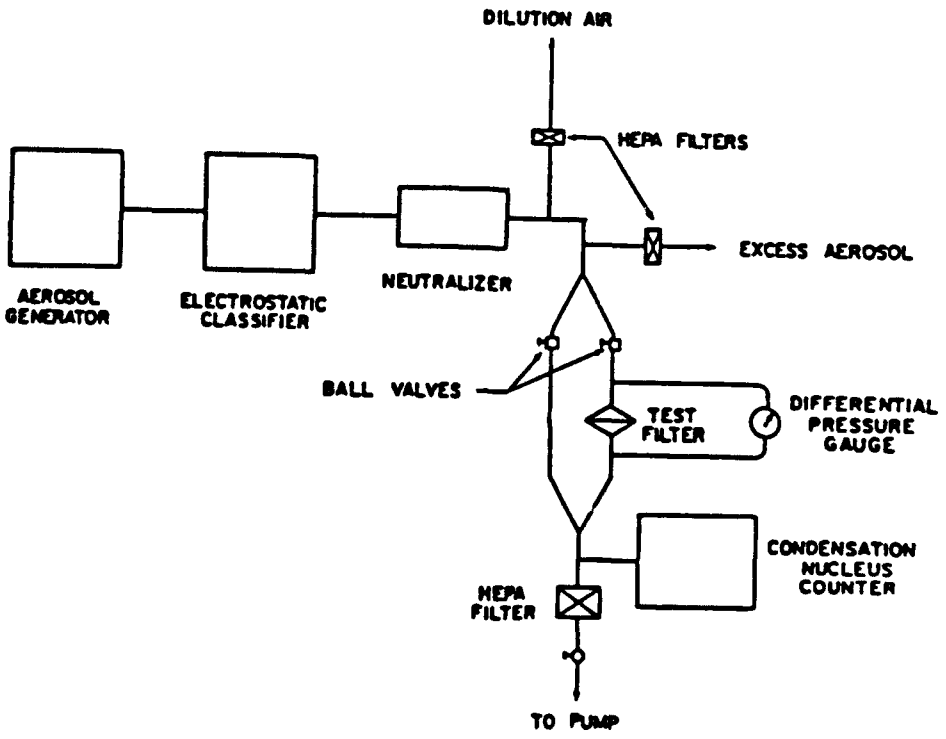

Figure 7. System for measuring the fractional efficiency of filters with monodisperse aerosols

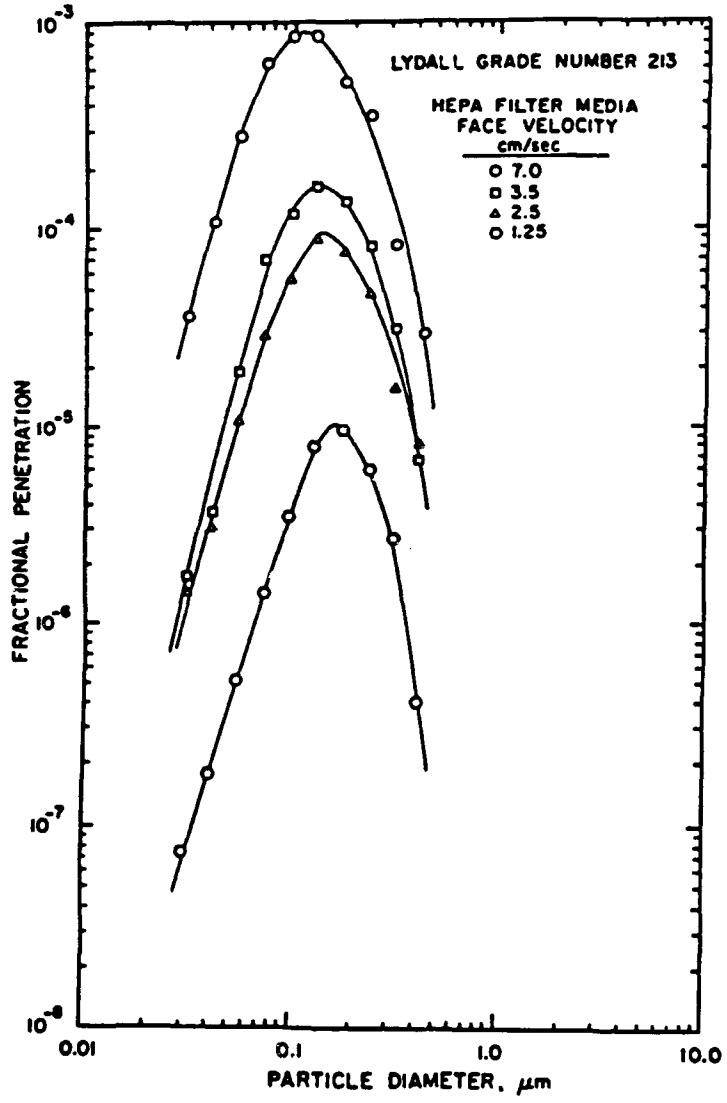

Figure 8. Fractional efficiency of a HEPA filter

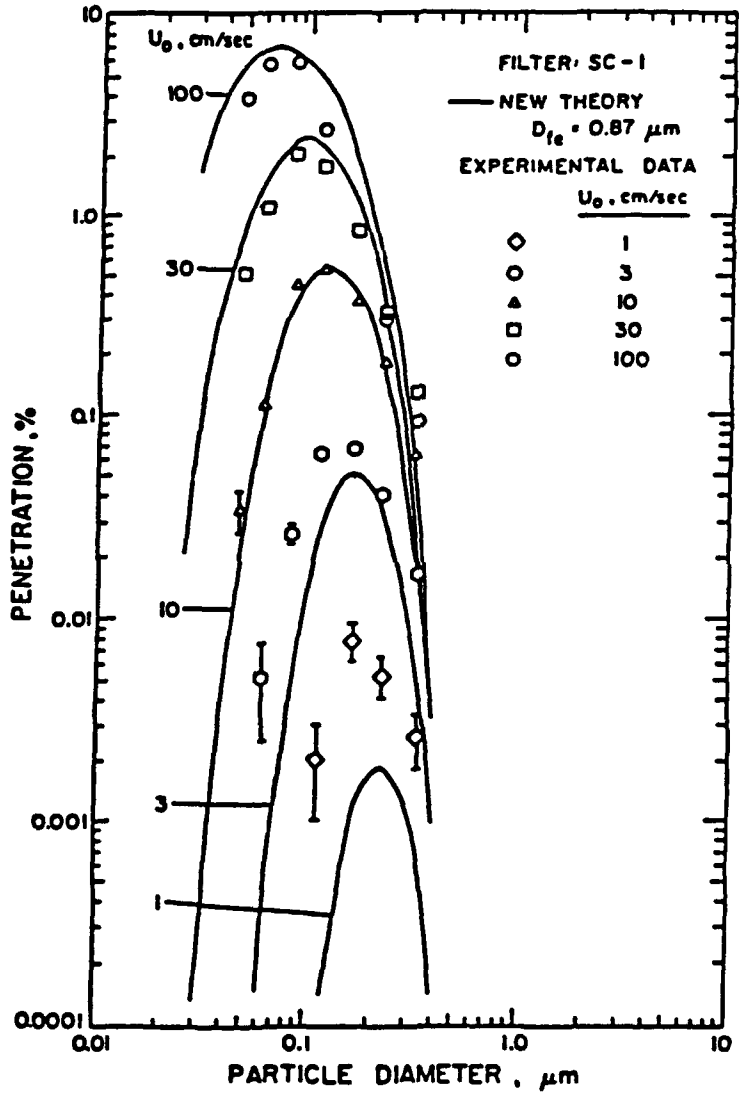

Figure 9. Comparison of theoretical and experimental filter efficiency for the Millipore SC membrane filter of 8 μm pore diameter

SECTION II: PARTICLE PRODUCTION AND DISSEMINATION

Blank

Particle Generation in Aerosol Reactors

Dr. David T. Shaw,
State University of New York, Buffalo

Abstract by Erica R. Riley, CRDEC

The decomposition of metal carbonyls is a convenient system to study in addressing the problem of chain aggregate formation in aerosol reators. Carbonyls are readily dissociated by irradiation as well as by direct thermal application. Dissociation products combine with available species to form metal or metal oxide particles that subsequently aggregate into chain-like morphologies. Product morphology can be controlled by using alternate methods of decomposition and by adjusting operating parameters of the various reactors.

The system used in these studies was the decomposition of iron pentacarbonyl in the presence of an oxygen source to form chains of iron oxides:

$$Fe(CO)_5 \xrightarrow{light\ or\ heat, O_2} Fe_2O_3$$

In this type of formation, the initial step is decomposition of the carbonyl to provide atomic iron and molecular carbon monoxide. This step is followed by nucleation of iron oxide particles and growth of these nuclei by surface condensation. These spherical particles generally reach sizes on the order of 200 angstroms before they aggregate into chain structures. The chains can then coagulate and grow further by additional condensation. Phenomena associated with each of these steps can affect product morphology.

There are four well-known methods for dissociating the carbonyl in this type of system and each method provides slightly different products. The most popular of this is simple thermal decomposition. In this method carbonyl vapor is carried in a hot gas stream to a heat sone (T > 160C) where the reactions occur. Generally this produces spherical particles with diameters on the order of the magnetic domain size, i.e. d > 200 angstroms. The formation of chain aggregates of magnetic materials by this method can be further controlled by the application of magnetic fields. Direct thermal dissociation can also be achieved in a flame generator. In this type of process the characteristics of the flame itself become important factors. As the particles enter the atmosphere they pass through the high temperature part of the flame and experience rapid cooling effects, dropping in temperature at a rate of 10^6 degrees per second. The spherical particles associated with this type of process are generally less than 200 angstroms in diameter.

The other two methods are associated with laser irradiation. Using a CO_2 laser operating at 10.6 microns, a 0.7 volt 50 nanosecond pulse causes "instant" vaporisation of carbonyl droplets. The product of this system is γFe_2O_3 . Departing from the traditional thermal decomposition process, these reactions can be initiated by photodissociation of the carbonyl. This has been done using an axcimer laser operating at 193 nanometers. The ultraviolet radiation dissociates the molecules without heating. Several purposes are served by this approach. The nuclei are cold and inhibit coagulation and aggregation. The product of this process is ultrafine (~ 200 angstrom) particles of αFe_2O_3 . This material is of interest to the semiconductor and microcircuit community, where there is great need of smooth nonmagnetic materials.

In all of these processes the product parameters such as diameter, crystal structure, aggregate length and diameter, and degree of coagulation, can be adjusted through process parameters. These parameters include but are not limited to application of magnetic fields, adjustments in heating and cooling rates, changes in gas flow rates, temperature ranges and time in generator, and the use of various atmospheric environments.

Blank

MATERIAL SYNTHESIS BY AEROSOL PROCESSES

Sotiris E. Pratsinis
Department of Chemical and Nuclear Engineering
Center for Aerosol Processes
University of Cincinnati
Cincinnati, OH 45221-0171

Aerosol process is any operation or series of operations that causes a physical or chemical change to a gaseous suspension of solid or liquid particulates. Individual particulate sizes may range from molecular clusters (<10A) up to 10μm particles (Friedlander, 1982).

Traditionally aerosol science has been devoted to the prevention of the deleterious effects of aerosols on human health and environment. Aerosol engineering is a new discipline aiming in developing industrial aerosol processes for manufacture of high technology materials (optical waveguides and advanced ceramics) and particulate commodities (carbon blacks and titania pigments).

Aerosol processes are advantageous for manufacture of particulates since they do not require the several tedious operations and high liquid volumes of wet chemistry. Thus, the 'chloride' process has gradually substituted the 'sulfate' process in industrial scale manufacture of titania pigments (Solomon and Hawthorne, 1983). Aerosol processes can be used for production of highly pure materials. Hence, in lightguide fabrication technology aerosol ('vapor' deposition) processes phased out the double crucible process for manufacture of low

loss fibers for telecommunications (Nagel et al., 1982; Kim and Pratsinis, 1988). Reactant mixing is achieved in much shorter time scales in aerosol than in wet chemistry processes. These processes are also energy efficient operations for manufacture of particulates. A typical example is the production of silicon for photovoltaic applications. There, the power consumption per unit silicon mass can be an order of magnitude lower in an aerosol reactor than in the classic Siemens process (Alam and Flagan, 1986).

Despite the widespread industrial applications of aerosol processes their design and operation relies heavily on experience and empiricism. As a result, it is not surprising that the particulate industry in United States has not made virtually any progress in the last 20 years (Merrow, 1985). In flame aerosol reactor technology, for example, though several patents on reactor design, feed additives and reactant mixing have been filed, the fundamentals of these systems yet have not been understood (Bowen, 1980).

On the other hand, most basic studies of aerosol processes have been focused on the investigation of a specific physicochemical system. Thus, relationships between process variables and product characteristics have not been developed in the convenient chemical engineering format: dimensionless numbers and monographs. Notable exceptions are a Levenspiellian analysis of standard chemical reactors with respect to product particle concentration, size, polydispersity, surface area and

yield (Pratsinis et al., 1986a); the analysis of the effect of reactant gas mixing on product particle characteristics (Kodas et al., 1987a); the analysis of particle production by condensation (Pesthy et al., 1983; Pratsinis et al., 1988); and the analysis of stirred tank aerosol reactors (Crump and Seinfeld, 1980; Pratsinis et al., 1986b). Although these studies were developed for rather idealistic laboratory scale systems, they provide valuable directions for the design of industrial aerosol processes (Kodas et al., 1987b).

Development of efficient and simple aerosol processes for manufacture of advanced materials and particulate commodities is a major research goal for several domestic and foreign industries. Design, scale up and control of these processes motivate the research for construction of comprehensive but compact models describing the behavior of industrial aerosol reactors. Invention and development of real time instruments measuring production rate, average size and polydispersity of highly concentrated aerosols is a pressing need of the particulate industry.

Alam, M.K., Flagan, R.C. Aerosol Sci. Technol. 5, 237 (1986).
Bowen, H.K. Mater. Sci. Eng. 44, 1 (1980).
Crump J.C., Seinfeld, J.H. AIChE J. 26, 610 (1980).
Friedlander, S.K. Aerosol Sci. Technol. 1, 3 (1982).
Kim, K.S., Pratsinis, S.E. AIChE J. 34, June (1988).
Kodas, T.T., Friedlander, S.K., Pratsinis, S.E. Ind. Eng. Chem. Res. 26, 1999 (1987a).
Kodas, T.T., Sood, A., Pratsinis, S.E. Powder Technol. 50, 47 (1987b).

Merrow, E.W. Chem. Eng. Prog. 80(5), 15 (1985).
Nagel, S.R., MacChesney, J.B., Walker, K.L. IEEE J. Quant. Elec. QE-18, 459 (1982).
Pratsinis, S.E., Kodas, T.T., Sood, A. Ind. Eng. Chem. Res. 27, 105 (1988).
Pratsinis, S.E., Kodas, T.T., Dudukovic, M.P., Friedlander, S.K. Ind. Eng. Chem. Proc. Des. Dev. 25, 634 (1986a).
Pratsinis, S.E., Friedlander, S.K., Pearlstein, A. AIChE J. 32, 177 (1986b).
Solomon, D.H., Hawthorne, D.G. Chemistry of Pigments, Wiley, 1983.

This work was supported in part by NSF grant CBT-8707144.

pp/sp3

AN OVERVIEW OF PARTICLE GENERATION FOR OBSCURATION

E.R.Riley

Chemical Research, Development and Engineering Center
Aberdeen Proving Ground, MD. 21010-5423

1. INTRODUCTION

Theoretical studies of the interactions of electromagnetic radiation with particulate clouds have provided information about the particle parameters required to maximize extinction. These parameters are generally related to the size, composition, shape, aspect ratio, conductivity, and optical constants associated with the individual particles. Designing and generating particles to produce any specified result in EM interactions involves proper choice of the material and its generation technique. Every method available for particle generation is limited in the types of materials that can be addressed by the technique. The ability to tailor a particle to specific meeds depends on full control of a wide variety of processes. A number of techniques will be discussed here, including chill block melt spinning, thermal decomposition of organometallics, spray drying, vapor depositions, plasma and flame spray techniques and combustion synthesis. Each has unique abilities to provide particles with specific properties.

2. TECHNIQUES

2.1. Chill Block Melt Spinning

The concept of chill block melt spinning has been used for may years to produce glassy metals and alloys. A stream of molten metal is impinged on a rapidly spinning wheel, cup or disk that is cooled to room temperature or below. The rapid transfer of thermal energy from the melt to the wheel results in solidification at rates that preclude classical crystallization. This allows formation of solid metal phases, stable at room temperature, that would otherwise not form. Historically researchers have concerned themselves with the problem of forming large sheets of glassy metals; however taking the opposite approach provides a convenient method of rapidly producing fine particles. Particle size can be controlled via such parameters as the speed of the spinning block, feed rate of the melt to the block(s), orifice diameter, melt viscosity, melt velocity, and cooling rate. Particle shape can be controlled by the geometry of the melt spinner, e.g. the shape of the block or combination of blocks, distances between blocks and thermal variations throughout the system. One example of a versatile melt

spinner is a spinning cup surrounded by rotating cylinders. The cup alone produces needles, cylinders alone produce ribbons or sheets, and both in tandem produce flakes.

2.2 Thermal Decomposition

Thermal decomposition of organometallic vapors can be used for a variety of applications. The material to be decomposed, the thermodynamically stable products, and the temperature, atmosphere and pressure used in the process all control the product characteristics. Many of these processes result in ultrafine irregular particles formed by the laws of nucleation and condensation. However, depending on the identity of the materials involved, additional controlling parameters can be used to alter the morphological characteristics of the product. One of the most useful of these parameters is the addition of a variable magnetic field. Proper use of this in the formation of ferromagnetic particles can result in fibers or whiskers of controllable diameter and length. This control is valuable in light of the theoretical significance of aspect ratio in attenuation mechanisms.

2.3 Spray Drying

Spray drying is extremely valuable in cases where the goal is fine crystals of soluble material. The size and crystallinity of the particles produced depends on the temperature profile of the system used, the solubility and concentration of the material in the solvent, and the droplet size, speed, and number concentration in the drying zone. The effect of varying these parameters is generally to control the rate of solvent evaporation and to control the population in the drying zone, thus controlling the kinetics of the nucleation and condensation processes. The actual effects of parameter controls on the spray drying process have been thoroughly studied for numerous solute/solvent systems. The experimental observations in these studies are effectively correlated with theoretical models.

2.4 Vapor Deposition

Deposition processes are generally recognized for their value in formation of thin films and coatings. There are a number of different deposition technologies ranging from purely physical vapor depositions to depositions involving chemical and electrical processes. All involve heating of a material, usually in vacuum, to generate a vapor phase. The vapors travel to a substrate surface and condense. Factors controlling the product include pressure, identity of the material being evaporated and of any gases existing in the zone, identity, texture, and cleanliness of the substrate, concentration of vapors, rates of evaporation and condensation, and stability of the material being evaporated. This last factor is often used to advantage in chemical processes. Coevaporation of two reactive materials, or evaporation of a

substance into a reactive gas, can provide deposition of a reaction product. This type of process is called chemical vapor deposition and there are numerous variations on the theme. Use of these processes in the generation of particulates is limited to cases where the desired size is in the realm approachable by mechanical manipulation. Ultrathin flakes may be produced via deposition through a screen onto a substrate that is later removed. Mechanical cutting of continuous deposited films can also provide flakes or ribbons. The greatest advantage to these techniques is direct control over the flake production process. This can provide multilayer flakes or flakes of materials which do not naturally assume this shape.

2.5 Plasma and Flame Spraying

Plasma and flame spray techniques are also traditionally used in coatings applications. A plasma or flame torch is used to vaporize a material and accelrate the vapor towards a substrate. Controlling parameters include plasma energy, thermophysical properties of the material being sprayed, distance between source and substrate, cleanliness of substrate, atmosphere, and temperature profiles. Several methods can be used to adapt these techniques to particle production. If no substrate is present the vapors will nucleate and condense in flight as particles such as the case for carbides and nitrides of silicon forming chain aggregates. Control of the nucleation and condensation rates by control of temperatures and concentrations throughout the zone can provide variation in particle morphology. Again, size and shape control can be achieved through geometric considerations and refined morphology can be achieved using electromagnetic fields strategically applied. The advantage of this technique is its applicability to high refractory materials.

2.6 Combustion Synthesis

Combustion synthesis of ceramics is one of the fastest and most cost effective methods of producing high density ceramic particulates. The technology takes advantage of the thermodynamic stability of the product relative to the reactants and uses the reaction exotherm to feed the reaction and to purge the products of impurities. The starting materials are generally powders in elemental form. These are intimately mixed and the reaction is initiated by an electrical discharge or sudden local thermal flux. A typical example is the reaction of titanium and carbon to form titanium carbide, or titanium and boron to give the boride. In these methods, the manner of particle size and shape control depends on the alloy system in use. In some cases the product strictly mimics the morphology of the precursors.

Blank

CHEMICAL REACTIONS IN AEROSOLS - A NEW TECHNIQUE FOR PREPARATION OF COLLOIDS OF NARROW-SIZE DISTRIBUTION

Richard E. Partch
Department of Chemistry and
Center for Advanced Materials Processing
Clarkson University
Potsdam, NY 13676

A novel technique has been developed for the preparation of spherical colloidal organic or inorganic particles which can be of simple or mixed composition, or coated. The procedure consists in contacting liquid aerosol droplets of one reactant with a co-reactant in the vapor phase. There are several distinct features of this technique which offer certain advantages over the commonly employed processes for the generation of fine powders. The so produced particles are always spherical and their diameter can be predetermined by the size of the initial aerosol droplets. The materials are of high purity because, in most cases, no extraneous ions, surfactants, or any other additives are involved in the process. Solids of defined mixed composition can be obtained from droplets of known contents in components. Finally, some extremely rapid reactions may be used in the aerosol processing, that are difficult to control by other procedures.

The described technique was employed in the preparation of spherical particles of narrow size distribution of titania (1), alumina (2), or mixed titania/alumina (3,4). In these cases, droplets of corresponding alkoxides (or mixtures thereof) were reacted with water vapor. Similarly, silica particles were prepared by exposing $SiCl_4$ aerosols to water vapor and mixed titania/silica and alumina/silica colloids were produced from the corresponding metal alkoxide and $SiCl_4$ (5).

Polymer colloids of styrene (6) or ethylvinyl/divinylbenzene (7) were generated from droplets of monomers in the presence of an initiator (trifluoromethanesulfonic acid) in the vapor phase. By this procedure, it was possible to obtain rather large particles (up to 30 um) which cannot be prepared by conventional techniques, such as emulsion polymerization.

Uniform spherical particles of polyurea were generated using droplets of diisocyanate derivatives and ethylenediamine vapor. Sequential use of metallorganics and organic monomers as starting materials yielded mixed particles such as polyurea/TiO_2 or polyurea/Al_2O_3 (8).

It is possible to coat inorganic cores with organic coatings by the aerosol technique. Titania produced as described above was wetted with diisocyanate derivatives in the aerosol phase and then mixed with the vapor of ethylenediamine. This sequence of reactions produced a polymeric coating on the titania cores. The

thickness of the coatings could be altered by varying experimental conditions (9).

Aerosol droplets can be obtained either by evaporation/ condensation or nebulization. In the former case, the droplet size and uniformity can be altered by the flow rate of the carrier gas and temperature of the apparatus. Nebulization results in droplets, and subsequently particles having wider size distribution but allows incorporation of nonvolatile components. Furthermore, microcapsules can be formed around nonreactive materials (10).

The so obtained colloidal powders find many applications, such as in medical diagnostics, as drug carriers, fillers, coatings, catalysts, or for various special uses n high-tech ceramics.

ACKNOWLEDGEMENT

This program is conducted in collaboration with Professor Egon Matijevic', Clarkson University.

REFERENCES

1. M. Visca and E. Matijevic', J. Colloid Interface Sci., 68, 308-319 (1979).

2. B.J. Ingebrethsen and E. Matijevic', J. Aerosol Sci., 11, 271-280 (1980).

3. B.J. Ingebrethsen, E. Matijevic' and R.E. Partch, J. Colloid Interface Sci., 95, 228-239 (1983).

4. B.J. Ingebrethsen and E. Matijevic', J. Colloid Interface Sci., 100, 1-16 (1984).

5. A. Balboa, R.E. Partch and E. Matijevic', "Preparation of Uniform Colloidal Dispersions by Chemical Reactions in Aerosols - IV. Mixed Silica/Titania Particles," Colloids Surf., 27, 123 (1987).

6. R.E. Partch, E. Matijevic', A.W. Hodgson and B.E. Aiken, J. Polymer Sci., Polym. Chem. Ed., 21, 961-967 (1983).

7. K. Nakamura, R.E. Partch and E. Matijevic', J. Colloid Interface Sci., 99, 118-127 (1984).

8. R.E. Partch, K. Nakamura, K.J. Wolfe and E. Matijevic', J. Colloid Interface Sci., 105, 560-569 (1985).

9. F.C. Mayville, R.E. Partch and E. Matijevic', "Preparation of Uniform Spherical Titania Particles Coated With Polyurea by

the Aerosol Technique," J. Colloid Interface Sci., 120, 123 (1987).

10. L. Durand-Keklikian and R.E. Partch, "Microencapsulation of Oil Droplets by Aerosol Techniques - I. Metal Oxide Coatings," J. Aerosol Sci., In Press.

Blank

COLLOIDAL PROCESSES FOR PARTICLE PRODUCTION

V.B. Menon, M.E. Mullins[1] and M.B. Ranade[2]
Research Triangle Institute
P.O. Box 12194
Research Triangle Park, NC 27709

INTRODUCTION

In recent years, the need for high purity, chemically homogeneous particles of uniform size and controlled shape has resulted in the development of a variety of unconventional techniques for ceramic powder production. The conventional powder preparation processes involving bulk mixing, calcination, comminution and classification have serious drawbacks when powders of high chemical purity and submicrometer size are required. The two approaches suitable for producing ceramic powders suitable for advanced ceramic applications are (i) vapor-phase synthesis, and (ii) colloidal synthesis. This paper describes the common colloidal processes for powder production with special emphasis on some of the more recent advances in the field.

Colloidal processing is the dominant route for the preparation of multicomponent oxide systems, because of the ease of mixing solutions of salts to precise ratios, which can then be converted to oxide powders without disturbing the chemical homogeneity of the solutions (Johnson, 1987). For nonoxide ceramic powders, vapor-phase processing still appears to be the more viable route. The various colloidal processes can be divided into two general categories; evaporation and precipitation. In the following sections each of these methods is discussed in greater detail.

EVAPORATION

All colloidal processes involve the dissolution of salts such as nitrates, sulfates, acetates, etc., in a solvent. Evaporation involves the removal of the solvent from a solution of the salt by drying. Simple evaporation by heating gives coarse crystals and is only suitable for single component solutions. For multicomponent systems this procedure results in a very inhomogeneous residue because of the different solubilities of the various components. The more common approaches to evaporation include spray drying or roasting, fluidized bed drying, freeze drying, and emulsion drying.

Spray Drying: Segregation can be minimized by dispersing the salt solution into fine droplets and drying the drops rapidly. In a spray dryer, a liquid

---

[1]Current address: Michigan Technological University, Houghton, MI.

[2]Current address: Particle Technology, Inc., College Park, MD.

solution is dispersed into a heated reactor chamber in the form of a mist of fine droplets. Typical droplet sizes vary from 1-30 μm while typical powder sizes are in the 0.5-20 μm range. The liquid is rapidly vaporized leaving residual particles of dry solid. These solids could, if necessary, be reacted to form products which can then be separated from the gas stream. Spray drying has been used for the production of ferrites and magnesium aluminates from sulfates (DeLau, 1970), and complex mixed oxides of metals such as La, Mg, Cu, Ti, for making elecrical interconnections of simple electrolysis cells (Roettanbacher and Schmidberger, 1983).

Spray Roasting: In this process spray drying and subsequent calcination to form metal oxide are combined into one operation. This process has been extensively used for the synthesis of oxide powders for ferrite production (Ruthner, 1985). Messing and coworkers (1987) have used a similar process to prepare powders of MgO and Al_2O_3-ZrO_2. This process, termed "evaporative decomposition of solutions", uses nitrates, acetates, chlorides, or sulfates as precursors for the oxide powder.

Fluidized Bed Drying: This technique is similiar to spray roasting except that the solution is trapped in a fluid bed for drying and decomposition. A pneumatic nozzle injects solution droplets into a heated fluid bed of the solid product. By varying the temperature, fluidizing gas flowrate and solution injection rate, the process can be made continuous, with periodic removal of product. Advantages of this process include: (i) absence of moving parts, (ii) formation of granulated powders of relatively high bulk density and large particle size, (iii) large capacity per unit volume of equipment, and (iv) excellent mixing and heat transfer rates.

Emulsion Drying: Spray and fluid bed drying are processes where drying is accomplished in the gas phase. In emulsion drying, the aqueous salt solution is dispersed in a matrix liquid such as kerosene and then dried. This gives a rather stable suspension of solid salt particles in kerosene. The particles are deflocculated, precipitated, filtered, washed and decomposed. Reynen et

al. (1983) reviewed the sequence of events that are part of a typical emulsion drying operation. A water-in-oil emulsion is prepared using suitable surface active agents with the aqueous phase containing the salts. Once the emulsion is formed, the solvent can be vaporized by evaporation using vacuum, heated immiscible oils such as petroleum or kerozene, freeze drying, or by combusting the emulsion.

Freeze Drying: In contrast to the methods described thus far for solvent volatilization, freeze drying makes use of sublimation rather than evaporation for solvent removal. The solution is dispersed into small droplets to minimize segregation and then rapidly refrozen. Solution droplets are sprayed into a bath of immiscible liquid such as hexane chilled by dry ice or acetone. The frozen droplets are recovered from the refrigerant and placed onto a cooled tray in a freeze drying chamber for the purpose of subliming the water. While freeze drying is quite successful in producing fine, homogeneous ceramic powders, high capital costs and energy requirements have prevented it from being used for large scale applications.

A variation of conventional freeze drying is emulsion freeze drying where the salt solution is encapsulated in an emulsion droplet. Figure 1 shows the difference between emulsion freeze drying and conventional freeze drying. In the latter case, an aqueous solution is atomized into the freezing solvent, while in the former case the emulsion is dispersed into the refrigerant. The advantage of emulsion freeze drying is that demixing, which is especially prevalent inside large droplets, is minimized.

Supercritical Expansion: Matson et al. (1986) describe a unique process, based on the rapid expansion of supercritical fluid solutions, for producing ceramic powders. When a salt solution is expanded through a nozzle from a high-temperature and -pressure regime to a low-pressure environment, particles of the solute material are produced by homogeneous nucleation. Particle size, agglomeration, and other characteristics can be controlled by manipulation of the solute concentration, temperature of the preexpansion fluid, and other parameters of the expansion process. Figure 2 depicts a schematic of the

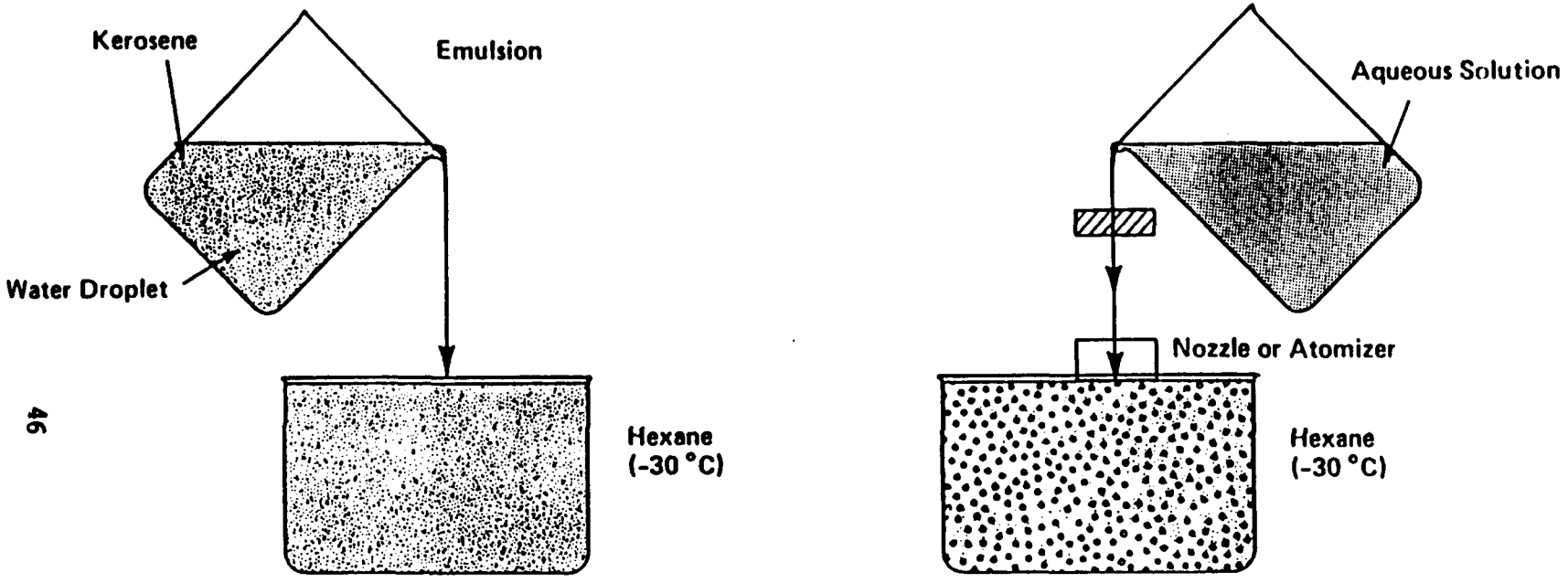

Figure 1. Comparison of freeze drying with emulsion freeze drying process.

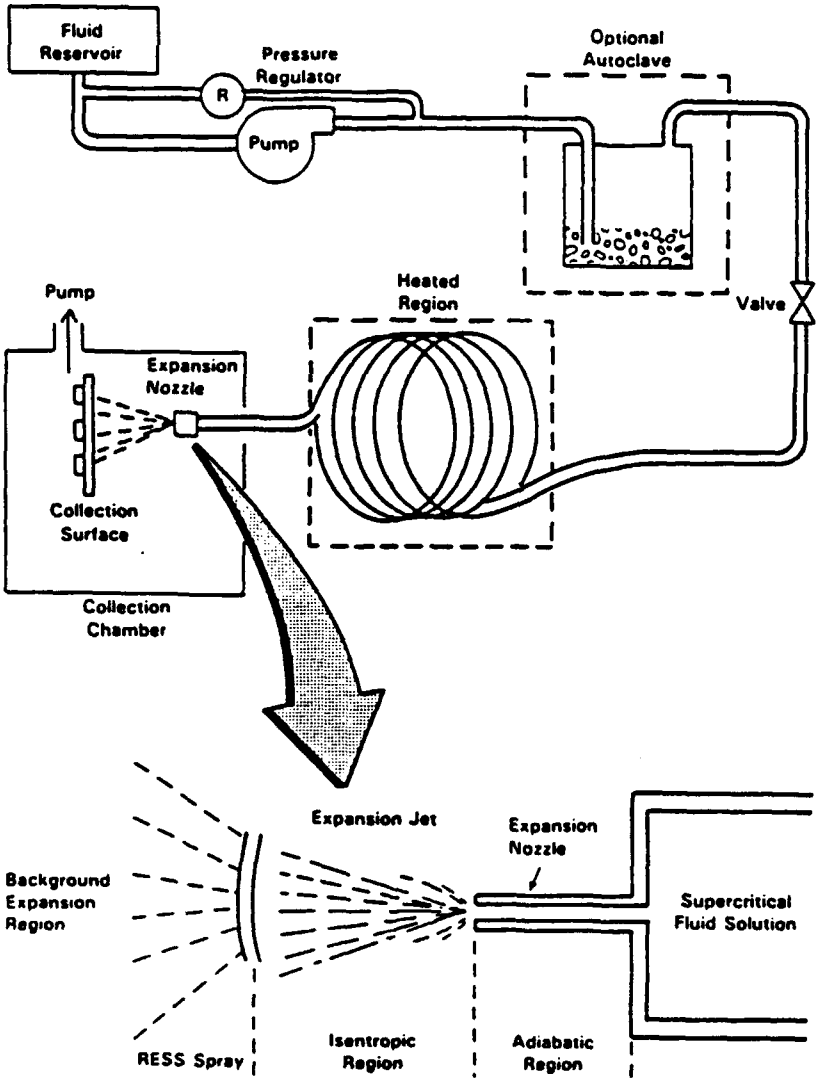

Fig. 2. Schematic of the RESS apparatus and (inset) the distinct stages occurring during the early part of the RESS expansion through a capillary nozzle (Matson et al., 1987).

experimental apparatus. The basic components of the system consist of a pump capable of producing pressure several times the critical pressure of the fluid of interest, a region in which the fluid is heated above its critical temperature, and a nozzle through which the solution is expanded to atmospheric pressure or below.

This technique, which is currently at the laboratory scale, has great potential for producing nonequilibrium amorphous powders that are not readily available by other, more conventional powder production methods (Matson et al., 1987). Materials that have been prepared using this method include SiO_2, GeO_2, and ZrO_2.

PRECIPITATION AND FILTRATION

Precipitation followed by removal of solids by filtration is one of the oldest techniques for preparation of inorganic and organic powders. In recent years a variety of inorganic colloids have been prepared in the form of well-defined particles of different shapes, including spheres (Matijevic, 1986, 1987). Precipitation of single cation salts is done on a large scale in the ceramics industry to prepare high purity oxides and carbonates. The important variables are (Johnson and Gallagher, 1978):

(1) pH of the aqueous solution: The influence of pH on the precipitation of hydroxides is obvious in that the OH^- concentration appears in the solubility product. e.g. The precipitation of $Al(OH)_3$ is:

$$Al^{3+} + 3OH^- = Al(OH)_3.$$

At very low pH there are insufficient OH^- ions in solution. At high pH, the soluble complex $Al(OH)_4$ is formed. A pH of 4-9 is necessary for $Al(OH)_3$ precipitation.

(2) Order of mixing and addition of precipitating agent: Generally the solution of cations is added slowly with stirring to a solution containing the precipitating agent. This allows an excess of the precipitating agent to be added and, the solubility products of all the cations are likely to be exceeded simultaneously. The opposite sequence of addition will result in cations that are precipitated with inhomogeneities.

(3) Rate of mixing: This parameter affects particle size; finely divided precipitates are formed by rapidly mixing cold concentrated solutions. Also, high mixing rates inhibit the formation of agglomerates.

(4) Presence of other ions in solution: The presence of high concentrations of electrolytes can destroy the electrical double layer around a particle and promote coalescence. The electrical charge distribution around each particle dictates whether particles will agglomerate or not. The composition and morphology of particles can also be greatly affected by the presence of other ions. Figure 3(a) shows ellipsoidal hematite particles precipitated by aging a water/ethylene glycol solution of ferric chloride. The effect of a small amount of phosphate ion on a similar system is demonstrated in Figure 3(b) (Matejevic, 1987). The presence of phosphate ions completely changes the morphology of the particles.

(5) Impurities: These can be incorporated into a precipitate due to adsorption on particles or by occlusion within flocculates. Slow growth, large particle sizes, and equilibrium produce the purest precipitates.

Other factors include temperature, solute concentration and pressure.

Major advantages of precipitation-based methods for powder production include the ability to form homogeneous particles of mixed metal oxides, and the capacity to produce equiaxed (regularly shaped) particles. A recent application of this type of powder preparation technique is the manufacture of 1-2-3 superconductors. Using salts of yttrium, barium, and copper in various stoichiometric ratios, a homogeneous powder of yttrium-barium-copper oxide can be precipitated.

Equiaxed, monodisperse particles that have been prepared by precipitation are SiO_2 (Barringer et al., 1984), TiO_2 (Barringer and Bowen, 1982), and Al_2O_3 (Sacks et al., 1984).

Precipitation by Alkoxide Hydrolysis: Alkoxides and other metallo-organics can provide a source of high-purity reactants for precipitation. In this process, a metal alkoxide is hydrolysed with alcohol and water to precipitate insoluble hydrated oxides. The hydrolysis reaction can be carried out either in an aerosol reactor or in an aqueous solution. For example, ZnO powder for high voltage devices has been produced by hydrolysis of ethylzinc-t-butoxide, dissolved in anhydrous toluene, in deionized water and ethanol. The ethanol is present to solubilize the organic liquid in the aqueous solution. Submicrometer size ZnO powder is formed quantitatively and can be removed by filtration (Heistand et al., 1986).

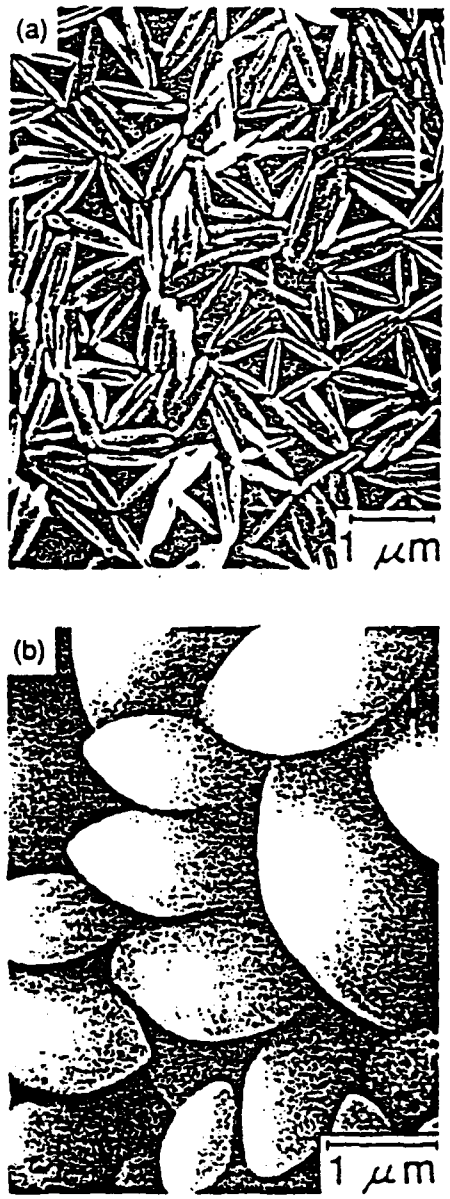

Fig. 3. Scanning electron micrograph of hematite particles obtained by heating at 100°C (a) for 7 days a 20 vol% ethylene glycol/water solution 0.05 mol · dm^{-3} in $FeCl_3$, and 0.03 mol · dm^{-3} in HCL; (b) for 2 days a 20% ethylene glycol/water solution 0.076 mol · dm^{-3} in $FeCl_3$, and 3 x 10^{-4} mol · dm^{-3} in $(NH_4)H_2PO_4$ (Matijevic, 1987).

Alkoxides have also been used to dope other preexisting ceramic particles. Thus, ZrO_2 has been added to α-Al_2O_3 particles by hydrolyzing zirconium alkoxide in a dispersion of alumina (Fegley et al., 1985).

Hydrothermal Precipitation: Often, alkoxide hydrolysis can be followed by hydrothermal reaction to give complete conversion of the metal precursor to the oxide. Titanium ethoxide [$Ti(OEt)_4$] hydrolysis results in partial conversion to TiO_2. The dispersion containing unreacted ethoxide, when heated in an autoclave at 200-300°C at 1.5 - 10 MPa pressure for 4-6 hours gives TiO_2. Figure 4 shows the sequence of steps involved in the hydrothermal conversion of Ti-ethoxide to TiO_2 and the subsequent processing steps to get a sintered ceramic product (Heistand et al., 1986).

Sol-Gel Precipitation: The sol-gel technique refers to the preparation of a sol (an aqueous colloidal suspension of the desired oxides in hydrated form) from nitrates or other salts, by controlled precipitation or digestion of precipitates. The sol is converted to a gel by partial dehydration or by adding ammonia in various forms. In some cases, dehydration is achieved by evaporation. The gel is dried to give low density spheres of high surface area and chemical homogeneity. These spheres can be sintered to theoretical densities at remarkably low temperatures. Very often, the powders are sintered in the gel state for ceramic applications.

Sol-gel processes have found their greatest application in nuclear fuel preparation and ceramics manufacture. Since the late seventies, sol-gel techniques have been used to prepare crystalline and noncrystalline solids from over fifty chemical systems (Mackenzie, 1986). A typical sol-gel process involves the formation of very small colloidal particles in solution by hydrolysis of organic compounds of metals to hydrous oxides (Figure 5). These particles are normally 2 to 3 nm in size. When particles of hydrated oxides of Fe, Th, Si, Ti, Zr, or Al are first formed in water, they are all in the above size range (Rijnten, 1970). Silicon ethoxide, n-zirconium propoxide, n-titanium butoxide, or tetra ethoxy silane are typical metallo-organic precursors for sol-gel preparation of powders (Perthius and Columban, 1986).

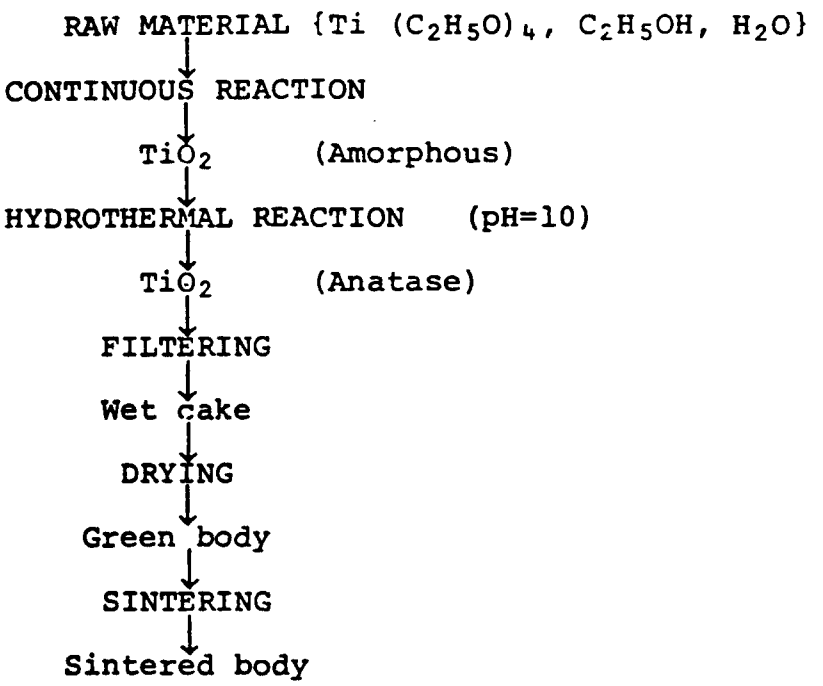

Figure 4. Hydrothermal treatment of TiO_2 powder (Heistand et al., 1986).

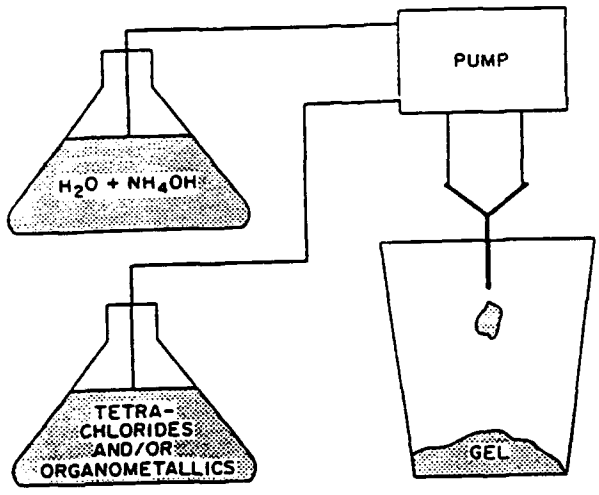

Fig. 5. Schematic of a sol-gel process apparatus (Fleming, 1987).

The hydrolysis reaction is achieved by adding a metal hydroxide, chloride, or nitrate in the aqueous phase. The hydrolysis of metal alkoxides gives a mixture of the corresponding hydroxide and oxide. Drying leads to the final powder. Ammonia and ammonium fluoride are catalysts for the gelation process.

Products prepared via the sol-gel route include contact lenses, filters, catalyst supports, coatings, films, radioactive waste containers, and nuclear fuel rods.

Emulsion Precipitation: This method is suitable for conducting reactions between species that are insoluble in each other. For example, yttrium oxide powders have been made from water-in-oil emulsions containing yttrium ions in the aqueous phase (Akinc and Celikkaya, 1986). Precipitation of yttrium hydroxide is accomplished by adding an organic base (triethanolamine) to the emulsion. Separation of the precursor by dissolution of the emulsion in alcohol, filtration, and subsequent calcination gives Y_2O_3. In this process, yttrium ions which are oil insoluble are reacted with the triethanolamine base which is water insoluble, by conducting the reaction at the oil-water interface.

Foam Precipitation: This is a novel method for preparing metal oxide powders with high aspect ratios. The process utilizes a colloidal foam reactor to prepare ceramic oxide flakes or powders (Menon, 1988). Figure 6 illustrates a schematic diagram of a typical foam reactor. An aqueous salt solution containing a surfactant is placed at the bottom of the reactor. A gas is then blown through the aqueous solution by means of a nozzle to generate a foam which rises up the reactor. The flowrates are adjusted in such a manner that the foam dries as it travels up the reactor. The precipitation reaction occurs within the foam bubbles and the solid powder is collected at the reactor outlet. Since the precipitation reaction occurs within the thin lamellar liquid walls separating individual foam bubbles, the particles that are formed have high aspect ratios. The powder collected at the reactor outlet can be calcined to obtain metal oxides. This reactor has been utilized to make flakes of Al_2O_3, ZrO_2, and Y_2O_3.

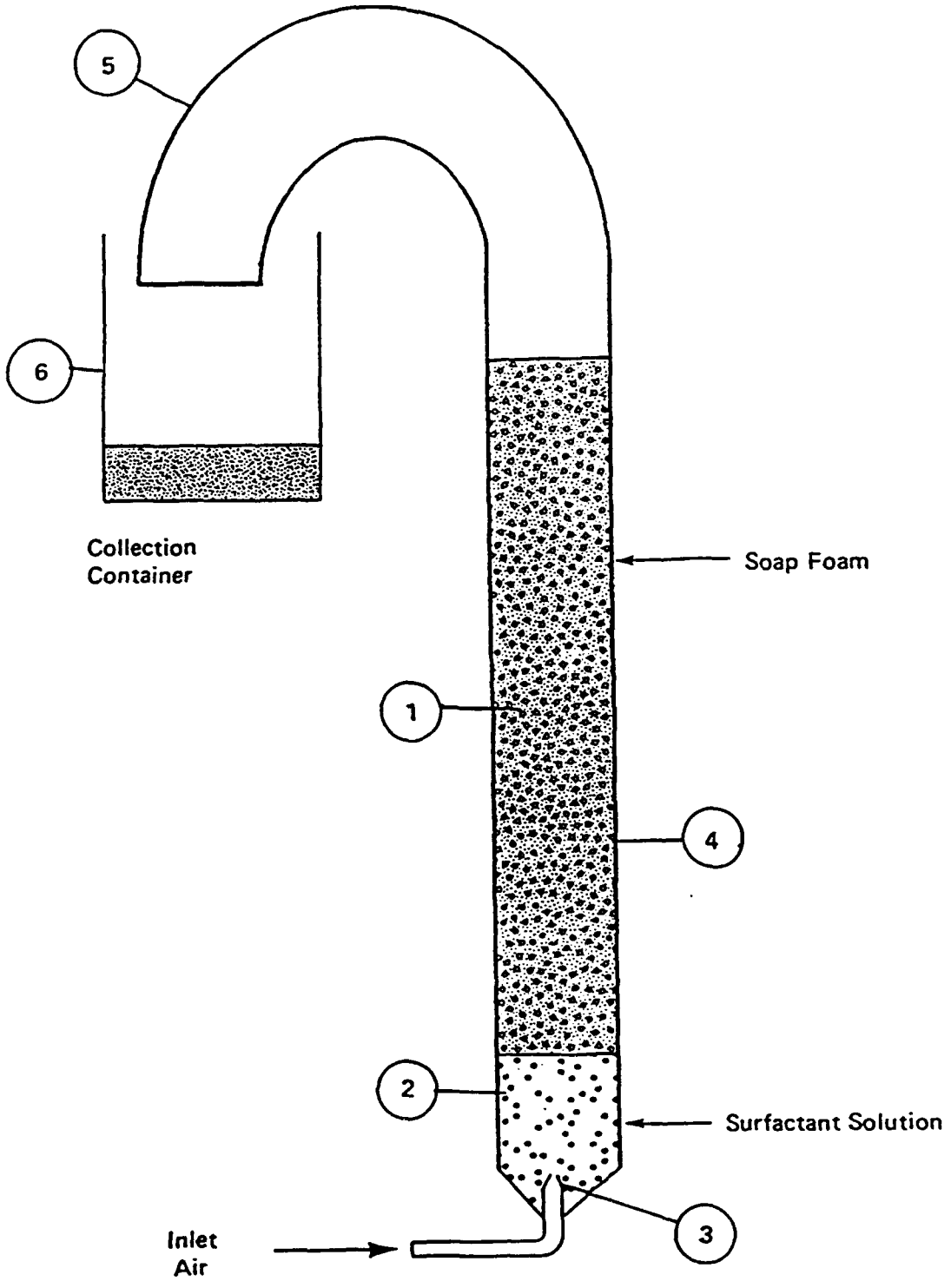

Figure 6. Schematic of a foam reactor (Menon, 1988).

Molten Salt Precipitation: This form of precipitation eliminates the need for an aqueous salt solution. The oxide precursors are mixed with a low-melting salt (such as a eutectic mixture of NaCl and KCl) and heated to temperatures above the melting point of the salt. The reactant oxides slowly dissolve in the molten salt and the desired compound precipitates because the product is only sparingly soluble in the molten salt. The product powder is obtained by dissolving the cooled salt (Johnson, 1987). This method yields particle sizes below 0.1 μm, with relatively narrow size distributions. Ferrites and barium titanates have been prepared by the molten salt method (Hayashi et al., 1985).

SUMMARY

A short review of the various liquid-based powder production techniques is presented. Advances in ceramics technology require the availability of submicrometer size particles of narrow size distribution and regular shape. Currently, these powders can only be prepared by colloidal and vapor phase methods. However, most colloidal techniques are limited to the production of metal oxides. Nonoxide ceramics such as carbides, nitrides, and diborides are becoming increasingly used in electronic and structural applications, and hence, there is a need for research in the field of nonoxide powder preparation by colloidal reactions.

REFERENCES

Akinc, M.K., and A. Celikkaya. 1986 "Preparation of Yttria Powders by Emulsion Precipitation," in Advances in Ceramics, Vol. 21 (eds. G.L. Messing, K.S. Mazdiyasni, J.W. McCauley and R.A. Haber), The American Ceramic Society, Columbus, OH., pp. 57-68.

Barringer, E.A., N. Jubb, B. Fegley, R.L. Pober, and H.K. Bowen. 1984 "Processing Monosized Powders," in Ultrastructural Processing for Ceramics and Glasses (eds. L.L. Hench and D.R. Ulrich), Wiley and Sons, New York, pp. 315-333.

Barringer, E.A., and H.K. Bowen. 1982 "Formation, Packing, and Sintering of Monodisperse TiO_2 Powders," J. Am. Ceram. Soc., 65: C-199.

DeLau, J.G.M. 1970 "Preparation of Ceramic Powders from Sulfate Solutions by Spray Drying and Roasting," Am. Ceram. Soc. Bull. 49:572.

Fegley, B. Jr., P. White, and H.K. Bowen. 1985 "Preparation of Zirconia-Alumina Powders by Zirconium Alkoxide Hydrolysis," J. Am. Ceram. Soc., 68: C-60.

Fleming, J.W. 1987 "Sol-Gel Processing of Glass Powders," in Advances in Ceramics, Vol. 21 (eds. G.L. Messing, K.S. Mazdiyasni, J.W. McCauley and R.A. Haber), The American Ceramic Society, Columbus, OH., pp. 155-162.

Hayashi, Y., T. Kimura, and T. Yamaguchi. 1985 "Preparation of Rod-Shaped $BaTiO_3$ Powder," Am. Ceram. Soc. Bull., 64: 1249.

Heistand, R.H., Y. Oguri, H. Okamura, W. C. Moffatt, B. Novich, E.A. Barringer, and H.K. Bowen. 1986 "Synthesis and Processing of Submicrometer Ceramic Powders," in Science of Ceramic Chemical Processing (eds., L.L. Hench and D.R. Ulrich), Wiley and Sons, New York.

Johnson, D.W.Jr. 1987 "Innovations in Ceramic Powder Preparation," in Advances in Ceramics, Vol. 21 (eds. G.L. Messing, K.S. Mazdiyasni, J.W. McCauley and R.A. Haber), The American Ceramic Society, Columbus, OH., pp. 3-19.

Johnson, D.W.Jr., and R.K. Gallagher. 1978 "Reactive Powders Solution," in Ceramic Processing Before Firing (eds. G.Y. Onoda, Jr., and L.L. Hench), Wiley Interscience, New York.

Mackenzie, J.D. 1986 "Applications of the Sol-Gel Method: Some Aspects of Individual Processing," in Science of Ceramic Chemical Processing (eds. L.L. Hench and D.R. Ulrich), Wiley Interscience, New York.

Matejevic, E. 1987 "Colloid and Interface Aspects of Ceramic Powders," in Advances in Ceramics, Vol. 21 (eds. G.L. Messing, K.S. Mazdiyasni, J.W. McCauley and R.A. Haber), The American Ceramic Society, Columbus, OH., pp. 423-438.

Matejevic, E. 1986 "Colloid Science of Composite Systems," in Science of Ceramic Chemical Processing (eds. L.L. Hench, and D.R. Ulrich), Wiley Interscience, New York.

Matson, D.W., R.C., Petersen, and R.D. Smith 1987 "Production of Fine Powders by the Rapid Expansion of Supercritical Fluid Solutions," in Advances in Ceramics, Vol. 21 (eds. G.L. Messing, K.S. Mazdiyasni, J.W. McCauley and R.A. Haber), The American Ceramic Society, Columbus, OH., pp. 109-121.

Matson, D.W., R.C. Petersen, and R.D. Smith. 1986 "Formation of Silica Powders from the Rapid Expansion of Supercritical Solutions," Adv. Ceram. Mater. 1: 242.

Menon, V.B. 1988 "A Novel Process for the Production of Ceramic Flakes," U.S. Patent Appl. Ser. No. 07/195,649.

Perthius, H., and Ph. Columban. 1986 "Sol-Gel Routes Leading to NASICON Ceramics," Ceram. Intl., 12: 39.

Reyner, P., H. Bastius, and M. Fiedler. 1983 "The Use of Emulsions in the Preparation of Ceramic Powders," in Ceramic Powders (ed. P. Vincenzeni), Elsevier, Amsterdam, pp. 499-504.

Rijnten, J.J. 1970 in Physical and Chemical Aspects of Sorbents and Catalysts (ed. B.G. Lindsen), Academic Press, London.

Roettenbacher, R., and R. Schmidberger. 1983 "Preparation of Special Ceramics for High Temperature Applications," in Ceramic Powders (ed. P. Vincenzini), Elsevier, Amsterdam, pp. 539-546.

Ruthner, M.J. 1985 "Spray-Roasted Iron Oxides: The Nature of Minor Impurities," in Advances in Ceramics, Vol. 15 (ed. F.F.Y. Wang), The American Ceramic Society, Columbus, OH., pp. 103-107.

Sacks, M.D., T.Y. Tseng, and S.Y. Lee. 1984 "Thermal Decomposition of Spherical Hydrated Basic Aluminum Sulfate," Am. Ceram. Soc. Bull., 63: 301.

Sproson, D.W., and G.L. Messing. 1987 "Ceramic Powder Synthesis by Thermal Reaction of Atomized Solutions," in Advances in Ceramics, Vol. 21 (eds. G.L. Messing, K.S. Mazdiyasni, J.W. McCauley and R.A. Haber), The American Ceramic Society, Columbus, OH., pp. 99-109.

LIPID TUBULE MICROSTRUCTURES: FORMATION, METALLIZATION, AND APPLICATIONS

Dr. Paul Schoen
NRL
Washington, DC

ABSTRACT

The polymerizable lipid, $DC_{8,9}PC$, has been shown to form hollow, cylindrical microstructures, called tubules, whose lengths range from 10's to 100's of microns and whose diameters are about 0.4 microns. We have been investigating their mechanisms of formation, their molecular structure, techniques for controlling their growth, and for metallizing and encapsulating them in polymer matrices.

Blank

DISPERSION AND DISSEMINATION OF DRY POWDERS

M.B. (Arun) Ranade
Particle Technology, Inc.
Building 335
College Park, MD 20742

Dispersion of dry powders is often required to produce airborne obscuration smokes. The effectiveness of obscuration smoke strongly depends on the ability to separate individual primary particles in the dissemination. High aspect ratio particles of micrometer or smaller dimensions are very effective smokes for a wide wavelength coverage. Spherical submicrometer particles such as titania are also effective in visible range. These size features also make their dissemination and dispersion difficult because of high interparticle attraction resulting in their agglomeration. Dispersion of dry powders is also needed in using aerosol instruments for size analysis and also for size classification of powders in narrow size fractions.

Dry powders may contain loose agglomerates, hard aggregates and depending on particle size, shape, and other physical properties may be free flowing or cohesive. Successful dispersion of powders in air will depend on these factors as well as the energy used in the dispersion process.

Forces between solids are predominantly attractive in nature and cause adhesion of particles to each other and to surfaces. These forces become increasingly significant for fine particles since the particle mass varies to the third power of the particle size. The principle forces encountered in most particle adhesion problems arise out of molecular interactions, electrostatic interactions, mechanical interlocking, liquid bridges, double-layer repulsion and chemical bonds such as hydrogen and metallic bonds.

The tensile and shear strengths of powders are determined by interparticle forces and influence the dispersibility of powders in fluids. Dispersion in air requires separation of adhering particles from agglomerates and/or external surfaces on which the particles are collected. Fine powders dispersion in air as individual micrometer or smaller size particles is especially difficult since molecular interactions are stronger in air than in liquids, and surfactants cannot be used to create repulsion. Environmental parameters such as humidity also make dispersion difficult. Even non-hygroscopic powders of micrometer and smaller dimensions clump at relative humidities >60%.

For efficient particle dissemination two basic particle attributes must be considered: (1) particle surface composition and (2) particle size and geometry. Particle surface composition plays a major role in the adhesion between particles which in turn affects a powders dissemination characteristics. Particle hardness (deformability), chemical composition, and the chemical

composition of any liquids used to assist in the filling techniques have a profound effect on the van der Waals interactions or on any capillary bonding effects that may be present.

Ranade and Goyal (1976) studied dispersion of spherical aluminum powders in vacuum. It was shown that the dispersibility of the powder correlated well with the powder tensile strength as well as with the measured force of adhesion between aluminum spheres to plates. Effectiveness of several powder treatments were evaluated by measurement of dispersibility and tensile strengths. Flow agents such as fumed silica improved flow but not the individual particle separation. A steam treatment which increased surface hardness reduced the tensile strength of the powder and improved dispersibility.

Ranade, et al. (1984), also developed the steam treatment and another silation treatment which produced a thin layer of silica for aluminum flakes (0.2 μm thick, 1-14 μm in diameter). It was shown that the treatments retained the desired infrared absorption of the material when only a surface structure modification rather than complete conversion to hydroxide using the steam treatment. Dispersibility of the powder was significantly improved.

Dissemination of powders involves two steps: (1) delivery of the powder to the dispersion apparatus and (2) dispersion and entrainment in an air stream.

Delivery of powders to the dispersion device suffers from all the problems associated with powder flow. A metered powder may be dispersed and agglomerates broken up by using the energy of a turbulent air jet, or by impacting the particles on a solid surface or by collisions between fluidized bed particles. The resulting aerosol may possess appreciable electrical charge created by particle collisions with each other and the hardware. Such charges are strongly dependent on environmental variables such as humidity and specific powder and construction materials. Charge neutralizers may be needed to ensure reproducible dispersions.

DISPERSION HARDWARE

Ejectors using compressed air can be used to entrain powder particles which are subjected to mixing with high speed jets. Successful dispersion results if the energy in the jets is adequate to overcome interparticle forces. Sonic and sub-sonic jets are used. The sub-sonic jets are usually effective for non-cohesive powders and sonic velocities are necessary for cohesive powders. The powder delivery to the jet is by aspiration from a container or a fluid bed. These devices can be used on a continuous basis with the help of a rotary turntable or a moving rack on which the particles may be packed in grooves and cavities.

A typical fluidized bed dispersion device requires higher air flow rates to achieve better dispersion, but an upper limit for the flow rate is set by the onset of air entrainment of the dispersion aids in the effluent stream. Large beads (100-200 micrometers) are often used to achieve a stable fluidized bed and to break up agglomerates. Mechanical vibrations to a mixer or fluidized bed may help in improving dispersion. An ultrasonic vibrating generator is one such variation. The powder is placed on a cylinder which is vibrated in an ultrasonic bath (frequency around 50 KHz) filled with water. Compressed air flows through the bed of particles which may additionally be mechanically vibrated. The performance of a vibrating bed generator is governed by factors such as the amplitude and frequency of the mechanical vibrations, particle size, number concentration and shape. Fluidized bed generators are subject to very high levels of electrical charges caused by the multiple collisions and use of charge neutralizers is essential.

The NBS dust generator carries the powder through the spaces between the teeth of a metering gear. The powder is sucked up from between the teeth by a compressed air ejector which is positioned diagonally to extract the powder. An impactor plate at the ejector removes any large agglomerates. The NBS generator can achieve high output concentrations.

Batch dispersion of powders can also be achieved on a small scale using a shock wave. The shock wave is generated by the rupture of a diaphragm separating a high pressure region from a low pressure region. Since extremely high shock speeds can be achieved, dispersion efficiencies are also higher than most other methods.

Conditioning of the dispersed dust may be necessary to remove large agglomerates not broken by the dispersion process. An inertial separator such as a cyclone or an impactor may be used to cut off the size of the dust at a required upper size. An accumulation chamber may be used to remove large particles by gravity settling and to smooth out concentration and pressure fluctuations.

If the dispersion process produces highly charged aerosols neutralization may be achieved using a bipolar ion generator using an AC corona or a radioactive source such as Kr-85.

REFERENCES

Ranade, M.B. and A. Goyal, "Research on Coatings or Surface Treatment of Metal Powders," Final Technical Report, RADC-TR-76-355, 1976.

Blank

SECTION III: SAMPLING AND MEASUREMENT OF AIRBORNE PARTICLES

Blank

AEROSOL SAMPLING AND MEASUREMENT

James W. Gentry
University of Maryland
College Park, MD

Arguably the majority of instruments used to measure the aerosol size distribution are based upon aerodynamic classification. These instruments incorporate one of three mechanisms -- the persistence of particle inertia relative to the carrier gas is exploited, the steady-state velocity in an electrical or gravitational field is utilized, or the average behavior of the particles undergoing stochastic fluctuations in position or velocity is exploited. Each of these mechanisms is characterized by a different dimensionless parameter and each serves as the basis for specific instrumentation. As a first approximation they can be assumed to cover different size ranges with the largest particles classified by inertial mechanisms and the smallest particles determined from measurements of the diffusion coefficient. There is considerable overlap among the mechanisms for the different size ranges.

In selection of the appropriate instrument several criteria must be considered. These include the methodology for particle measurement (is the mass or the particle number measured?; are single particles or an averaged variable measured?; is the measurement on-line or at ambient conditions?), the procedures used for data analysis, and the morphology of the particles.

By far the most widely used inertial classifier is the sequential-stage cascade impactor. In this instrument the particle stream passes through a sequence of 6-8 successive stages. In each stage the direction of the flow stream is altered by 90 degrees due to the presence of a blocking surface. Particles with sufficient inertia are unable to follow the stream impact on the surface and are collected. The collection efficiency for these instruments can be characterized by the Stokes Number, a dimensionless parameter which is the ratio of the kinetic energy to the work necessary to overcome the drag resistance. Such instruments operate most effectively with larger particles (Dp > 2 m) and the measurements are based on an integral rather than individual particles. Most often the size is determined from gravimetric measurements of the mass collected on a stage. The mass may be determined by weight or less frequently by using a radioactively labeled aerosol. Such devices usually have a sharp separation around Stk = 0.25 and are operated as four or more stages in sequence. In recent years the cut-off size has been extended to smaller sizes by utilizing the increase in mobility which occurs when the mean free path of the carrier gas increases at low pressures. At these lower pressures there is an increased complexity in collection mechanisms. A second difficulty can arise for solid particles where there is bounce and eventual reentrainment. This is a more serious problem for larger particles. Generally the behavior of non-spherical particles is

not known, as their alignment in the flow field results in substantially different behavior than for isometric particles. Several different geometries of inertial impactors have been suggested including those of Casella, Anderson, May, Mercer, and Berner. However the behavior of each of the instruments are substantially the same.

Several other instrument designs have been based on the principle of the inertial impactor. These include the virtual impactor where the particles are decelerated by a dead space rather than a collecting surface and the Prodi inertial spectrometer where the particle stream is introduced parallel to the collection surface rather than perpendicular as in most inertial impactors. The latter shows a sharp separation and is especially suitable for electron microscopy. A second approach is a single particle counter based on the deceleration of a particle as it emits from a jet. Calibration has proved a problem for non-spherical particles and even large spherical particles where there is some deformation in the flow field. These instruments have been designed to overcome perceived complexities such as reentrainment, averaging over diverse shapes, comparatively broad size classes per instrument, and working with volatile particles. The key features of such instruments are the sharp separations and a robustness in the instrument so that it can be used in hostile and corrosive environments. In general it can not be used in-line.

The second mechanism for particle collection is based upon the mobility in a constant field such as elutriators (gravity), cyclones (radial acceleration) and electrostatic precipitators (electrical fields). These instruments usually are operated under conditions where the time required to reach equilibrium velocities are short compared to the residence times in the instrument. Compared to the inertial collectors the forces acting on non-spherical particles are better defined and more uniform. It is much easier to compare theoretical collections with experimental collections for particles in such collectors where there is less uncertainty in the description of the force field and the collection mechanisms are better understood. Usually bounce or reentrainment is not a problem. Disadvantages of such instrumentation are that the particles collected are not always available for microscopical analysis, the separation is not so sharp as for inertial devices, and in the case of electrical precipitators there are ambiguities imposed by multiple charging of the particles. Each instrument has its own dimensionless parameter. Typically particle collection is in the 0.2 to 2.0 micron range.

The most widely used of these classifiers are the cyclones and electrostatic precipitators which are used commercially for gas cleaning. These instruments can be scaled comparatively easily for large-scale particle collection and classification. When used for measuring aerosols, in the most common applications the fractional penetration -- the ratio of concentrations after to

before the collector are measured. The concentrations are determined either with single particle counters, from the total nuclei present, or the total electrostatic charge on the particles. Although mini-cyclones have been used directly to determine the charge distribution, most commonly they are used as the first stage in a measurement assembly. The larger particles are removed in the cyclone. Typically the particles collected in a cyclone are not available for microscopy. An important exception are spiral centrifuges (as the Goetz, Stoeber, and Vienna centrifuges) where the particles are sized by comparison with a calibration curve based on spherical particles. These instruments and elutriators (actually sedimentation chambers) have proven to be especially successful in determining the aerodynamic properties of non-spherical particles. Such instruments have the sensitivity to determine the Cunningham-Stokes correction factor from penetration measurements alone.

The most widely used of these instruments for aerosol measurements are based upon the principle of electrical mobility. In one instrument, the electrical aerosol analyzer, the aerosol is passed through a corona discharge. The particles are then passed through a variable-voltage electrostatic precipitator and collected in a Faraday cup. The total charge is then measured. The data consist of the charge as a fraction of voltage and as a consequence size. The voltages in the precipitation stage are varied according to a prearranged program. Aerosols with particles in the size range of 0.01 to 1.0 microns are measured, although there is substantial uncertainty for the smaller particle size range. The behavior of non-spherical particles depends on both the rate of diffusional charging and the mobility or drag resistance of the particles, both of which are uncertain. An instrument working on a similar principle is the differential mobility classifier. In this case the charging is from a radioactive isotope, and electrostatic forces are used to remove a narrow mobility window. This instrument works best in the 5-50 nanometer range. Multiple charging of the larger particles result in a polydisperse distribution. This instrument produces a monodisperse aerosol from a polydisperse cloud subject to the restrictions mentioned above. However there is a substantial reduction in the concentration of aerosol from 1000:1.

Both electrostatic and thermal precipitation have been used for collection of particles for microscopy. Generally the samples collected are small and sampling must take place over a relatively long time period. Thermal precipitation which is a relatively weak force is independent of the size (as a first approximation) and thus gives a representative distribution.

The last of the classes of measurement instruments described here is based on the behavior in a stochastic or random field. This is almost always due to thermal or Brownian diffusion. It can be characterized by a dimensionless parameter, the Peclet Number, which can be regarded as proportional to the diffusion coefficient divided by the product of velocity and a geometric

dimension of the collector (usually the length divided by the cross-sectional area). Such collectors are very insensitive to larger particles and are useful only for particles below 0.1 microns. However, a well designed instrument in the suitable size range can be very precise in the nanometer range being able to detect changes in the size of particles of less than one monolayer. The aerosol collected by this mechanism is not available for microscopy or other non-destructive testing. Particles of the size range used by this instrument are sufficiently small that they can not be normally detected by single particle counters. Almost always particles are detected using condensation nuclei counters in which vapor (alcohol or water) condenses on an otherwise undetectable nuclei. The droplets grow to a detectable size (about 2 microns) and the total light scattered is proportional to the number of nuclei. The minimum detection size of the nuclei depend on both the properties of the nuclei counter (expansion ratio, condensation fluid) but also on the composition of the nuclei.

The advantage of instruments based on the stochastic behavior of the particles are that measurements can be made on very small particles which are otherwise undetectable. The theoretical interpretation of the experimental measurements is less ambiguous than in the other two cases. Furthermore, diffusion coefficients can be measured unambiguously for non-spherical particles. The disadvantages are that the particles are not collected for microscopy or further analysis and the separation curves are broad especially for larger particles.

To summarize, instruments have been designed to exploit aerodynamic classification to measure the size and size distribution of aerosols. The criteria for selection of the appropriate instrument depends primarily on the size range of interest. It is convenient to classify the instruments as based on inertial effects, the mobility of a constant force field, and the stochastic behavior of the particles due to thermal motions. A number of instruments have been designed for special applications but as a first approximation, the inertial devices are most effective for large particles and have a sharp separation while instruments based on diffusion are for small particles and have a broad separation curve. Those instruments using a constant force field are intermediate in both the sharpness of separation and the size range. On the other hand, they are most frequently used for classification in industrial-scale operations and in the collection of particles for microscopy.

AEROSOL SAMPLING STUDIES

A.R. McFarland, W.D. Turner, C.A. Ortiz, N.K. Anand, M.G. Glass, R.E. DeOtte, Jr., S. Somasundaram and D.L. O'Neal. Department of Mechanical Engineering, Texas A&M University, College Station, TX 77843.

ABSTRACT

A study has been conducted to develop design criteria for the sampling of aerosols from the ventilation air of a nuclear storage pilot plant, the WIPP site. Tests were conducted with models of the exhaust ducting to determine the minimum length of straight ducting which would provide a suitable location for single point sampling. For the duct configuration recommended for the post-HEPA filter location, the velocity and concentration profiles were fully developed at a distance of 11.5 diameters from the duct entrance.

A new type of sampling probe was developed which offers advantages over isokinetic probes in situations where it is desired to continuously monitor aerosol concentration. The device consists of an aerodynamic shroud that is placed concentrically about the actual sampling probe. The shroud decelerates the aerosol stream prior to the stream being sampled by the probe. Wind tunnel tests show the concentration ratio of the shrouded probe to be 0.93 to 1.11 for 10 μm aerodynamic diameter particles over the range of wind speeds of 400 to 2700 ft/min with the probe operated at a fixed flow rate of 6 cfm.

The loss of aerosol particles in transport systems has been modeled and an empirical expression has been developed to permit calculation of the diameter of a horizontal tube which permits maximum penetration of aerosol.

Potentially radioactive aerosols are collected by devices known as CAM samplers. The CAM samplers purchased for the WIPP-site originally had internal wall losses of 76% of 10 μm particles. After a re-design of the internal elements of the sampler, the losses were reduced to 14%.

INTRODUCTION

The U.S. Department of Energy is currently constructing a pilot plant storage site for low level nuclear wastes at Carlsbad, NM. The facility, called the WIPP-site, consists of a region mined in a salt stratum at a depth of 2100 ft below ground level. During the next 25 years, while storage tests are being conducted, the storage region will be provided with ventilation air at a flow rate of 420,000 cfm. The exhaust air will be discharged from the storage region through a 14 ft diameter shaft and, at the surface, the exhaust air will normally be vented to the atmosphere through induced draft fans. If an emergency condition were to develop, where radioactive

particulate matter were to be present in the exhaust air, the 420,000 cfm flow rate of ventilation air would be reduced to 60,000 cfm and the flow stream would be diverted through HEPA filters prior to being discharged to the atmosphere. An emergency situation would be put into effect by a signal from a continuous air monitor (CAM) aerosol sampler located either in the storage region or in the exhaust ducting. A large number of CAM samplers will be placed at strategic locations in the storage region and many of these samplers will have transport tubes connecting the sampler with the local environment from which the sample is to be collected. As a design goal, the penetration of aerosol through the tubing should be maximized.

There are two sampling stations in the exhaust ducting system -- one is located at the ground-level elevation of the 14-ft duct just upstream of an elbow. The second location is in exhaust duct leading from the HEPA filters. The samplers in the 14-ft duct are intended to provide an alarm in case of an inadvertent release of radioactivity and to monitor the dose to which the underground areas and the HEPA filters would be exposed. The samplers located in the post-HEPA ducting are intended to monitor the release of radioactivity to the atmosphere in an emergency situation.

RESULTS AND DISCUSSION

1. Modeling of Ductwork.

In the prototype of the post-HEPA ducting, a flow rate of 60,000 cfm will be drawn from the HEPA filters through an induced draft fan and thence through a length of horizontal ducting before being discharged to the atmosphere. It is desired that the length of horizontal ducting be sufficient to allow the velocity and concentration profiles to become fully developed. This length of ducting was determined through tests with model ducts. There is some controversy in the literature relative to the scaling the entrance lengths in turbulent flow. For example AMCA (1) suggests that a model and prototype will have similar flow patterns if the two are operated at the same velocity. Others, e.g., Parker et al. (2), relate the entrance distance to the duct Reynolds number, and still others claim there to be fixed range of dimensionless distances, L/D, required for the flow in the model or prototype to become fully developed regardless of Reynolds number or velocity (3). Here L is the distance from the duct entrance (from the fan discharge location in the post-HEPA filter duct at the WIPP-site) and D is the duct diameter. Because of the controversy, we did the scaling based upon both equal velocity and nearly-equal Reynolds numbers between model and prototype.

The typical velocity profile development at the post-HEPA location is illustrated in Figure 1. The data show the profiles from a location 1.0 duct diameters downstream from a fan discharge to a location that is 11.5 diameters downstream from

the fan. It may be noted that at the 1.0 diameter location there is backflow while at the 11.5 diameter location the profile is fully developed. These test data were for a situation in which the model and prototype velocities were matched. When the Reynolds numbers of the model and prototype were matched, the velocity profiles were also fully developed at the 11.5 diameter location.

Concentration profiles at a distance of 12 diameters downstream from the duct entrance are shown in Figure 2. Experimentally, 10 μm aerodynamic diameter particles were introduced at the side wall of the duct at the entrance section. Samples of the aerosol were collected on a filter rake at the 12 diameter location. It may be noted the concentration profile is well developed.

Based upon the results of this work, a 10-ft diameter duct was constructed at the WIPP-site. The sampling location is placed at a distance of 11.5 diameter from the entrance.

Modeling work was also done to determine the location of the sampling points in the 14-ft exhaust duct that leads from the underground storage area to the surface. Test results showed the velocity profile was acceptable (within $\pm$10% of a symmetrical fully developed profile) at an upstream distance of 1.5 diameters from the elbow at the surface location.

2. Shrouded Aerosol Sampling Probe. The use of a shroud about an aerosol sampling probe tends to reduce the internal wall losses in the probe. The shrouded probe which we developed, Figure 3, is designed to sample at a rate of 6 cfm through a 1.18-inch diameter probe. The shroud is 4-inches in diameter and causes a 40% reduction in the free stream velocity. With reference to Figure 4, the concentration ratio of the shrouded probe is compared with that of an isokinetic probe for a particle size of 10 μm aerodynamic diameter and a sampling rate of 6 cfm. Here, the concentration ratio is the concentration of aerosol which penetrates through the probe divided by the free stream aerosol concentration. The experimental data were collected using an oil droplet aerosol for which the attachment coefficient should be unity, i.e. the particles would adhere to any surface with which they might come in contact. It may be noted the concentration ratio of the shrouded probe varies only from 0.93 to 1.11 over the velocity range of 400 to 2700 ft/min while that of the isokinetic probe varies from unity to 0.61 over the same range of air speeds. Wall losses in the isokinetic probe account for the limitations of that device. Where continuous monitoring is needed, the shrouded probe has a distinct advantage over a typical isokinetic probe.

3. Gravitational and Turbulent Deposition of Aerosols in Tubes. A model was developed to combine gravitational and turbulent depositional effects and the model was numerically evaluated for a variety of physical situations. In this model, we used the equations of Agarwal (4) to calculate turbulent depositional

velocities and combined that velocity with the gravitational depositional velocity through use a special constraint. One of the results of this study was the development of an expression for determining the optimal size of tubing for transporting aerosol particles of a given size at a given flow rate through horizontal tubing. With reference to Figure 5, the penetration of 10 μm diameter aerosol particles for a flow rate of 2 cfm is plotted as a function of tube diameter. For tubes that are smaller than the optimal diameter, the penetration drops dramatically with decreasing tube size due to increased turbulent deposition. On the other hand, for tubes larger than the optimal size there is a gradual decrease in penetration with increasing size due to increased gravitational deposition. Based upon a regression of the data such as those shown in Figure 5, we developed an expression for the optimal diameter of horizontal tubes, namely:

$$D_{opt} = 1.75Q^{0.47} D_a^{0.21}$$

where D_{opt} is the optimal tube diameter (mm), Q is the flow rate (L/min), and D_a is the aerodynamic particle diameter (μm). Because of the steep drop in penetration for tube sizes smaller than the optimal size, for most applications it is recommended the actual tube diameter be selected to be somewhat larger than the optimal size.

These results have been incorporated into a workbook for calculating particle losses in sampling systems where the overall system may include inlet anisokinetic effects, losses in horizontal, inclined and vertical tubes and losses in bends (5).

4. Redesign of CAM Samplers. The CAM samplers that were purchased for the WIPP-site consisted of a radioactive detector placed in close proximity (~1/4-inch) to an aerosol collection filter. The detector tube and filter are approximately the same diameter. A flow rate of 2 cfm is drawn into the CAM sampler through a 0.62-inch diameter tube, however the tube is flattened to a rectangle of approximately 0.13 inches x 0.62 inches at the entrance to the chamber which contains the filter and detector tube. Ideally, the flow would pass from the entrance tube and then into the gap between the filter and detector. Decay of radioactive materials collected on the filter would be continuously monitored with the detector. Tests with 10 μm diameter aerosol particles showed 76% of particles introduced into the 0.62-inch diameter tube were inadvertently deposited on the internal walls of the sampler rather than collected by the filter. We redesigned the flow chamber that surrounds the detector tube and filter and eliminated the flattened entry tube. In addition we were able to reduce the spacing between the filter and detector tube to 0.20-inches (from the standpoint of nuclear counting efficiency, it is desirable to have the two elements as close as practical). The redesigned sampler showed internal wall losses of 14%.

ACKNOWLEDGMENT

Funding for this research was provided by the U.S. Department of Energy, WIPP Project Office under Contract DE-AC04-86AL31950 to Westinghouse Waste Isolation Division. Westinghouse, in turn, funded us under Subcontract No. 94-WLM-26907-SD. We wish to thank Mr. Kevin J. Shenk of Westinghouse for his helpful suggestions during the course of this work.

REFERENCES

1. Air Movement and Control Association, Inc. (AMCA). Fan Application Manual - Fan and Systems. AMCA Publication 201. AMCA, Arlington Heights, IL. (1985).

2. Parker, J.D., J.H. Boggs and E.F. Blick. Introduction to Fluid Mechanics and Heat Transfer. Addison-Wesly Publishing Co., Inc., Reading, MA. (1969).

3. Incropera, F.P. and D.P. DeWitt. Fundamentals of Heat and Mass Transfer. Second Ed. John Wily and Sons, New York. (1985).

4. Agarwal, J.K. Aerosol Sampling and Transport. Ph.D. Thesis. University of Minnesota, Minneapolis. (1983).

5. Anand, N.K. and A.R. McFarland. Particle Penetration through CAM-Sampler Aerosol Transport Lines. Report No. 5897/01/01/88/NKA, Aerosol Technology Laboratory, Department of Mechanical Engineering, Texas A&M University, College Station, TX. (1988).

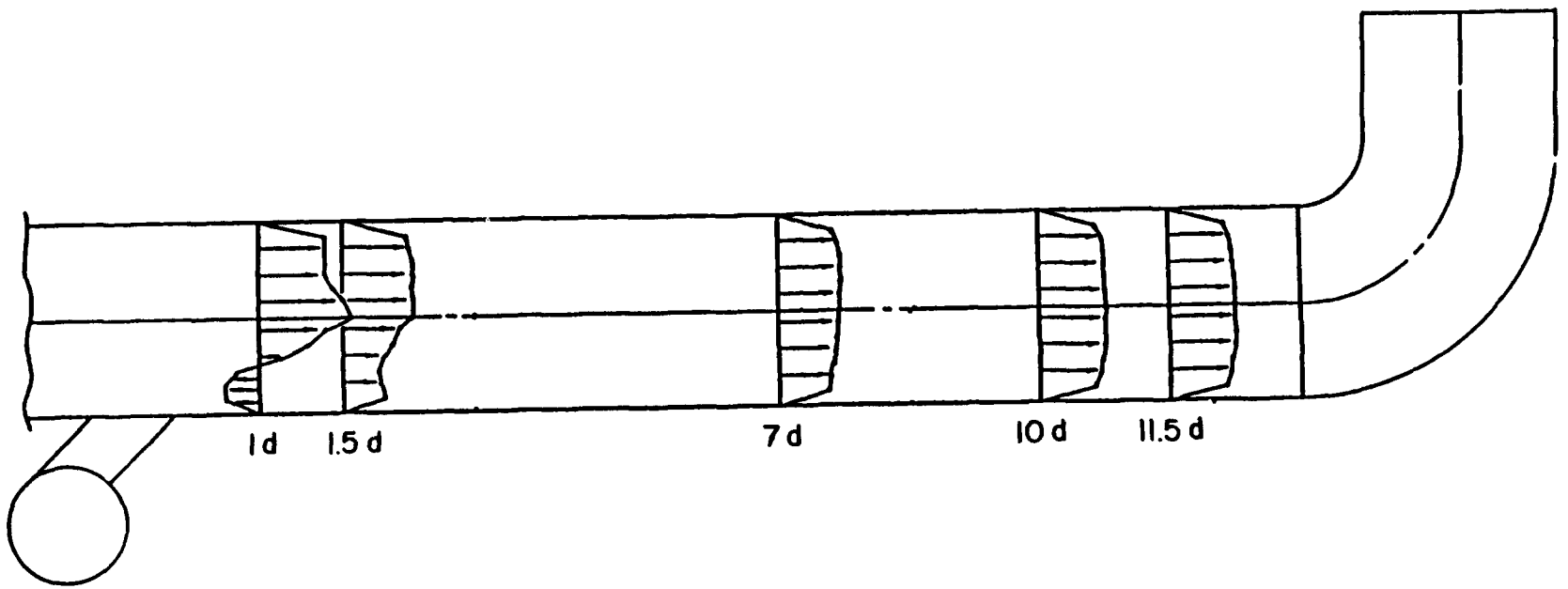

FIGURE 1. Development of velocity profiles in a model duct. Values given below duct are downstream distances in units of duct diameters. Air velocity = 2200 ft/min. Duct diameter = 14 inches.

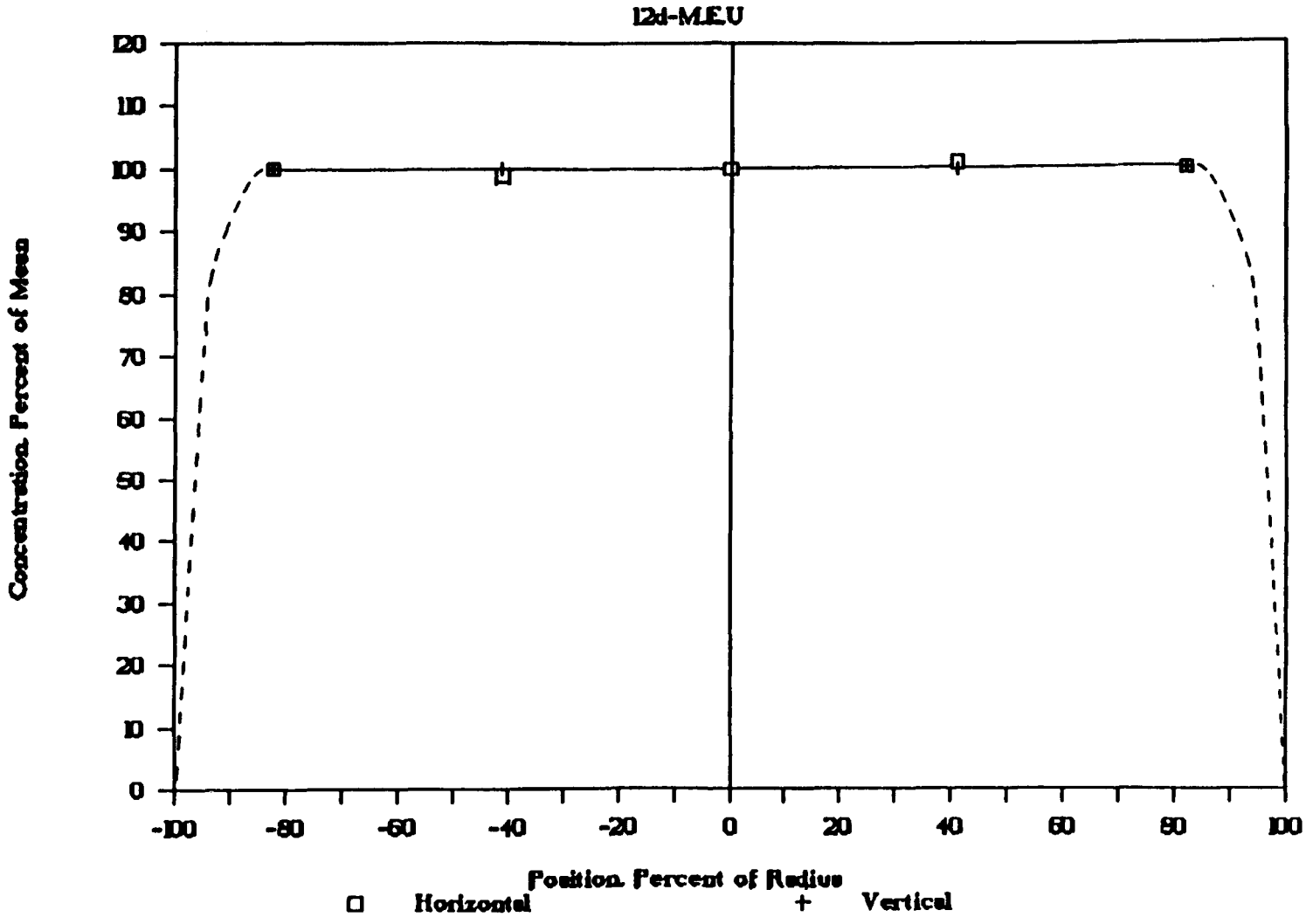

FIGURE 2. Concentration profile at a distance of 12 diameters from the entrance section of a model duct. Air velocity = 2200 ft/min. Duct diameter = 34 inches.

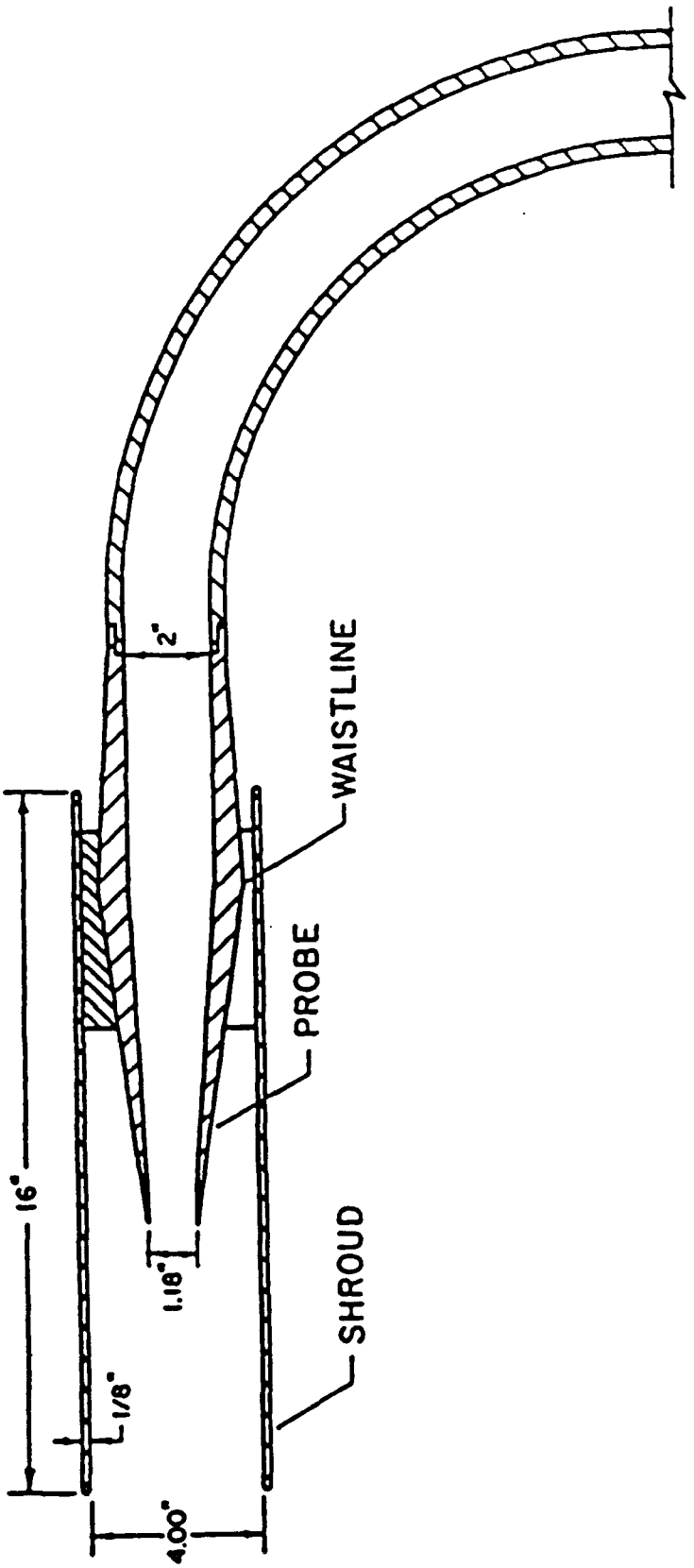

FIGURE 3. Shrouded probe aerosol sampler.

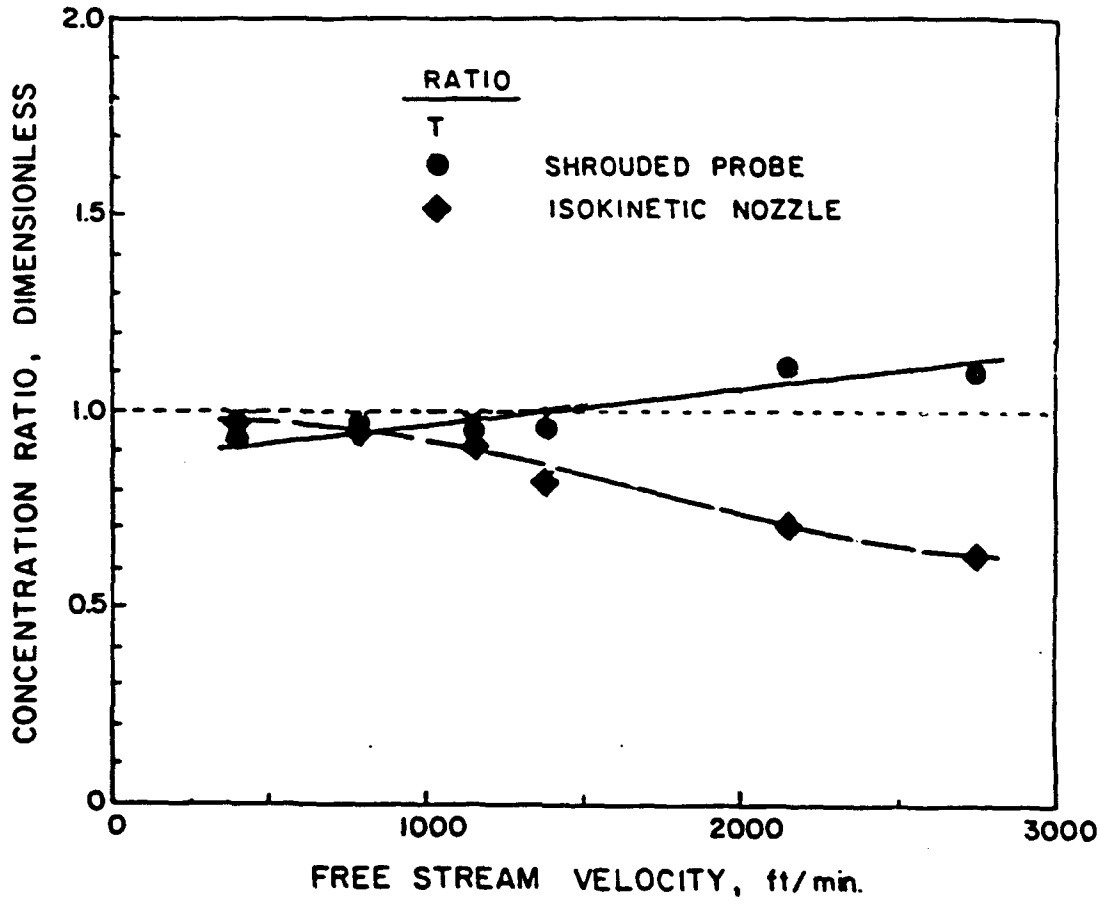

FIGURE 4. A comparison of concentration ratios determined with the shrouded probe and with isokinetic probes. Aerodynamic particle diameter = 10 μm. Sampling rate = 6 cfm.

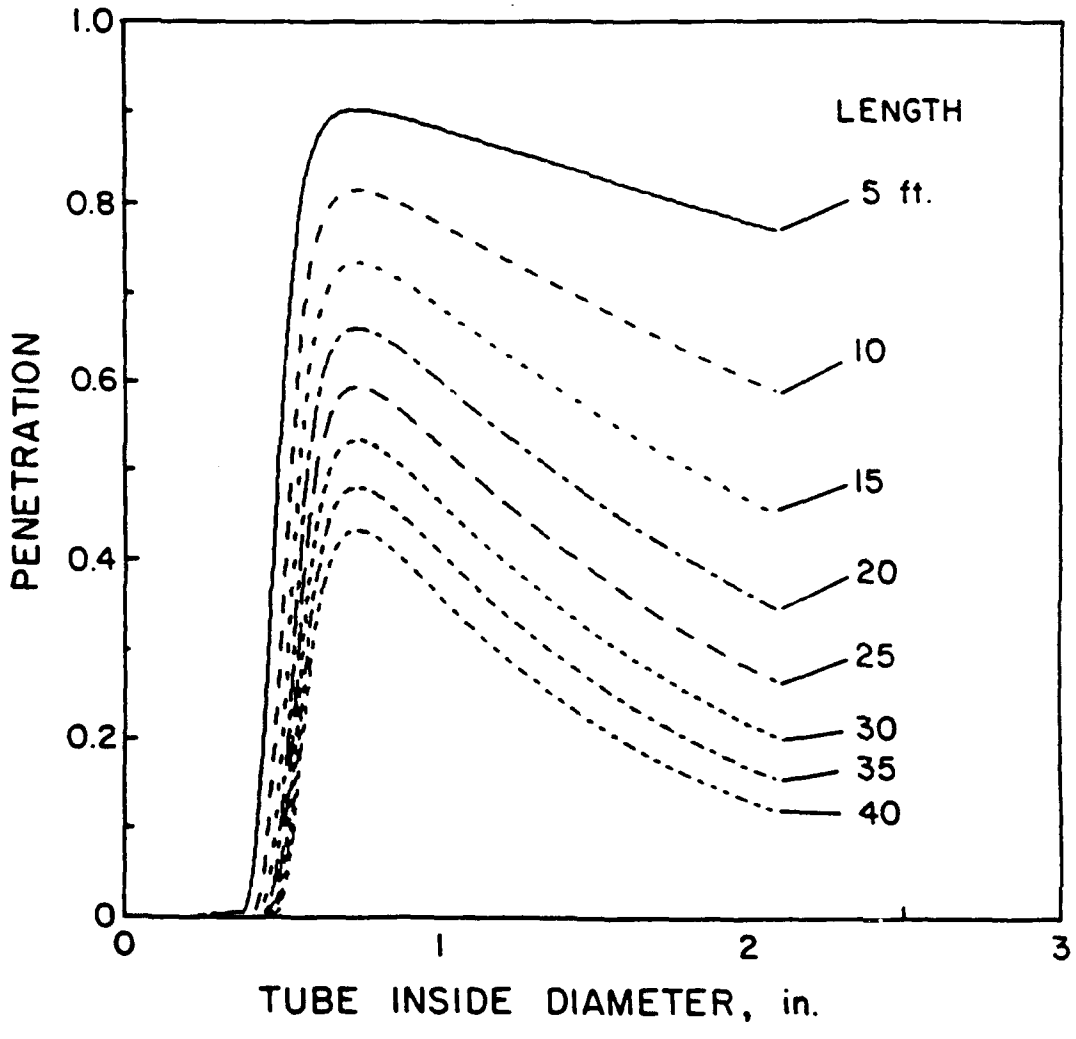

FIGURE 5. Penetration of aerosol particles through horizontal tubes with circular cross sections. Aerodynamic particle diameter = 10 μm.

Optical Properties of Smoke Agglomerates

George Mulholland, Nelson Bryner, and Raymond Mountain
National Institute of Standards and Technology
Gaithersburg, Md 20899

Light scattering has recently been used to determine the fractal dimension, d_f, of clusters of particles formed into agglomerates. The usefulness of the fractal dimension is that it makes it possible to concisely characterize a set of statistically similar, but geometrically irregular objects. Here we present results on the scattering properties of agglomerates grown via computer simulation and also report preliminary experimental results on the optical properties of "fresh" and cloud processed smoke.

Theory

The agglomerates are generated using a simulation method which mimics the process of agglomeration which occurs when diffusing primary particles stick together forming an irregular mass. We begin a simulation by distributing 4,000 primary particles at random positions in a cubic box which is subject to periodic boundary conditions. The diffusive motion of a particle of mass m is described by the Langevin equation. The diffusive motion of the particle is supplemented by the condition that if any two primary particles touch, they stick forming a larger, rigid cluster. This cluster continues to diffuse according to the Langevin equation but with a changed mass. This process continues until clusters ranging in size from 10 - 700 primary units are formed. This growth process is known in the fractal literature as cluster-cluster aggregation.

Once the set of agglomerates has been generated, the V-V scattering intensity is calculated using the Rayleigh-Debye theory in which each primary particle acts as a dipole source for scattered radiation. It is the difference in phase of the light scattered from the separate primary particles that determines the overall scattered field. The scattering cross section, σ, is obtained as

$$\sigma = C \left|\Sigma \exp(i\mathbf{q}\cdot\mathbf{r}_j)\right|^2 = C\, S(\mathbf{q}),$$

where $S(\mathbf{q})$ is the structure factor of the cluster and the coefficient C is a function of the wavelength of light and the polarizability of the primary particle. The quantity $\mathbf{q}$ is the standard momentum transfer vector with magnitude given by $|\mathbf{q}| = (4\pi/\lambda)\sin(\theta/2)$, where λ is the wavelength and θ the scattering angle.

The orientation averaged structure factor is defined as I(q). The entire set of I(q) curves for 48 clusters ranging in size from 10 - 700 primary particles can be correlated when the results are plotted as $I(q)/N^2$ vs $R_g q$, as illustrated in Fig. 1. The quantity N refers to the number of primary particles in the cluster and R_g is the radius of gyration of the cluster.

The scaling property of these light scattering results indicates that the pair distribution function for the clusters should be a function of r/R_g, where r is the distance between a pair of primary particles. That is because the

intensity and this function are Fourier transform pairs. That R_ξ is the proper length scale is illustrated in Fig. 2 where the pair distribution functions, $G(r/R_\xi)$, for the set of 48 clusters are plotted in Fig. 2.

Experiment

To provide data for testing theories of the optics of fractal clusters and for use in assessing the potential climatic impact of smoke produced by nuclear weapons initiated mass fires, we have measured the extinction, scattering, and absorption coefficient of "fresh" acetylene smoke and for cloud processed acetylene smoke. A transmission cell-reciprocal nephelometer similar to Gerber's (1982) design was used to measure simultaneously the extinction and total scattering coefficient of the smoke. The absorption coefficient was obtained by subtracting the scattering coefficient from the extinction coefficient.

The smoke was produced by burning acetylene in a laminar diffusion burner. The cloud processing of the smoke was performed in a 9 liter scaled-up version of the Pollak expansion cloud chamber at an over pressure of 160 mm Hg. A sudden expansion produced a cloud of water droplets with the smoke particles acting as nuclei. The droplets were evaporated, and the "processed" smoke was passed into the 9 liter optical cell. The light transmission through the cell, the total scattering, both at λ=633 nm, and the mass concentration of the smoke were measured simultaneously as the cloud processed smoke moved through the cell.

The cloud processed smoke is observed by electron microscopy to be more compact than the "fresh" smoke. The specific scattering cross section, σ_s, of the cloud processed smoke is almost twice as large as that for the fresh smoke, while the specific absorption cross section, σ_a, is not affected by the cloud processing. Both of these results are consistent with the Berry-Percival optical theory for fractal clusters based on an estimated cluster size of about 400 primary particles, each with a diameter of 35 nm.

It is predicted that for cluster with 10,000 or more primary particles, the absorption and scattering coefficient of the cloud processed soot would be a factor of two less than that for the "fresh" smoke. The implication of this effect on the global climatic impact of mass fires initiated by a major nuclear is a topic of much interest.

We would like to acknowledge C.F. Rogers, J.G. Hudson, and J. Hallett from Desert Research institute, Reno, for constructing the expansion chamber and assisting in the experiment.

Gerber, H.E., Light Absorption by Aerosol Particles, ed. by H.E. Gerber and E.E. Hindman, Spectrum Press, Hampton Virginia, 231-241, (1982).

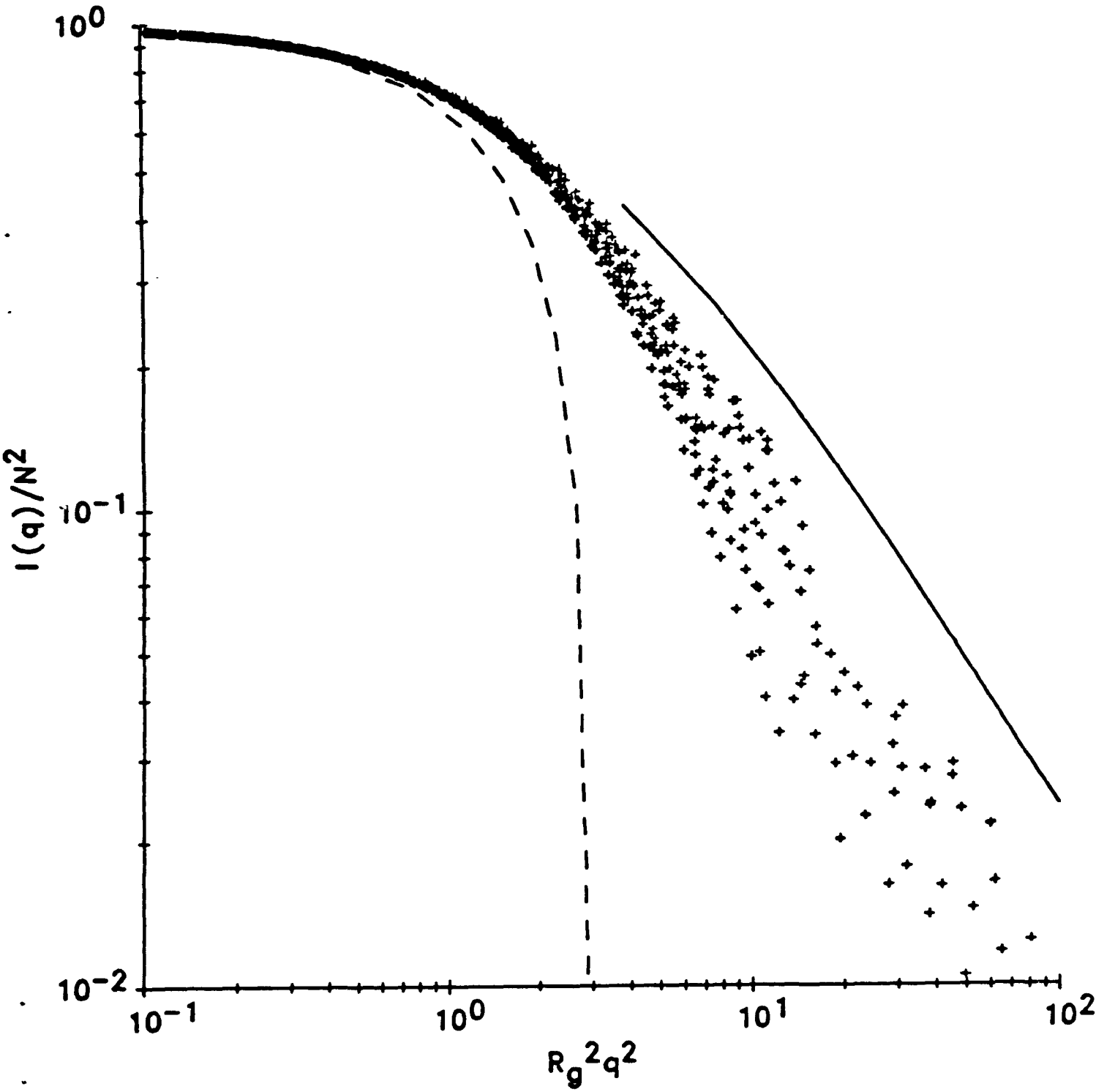

Fig. 1. The scaled V-V intensity of the scattered light for the 48 agglomerates. In each case, the calculated value of the radius of gyration, R_g, was used to determine $R_g q$. The Fisher-Burford form based on an exponential cutoff function is represented by the solid line, and the hard sphere type cutoff function suggested by Hurd and Flower is indicated by the dashed line.

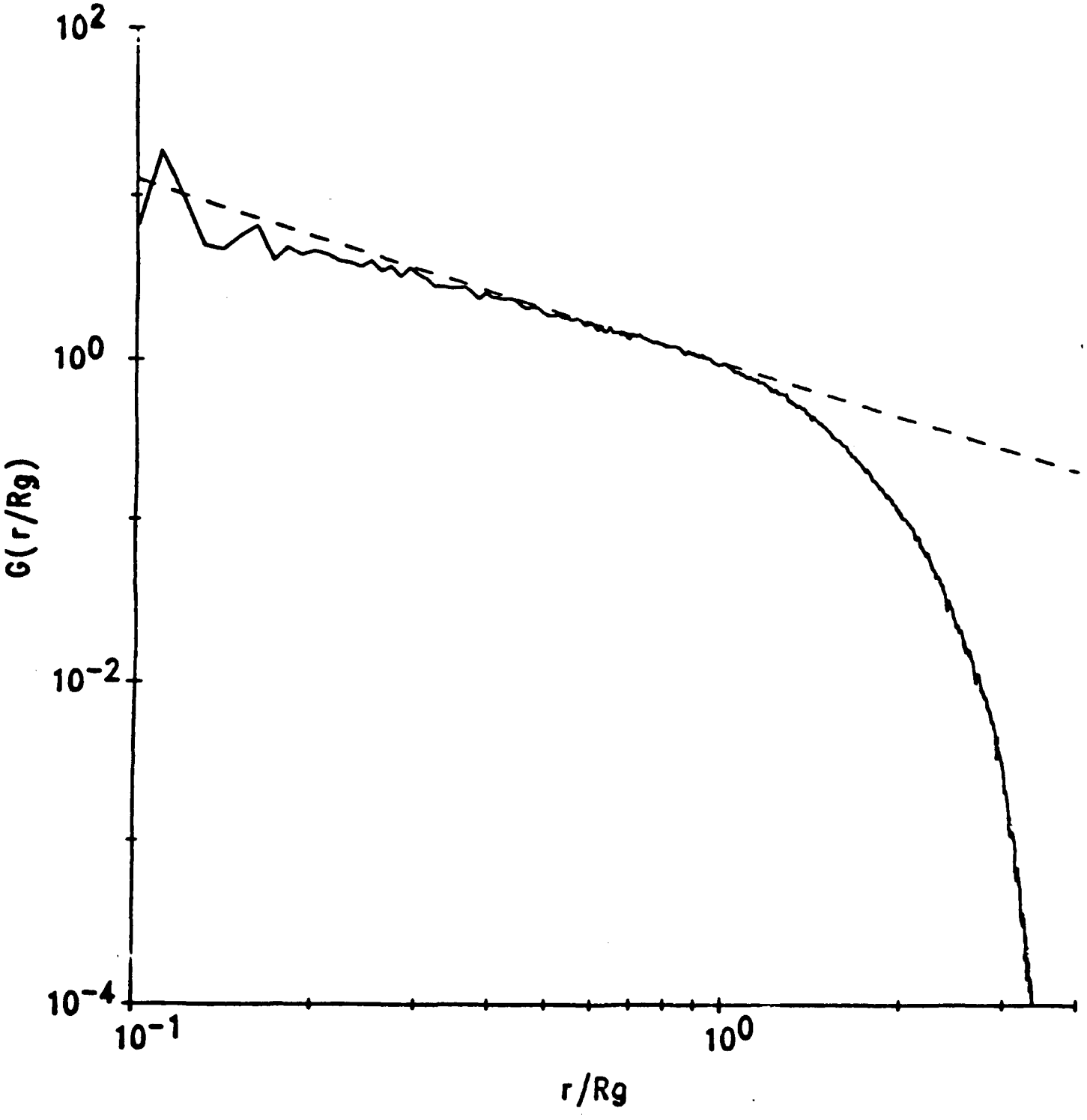

Fig. 2. The distribution of pairs, $G(r/R_g)$ is a scaled function of r/R_g. The dashed line is the result for a fractal of infinite extent with fractal dimension equal 1.9.

AEROSOL MASS CONCENTRATION MEASUREMENTS BY X-RAY FLUORESCENCE

George M. Thomson
U.S. Army Ballistic Research Laboratory
Aberdeen Proving Ground, Maryland 21005

ABSTRACT

The Ballistic Research Laboratory has developed two devices for measuring the mass concentration of aerosols containing elements having atomic number Z > 24 appearing as droplets or particles. While the two devices differ in details and in the densities of the aerosols they address, both operate on the same principle - x-ray fluorescence (XRF). In XRF one bombards the particles with x-rays of known energy. These primary x-rays ionize the inner shells of any atoms they encounter, and sometimes cause these atoms to fluoresce; that is, to emit x-rays of their own at lower energies characteristic of their species. If the atomic number Z of the atom is large enough, the fluorescent x-rays can be detected. Their abundance reveals the concentration of the aerosol and their energy its elemental identity.

The first device is intended for aerosols with low mass concentrations. Prior to irradiation it separates out the particles by pumping the aerosol at a known adjustable rate (0 - 0.1 cubic meters/min) through a section of a tape made of filter paper. Motion of the tape is incremented so that each section filters the airstream for a fixed period of time. As the tape advances, new sections intercept the airstream while exposed sections move before an annular 25 mci Cd-109 radioactive source. Here the trapped particles are bombarded with 22 keV x-rays. Those resulting fluorescent x-rays emitted axially to the source annulus pass through its central opening and onto a gas proportional counter. When this occurs, the counter generates an electrical charge pulse proportional to the energy of each impinging fluorescent x-ray photon. Digital circuitry then ascertains the number of photons at each energy detected in the counting/pumping period - raw data that reveals the abundance of each individual qualifying element in the aerosol simultaneously. Note that the x-ray method is independent of the state of chemical combination of the target product and it can sense one, two, or more elements simultaneously.

The device has been tested and calibrated for over a dozen elements. A summary of its response to some elements often the subject of worker safety concerns are listed in Table 1. The response is measured in terms of the minimum level at which the mass concentration can be determined with 10% accuracy in the time cited. The left-hand column shows values of the currently accepted threshold limited values for permitted 40 hr week worker exposure.

During development of the first detector, it was realized that the extremely high sensitivity of XRF held promise for eliminating a long-standing problem in dense metal aerosol work - the necessity of having to extract particles out of the air prior to assessment in a fashion which gives samples that are truly representative of the aerosol. Accordingly we have designed XRF system that operates directly on the aerosol as dispersed, and provide non-invasive concentration measurements rapidly, simply and reliably for most materials with atomic number above 24.

The direct system uses a thermionic x-ray tube in place of a radioisotope to ionize the target. In operation, a flux of x-rays produced by the tube is sent directly out into the aerosol. Some of the x-rays impact upon the metal particles, ionizing them and inducing fluorescence. The characteristic, fluorescent x-rays are then detected and analyzed by methods similar to that of the first device.

A proof-of-principle monitor has recently been constructed which incorporates an interchangable anode structure. This feature allows one to adjust the energy of the primary x-ray flux by proper selection of an anode material. Using germanium and gold anodes and operating at 20kV, 1 ma (a penetration and power level far less than that of, say, a medical device), XRF was recently employed in tests targeting a two dimensional simulation of an iron aerosol. The results show that in a minute or less one can assess mass concentrations from a few milligrams up to several grams per cubic meter. It is expected that with increased x-ray fluxes and improved spectral purity of the primary x-rays one can realize better sensitivity, lower minimum measurable concentrations and more rapid function.

TABLE 1.

element	min. QUANTITATIVELY MEASUREABLE conc., +/- 10% std. dev. (micrograms/cu. meter) 4 min. sample	10 min. sample	Permissible concentration 40 hr/wk worker exposure (micrograms/cu. meter)
Uranium	24.8	4.0	200 soluble & insoluble
Lead	39.0	6.2	150 inorganic dusts & fumes as Pb
Mercury	27.0	4.3	100 dusts and mists of inorganic compounds,
Chromates	68.3	10.9	50 Chromium (VI) as Cr; 500 Chromium (II) & (III) as Cr; metal
Arsenic	18.3	2.9	200 dusts and mists of inorganic compounds
Copper	26.2	4.2	200 as fume; 1000 as dusts & mists
Iron	47.7	7.6	1000 for soluble iron salt as Fe; 5000 for Iron oxide fumes as Fe
Zinc	24.4	3.9	5000 for Zinc Oxide fume; 10,000 for Zinc Oxide dust

Blank

INVERSION OF AEROSOL SPECTRAL TRANSMITTANCE TO DETERMINE SIZE DISTRIBUTION OF CONCENTRATION

Dr. Janon Embury
U.S. Army
Chemical Research, Development and Engineering Center
Aberdeen Proving Ground, MD 21010

INVERSION PROBLEM

In general the inversion problem is that of finding the solution f(x) to the Fredholm Integral Equation:

$$g(y) = \int_a^b K(y,x) f(x) dx \ .$$

The specific problem of inverting aerosol spectral transmittance measurements to obtain a size distribution may be written:

$$T = \frac{I}{I_o} = \exp \left\{ - \ell \int_o^\infty \pi r^2 Q_E(\tfrac{r}{\lambda}) n(r) dr \right\} \ ,$$

thus:

$$g(\lambda) = \frac{\log T}{\pi \ell} \ ,$$

$$K(\lambda, r) = r^2 Q(\tfrac{r}{\lambda}) \ ,$$

$$f(r) = n(r) \ .$$

LOG NORMAL SIZE DISTRIBUTION

Rather than measuring transmittance at "N" wavelengths to obtain the population density $n(r_i)$ in Bins $1 \leq i \leq N$ we will choose a function with two parameters, σ_G and r_{MMD}, to fit the data. Thus only two wavelengths will be necessary for the inversion:

$$n(r) = \frac{1}{r \ln \sigma_G (2\pi)^{1/2}} e^{\frac{-(\ln r - \ln r_G)^2}{2 \ln^2 \sigma_G}},$$

where:

$$r_p = r_G e^{p \ln^2 \sigma_G}.$$

TABLE 1. Value of p for various diameter definitions (Reist, 1984).

Definition Number	To Get	Let *p* Equal
1	Mode	-1
2	Geometric mean or median	0
3	Arithmetic mean	0.5
4	Diameter of average area[a]	1
5	Diameter of average mass	1.5
6	Surface median diameter	2
7	Surface mean diameter[b]	2.5
8	Volume median diameter	3
9	Volume mean diameter	3.5

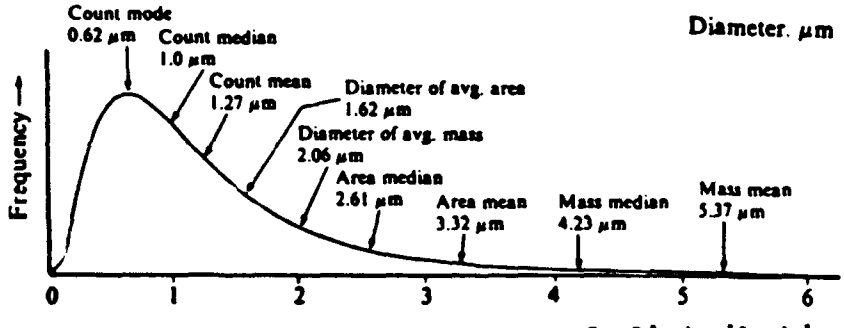

FIGURE 1. Example of log-normal distribution. Definition of terms: $d_g = 1.00$, $\sigma_g = 2.00$ (Reist, 1984)

EXPRESSIONS FOR THE KERNEL $r^2Q(r/\lambda)$

Actually the extinction efficiency factor is a function not only of r/λ but also the refractive index m, i.e., $Q(m,r/\lambda)$.

For intermediate values of m:

$$\frac{r}{\lambda} >> 1, \quad \frac{|m|r}{\lambda} >> 1 \quad \text{(Geometric Optics Limit);}$$

$$Q_E \approx 2 ,$$

$$Q_S \geq 1 \quad \text{(Due to Diffraction);}$$

$$\frac{r}{\lambda} << 1, \quad \frac{|m|r}{\lambda} << 1 \quad \text{(Rayleigh Limit);}$$

$$Q_E = Q_A + Q_S ,$$

$$Q_A = -4\left(\frac{2\pi r}{\lambda}\right) \mathrm{Im}\left(\frac{m^2 - 1}{m^2 + 2}\right) ,$$

$$Q_S = \frac{8}{3}\left(\frac{2\pi r}{\lambda}\right)^4 \left|\frac{m^2 - 1}{m^2 + 2}\right| .$$

EXPRESSIONS FOR THE KERNEL (continued)

For refractive index near one $|m - 1| \ll 1$:

$\frac{r}{\lambda}$ = arbitrary, $\frac{r|m - 1|}{\lambda} \ll 1$ (Rayleigh-Gans Limit);

$$Q_A = -4\left(\frac{2\pi r}{\lambda}\right) \mathrm{Im}\left(\frac{m^2 - 1}{m^2 + 2}\right) ,$$

$$Q_S = |m - 1|^2 \left\{\frac{5}{2} + 2x^2 - \frac{\sin 4x}{4x} - \frac{7}{16x^2}(1 - \cos 4x)\right.$$

$$\left. + \left(\frac{1}{2x^2} - 2\right)\left(\gamma + \log 4x + \int_x^\infty \frac{\cos u}{u}\, du\right)\right\} ,$$

where:

$$x \equiv 2\,\frac{\pi r}{\lambda} ;$$

$\frac{r}{\lambda} \gg 1$, $\frac{r|m - 1|}{\lambda}$ = arbitrary (Anomalous Diffraction);

$$Q_E = 2 - 4\, e^{-\rho \tan\beta}\, \frac{\cos\beta}{\rho} \sin(\rho - \beta)$$

$$-4\, e^{-\rho \tan\beta} \left(\frac{\cos\beta}{\rho}\right)^2 \cos(\rho - 2\beta) + 4\left(\frac{\cos\beta}{\rho}\right)^2 \cos 2\beta ,$$

where:

$$m = n - ik ,$$

$$\tan\beta = \frac{k}{(n - 1)} ,$$

$$= \frac{4\pi r}{\lambda}(n - 1) .$$

EXPRESSIONS FOR THE KERNEL (continued)

Large refractive index typical of metals in the far infrared and microwave regions:

$$\frac{r}{\lambda} << 1, \quad \frac{\eta^{1/2} r}{\lambda} << 1 ,$$

where:

$$m^2 = \epsilon - i\eta \approx i\eta = i\frac{4\pi\sigma}{\omega} ;$$

$$Q_A \approx Q_E \approx \frac{12(\frac{2\pi r}{\lambda})}{\eta} + \frac{2\eta}{15}(\frac{2\pi r}{\lambda})^3 ;$$

$$\frac{r}{\lambda} << 1, \quad \frac{\eta^{1/2} r}{\lambda} = \text{arbitrary} ;$$

$$Q_A \approx Q_E \approx \frac{6}{(2\eta)^{1/2}}\left(\frac{-\lambda}{\pi r(2\eta)^{1/2}} + \frac{\sinh\frac{(2\eta)^{1/2} 2\pi r}{\lambda} - \sin\frac{(2\eta)^{1/2} 2\pi r}{\lambda}}{\cosh\frac{(2\eta)^{1/2} 2\pi r}{\lambda} - \cos\frac{(2\eta)^{1/2} 2\pi r}{\lambda}}\right) ;$$

$$\frac{r}{\lambda} << 1, \quad \frac{\eta^{1/2} r}{\lambda} >> 1 ;$$

$$Q_A \approx Q_E \approx \frac{6}{(2\eta)^{1/2}} - \frac{6}{\eta x} ;$$

$$\frac{r}{\lambda} = \text{arbitrary}, \quad \frac{\eta^{1/2} r}{\lambda} >> 1 ;$$

$$Q_S \approx Q_E, \; Q_A = \frac{8}{3}(\frac{2}{\eta})^{1/2} ;$$

$$\frac{r}{\lambda} >> 1, \quad \frac{\eta^{1/2} r}{\lambda} >> 1 ;$$

$$Q_S \approx Q_E = 2, \; Q_A = \frac{8}{3}(\frac{2}{\eta})^{1/2} ;$$

TABLE 2. Boundary regions of the m-x domain. (van de Hulst, 1957).

Region	ρ	$m-1$	$x(m-1)$	Chapter or Section	Extinction Formula
61	0	0	0		$Q = (32/27)(m-1)^6x^4$
1	arb	0	0	7.2 (Rayleigh-Gans)	
12	1	0	0		$Q = 2(m-1)^2x^2$
2	1	0	arb	11 (anomalous diffraction)	
23	1	0	1		$Q = 2$
3	1	arb	1	12 (large spheres)	
34	1	1	1		$Q = 2$
4	arb	1	1	10.6 (total reflector)	
45	0	1	1		$Q = (10/3)x^4$
5	0	1	arb	10.5 (optical resonance)	
56	0	1	0		$Q = (8/3)x^4$
6	0	arb	0	6.3 (Rayleigh scattering)	

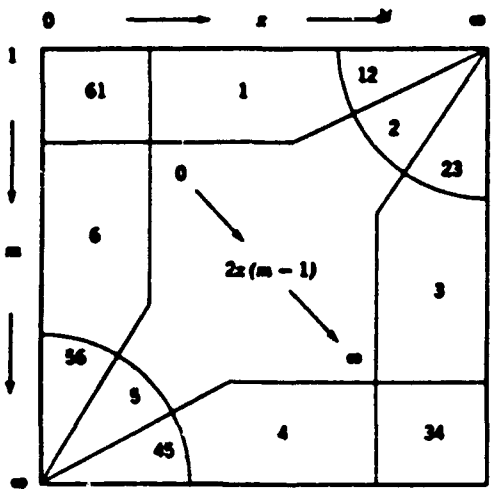

FIGURE 2. Survey of limiting cases in the m-x domain (van de Hulst, 1957).

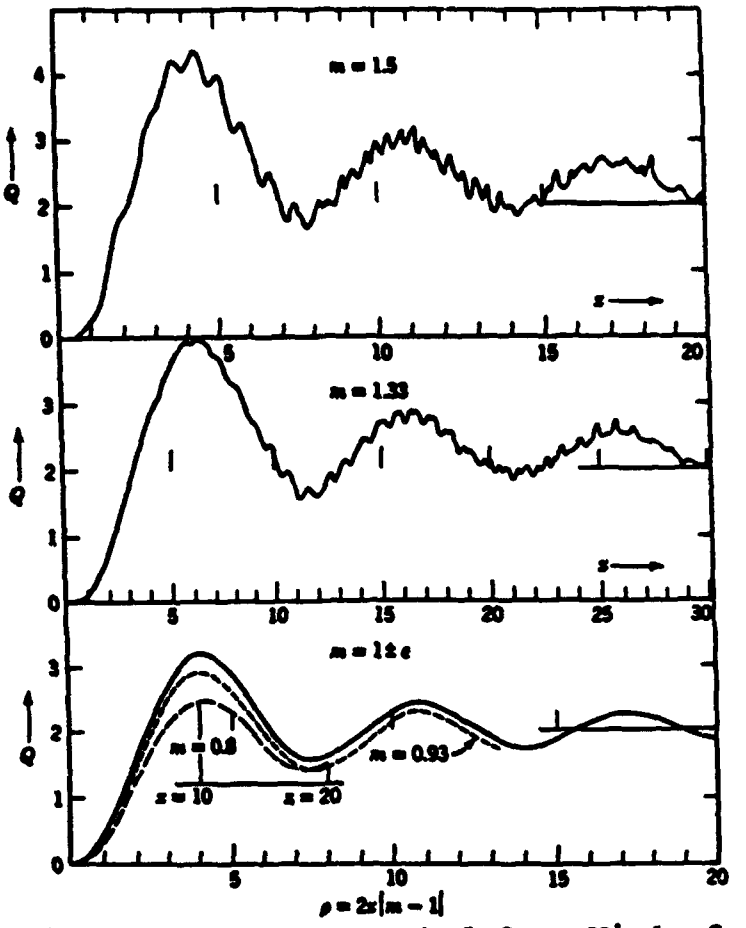

FIGURE 3. Extinction curves computed from Mie's formulae for m = 1.5, 1.33, 0.93, and 0.8. The scales of x have been chosen in such a manner that the scale of $\rho = 2z|m - 1|$ is common to these four curves and to the extinction curve for $m = 1 \pm e$ (van de Hulst, 1957).

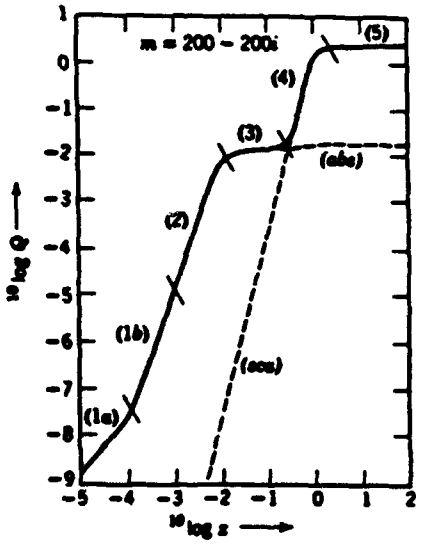

FIGURE 4. Logarithmic sketch of the extinction curve for spheres with m = 200 - 200i (van de Hulst, 1957).

DEPENDENCE OF REFRACTIVE INDEX ON WAVELENGTH

Bound electrons and ions - Lorentz Multiple Oscillator Model for dielectrics:

$$m^2 \equiv \epsilon = \epsilon_o + \sum_j \frac{\omega_{p_j}^2}{\omega_j^2 - \omega^2 - i\gamma_j\omega} .$$

Conductors - the Drude Model:

$$\epsilon = 1 - \frac{\omega_p^2}{\omega^2 + i\gamma\omega} = \epsilon' + i\epsilon'' ,$$

$$\epsilon' = 1 - \frac{\omega_p^2}{\omega^2 + \gamma^2} ,$$

$$\epsilon'' = \frac{\omega_p^2}{\omega(\omega^2 + \gamma^2)} ;$$

$$\gamma \equiv 1/\tau ,$$

τ = average time between collisions;

$$\sigma_{DC} = \frac{\omega_p^2}{4\pi\gamma} .$$

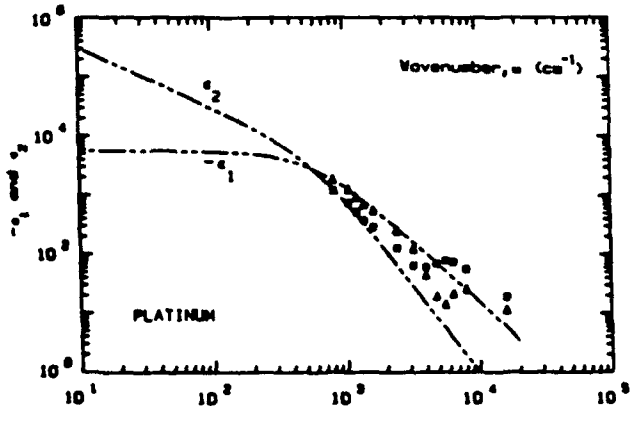

FIGURE 5. Platinum: $-\epsilon'(\omega)$ and $\epsilon''(\omega)$ vs. frequency. The dashed lines are the Drude Model fit (Ordal, et al., 1985).

TWO WAVELENGTHS IN THE GEOMETRIC OPTICS LIMIT

$$Q_E = 2 \ ;$$

$$\frac{\log T_{\lambda_1}}{\pi \ell} = \int_0^\infty r^2 (2) \frac{1}{r \ln \sigma_G (2\pi)^{1/2}} e^{\frac{-(\ln r - \ln r_G)^2}{2 \ln^2 \sigma_G}} dr \ ;$$

$$\frac{\log T_{\lambda_2}}{\pi \ell} = \int_0^\infty r^2 (2) \frac{1}{r \ln \sigma_G (2\pi)^{1/2}} e^{\frac{-(\ln r - \ln r_G)^2}{2 \ln^2 \sigma_G}} dr \ ;$$

Because $Q \neq f(\lambda)$, instead of two equations, there is only one equation. This allows a solution for either r_G or σ_G but not both.

ONE WAVELENGTH IN THE GEOMETRIC OPTICS LIMIT AND THE OTHER IN THE RAYLEIGH LIMIT

Geometric optics limit wavelength:

$$Q(\lambda_1) = 2 \ ;$$

$$\frac{\log T_{\lambda_1}}{\pi \ell} = \int_0^\infty 2r^2 \frac{1}{r \ln \sigma_G (2\pi)^{1/2}} e^{\frac{-(\ln r - \ln r_G)^2}{2 \ln^2 \sigma_G}} dr \ ;$$

Rayleigh limit wavelength absorption dominates:

$$Q(\lambda_2) = -4\left(\frac{2\pi r}{\lambda_2}\right) \mathrm{Im}\left(\frac{m^2 - 1}{m^2 + 2}\right) ,$$

$$\frac{\log T_{\lambda_2}}{\pi \ell} = \int_0^\infty r^2 \left(\frac{-4\left(\frac{2\pi r}{\lambda_2}\right) \mathrm{Im}\left(\frac{m - 1}{m^2 + 2}\right)^2}{r \ln \sigma_G (2\pi)^{1/2}}\right) e^{\frac{-(\ln r - \ln r_G)^2}{2 \ln^2 G}} dr \ ;$$

$$m = m(\lambda) \ .$$

Rayleigh limit wavelength scatter dominates:

$$Q(\lambda_2) = \frac{8}{3}\left(\frac{2\pi r}{\lambda_2}\right)^4 \left|\frac{m^2 - 1}{m^2 + 2}\right| \ ;$$

$$\frac{\log T_{\lambda_2}}{\pi \ell} = \int_0^\infty r^2 \left(\frac{\frac{8}{3}\left(\frac{2\pi r}{\lambda_2}\right)^4 \left|\frac{m^2 - 1}{m^2 + 2}\right|}{r \ln \sigma_G (2\pi)^{1/2}}\right) e^{\frac{-(\ln r - \ln r_G)^2}{2 \ln^2 G}} dr \ .$$

BOTH WAVELENGTHS IN THE RAYLEIGH LIMIT

Absorption dominates:

$$\frac{\log T_{\lambda_j}}{\pi \ell} = \int_0^{\infty} r^2 \left(\frac{-4 \left(\frac{2\pi r}{\lambda_j}\right) \mathrm{Im}\left(\frac{m^2 - 1}{m^2 + 2}\right)}{r \ln \sigma_G (2\pi)^{1/2}} \right) e^{\frac{-(\ln r - \ln r_G)^2}{2 \ln^2 \sigma_G}} \, dr \; ;$$

Note: $m = m(\lambda_j)$.

Scatter dominates:

$$\frac{\log T_{\lambda_j}}{\pi \ell} = \int_0^{\infty} r^2 \left(\frac{\frac{8}{3} \left(\frac{2\pi r}{\lambda_j}\right)^4 \left| \frac{m^2 - 1}{m^2 + 2} \right|}{r \ln \sigma_G (2\pi)^{1/2}} \right) e^{\frac{-(\ln r - \ln r_G)^2}{2 \ln^2 \sigma_G}} \, dr \; ;$$

$$m = m(\lambda_j) \; .$$

INVERSION TO OBTAIN MONODISPERSE AEROSOL CONCENTRATION

$$T = e^{-\langle (m,r,\lambda) \rangle_n c \ell} ;$$

$$c = \frac{\ln 1/T}{\langle (m,r,\lambda) \rangle_n \ell} ,$$

$$\alpha (m,r,\lambda) = GQ(m,r,\lambda)/\rho V ;$$

for:

$$r/\lambda >> 1, \; Q(m,r,\lambda) = 2 ;$$

$$\langle \alpha \rangle = \frac{2}{\rho V} \langle G \rangle_n ;$$

$\langle G \rangle_n = S/4$ (Convex Shapes Random Orientation);

$$c = \frac{\ln 1/T}{\frac{S}{2\rho V} \ell} .$$

TABLE 3. Surface area per unit volume for randomly-oriented particles.

Shape	Monodisperse	Polydisperse
Sphere (r = radius)	$\frac{3}{r}$	$\frac{3}{r_n} e^{\frac{-5}{2}(\ln\sigma)^2}$
Cube (a = edge)	$\frac{6}{a}$	$\frac{6}{a_n} e^{\frac{-5}{2}(\ln\sigma)^2}$
Flake (t = thickness)	$\frac{2}{t}$	$\frac{2}{t_n} e^{\frac{-1}{2}(\ln\sigma)^2}$
Filament (r = radius)	$\frac{2}{r}$	$\frac{2}{r_n} e^{\frac{-3}{2}(\ln\sigma)^2}$

INVERSION OF TRANSMITTANCE AS A FUNCTION OF TIME IN A STIRRED CHAMBER

$$T(t) = e^{-\ell \int_0^\infty r^2 Q(r/\lambda) n(r,t) dr} \quad ;$$

$$n(r,t) = n_o(r)\, e^{-\vartheta(r) t/H} \quad ;$$

$$n_o(r) = \frac{1}{(2\pi)^{1/2} r \ln\sigma_G} e^{\frac{-(\ln r - \ln r_G)^2}{2\ln^2 \sigma_G}} \quad ;$$

$$\vartheta(r) = \frac{2\rho g}{9\mu} r^2 \; .$$

For monodisperse aerosol in geometric optics limit:

$$\ln \ln \frac{1}{T(t)} = \ln(\pi \ell r^2) - \vartheta(r)\; t/H$$

$$= \ln(\pi \ell r^2) - \frac{2\rho g r^2}{9\mu H} t \; .$$

For non-spherical particle monodispersions:

$$\ln \ln \frac{1}{T(t)} = \ln\left(\ell \langle G \rangle_\lambda\right) - \vartheta t/H \; .$$

REFERENCES

Ordal, N.A., et al., Applied Optics, V.24, 4493, 1985.

Reist, P.C., Introduction to Aerosol Science, MacMillan, New York, 1984.

van de Hulst, H.C., Light Scattering by Small Particles, Wiley, New York, 1957.

SECTION IV: PARTICLE CHARACTERIZATION AND APPLICATIONS OF PARTICLE TECHNOLOGY

Blank

An Exercise in Particle Characterization

by J. K. Beddow
1153 Engineering Building
University of Iowa, Iowa City, Iowa 52242

Introduction

The problems associated with the characterization of matter in divided form have been the subject of increasingly intensive study during the last 40 years.[1] For much of this time great effort has been devoted to the problems of measuring particle size. There are now many different methods for measuring size all of which are based upon different physical principles. Consequently for non-spherical particles, the vast majority encountered in practice, each method yields different size data for the same sample. Although this state of affairs is unwelcome, it is nevertheless logical. There is clearly a need for a comprehensive theory that will include not only particle size, but shape, roughness, symmetry and many other of the features that collectively constitute the characteristics of the particle or particle set.

Morphological analysis provides a theoretical framework for this task in the following way:

- it provides an analytical theory and procedures for determining features including particle size, shape, roughness, symmetry for profiles, 2-dimensional surfaces, and 3-dimensional particles.[2,3]
- it provides a theory of particle characterization which enables the standardized set of features to be determined that fully characterizes the particle/particle set to the extent desired.[4]

At the present time particle profile morphological analysis can be conducted to yield size, shape, symmetry, roughness and other measures using a newly-available image analyzer. However, it is not yet possible to conduct a formal particle characterization because the theory is not quite finished.

This paper describes certain aspects of the theory of morphological profile analysis. The image analysis instrument is then described. Finally, some typical data are reported.

Morphological Analysis

Morphological Analysis is the science of the analysis of points in space. Researchers in the multidisciplinary field of particulate science and

technology have accessed this science at the microscopic level, initially in two dimensions (x,y) and more recently in three dimensions (x,y,z).

Morphological analysis is also applicable to more than three dimensions. For example, (x,y,z,t).

The essential steps in morphological analysis are:

- determination of the mathematical form of the particle representation.
- extraction of the features from the representations
- formulation and ranking of the significant features in order to characterize the particle or particle set.

Once the characterization step is completed, relationship between morphology and the physical behavior of the particulate material under study may be sought.

Fine Particle Representation

The first problem of representation is the particle profile. It is both the simplest problem to solve and that from which we learn the most. The shape is defined as the pattern of relationships among all of the points of the profile.

The initial choice of the (R-Θ) Fourier method to represent the profile was arbitrary and expedient. However, the (R-Θ) method illustrates the major aspects which are common to all particle representations. The profile consists of myriads of (x,y) co-ordinate points. The analysis reduces this x,y, data to an analytical relationship (the Fourier Equation of the Curve). This condensation of information is continued by the extraction of Fourier Coefficients. These are transformed into invariants. The invariants then represent the size, shape, and asymmetry of the particle profile. The sequence of steps is therefore.

- obtain data that measures the positions of points in space.
- convert the data to an analytical relationship.
- extract coefficients.
- transform to invariant form--these are the features.

The above represents the important steps in morphological analysis.

The morphological variational principle is the fundamental basis for a general theory of morphology:

A mathematical representation of the Boundary Function for surfaces may be derived by finding a "Normalized Function" which causes the surfaces area integral to take on stationary values.

Application of this principle hase resulted in the derivation from first principles of the relationships for the profile, 2-D , 3-D surfaces, fibers and flakes.[5-9]

Feature Extraction

Mathematically speaking, a feature of an object is described in terms of invariants and indeed a feature may well be an invariant. This is illustrated as follows.

A particle profile expressed in polar coordinates has the form:

$$R\theta = a_0 + \sum^{\infty} (a_n \cos n\theta + b_n \sin n\theta) \qquad (1)$$

The initial urge is to consider (a_n, b_n) as shape features. This is unwise because (a_n, b_n) vary as the particle is moved by rotation, for example. This means that (a_n, b_n) are definitely not invariants. They have to be transformed in order that the invariants might be obtained.

In general, features are moments of distributions. The deep significance of statistics in morphological analysis is shown by the **fundamental morphological principle** for size, R_0, in which R_0, the equivalent radius is defined

$$R_0^2 = a_0^2 + 1/2 \sum_{n=1}^{\infty} a_n^2 + b_n^2 \qquad (2)$$

In which πR_0^2 is the area of the profile

a_0 is the mean radius (the mean of the radial distribution)
a_n, b_n, are Fourier coefficients.

In words equation 2 reads

(The Size)^2 = (The mean radius)^2 + (The Shape Information) (3)

μ_2 is the second moment about the mean of the radial distribution, μ_2 is identical to $\frac{1}{2} \sum a_n^2 + b_n^2$. Therefore,

$$R_o^2 = a_o^2 + \mu_2 \qquad (4)$$

In words, equation 4 reads,

$$(\text{The Size})^2 = (\text{The Mean})^2 + \text{The second moment about the mean} \qquad (5)$$

Characterization

Particle characterization results from a non-simple process of information structuring. Particle characterization is defined as the communication of the description of the essential multidimensional properties of a particle or a collection of particles. Each multidimensional property constitutes a characterization vector which is determined by a measurement vector operating on a basis set of the property features. The resultant characterization comprises a set of mathematical descriptors and a corresponding set of verbal descriptors.

This theory is illustrated by referral to shape characterization in which $C_1 \ldots C_n$ are partial rotational symmetries and $J_1 \ldots J_2$ are partial reflection symmetries.

$$\begin{bmatrix} C_1 \\ C_2 \\ \cdot \\ \cdot \\ \cdot \\ \cdot \\ C_n \\ \sigma_1 \\ \sigma_2 \\ \cdot \\ \cdot \\ \cdot \\ \sigma_n \end{bmatrix} \quad \begin{bmatrix} C_{10} & C_{11} & C_{12} & \cdots & C_{1n} \\ C_{20} & C_{21} & C_{22} & \cdots & C_{2n} \\ \cdot & \cdot & \cdot & \cdots & \cdot \\ \cdot & \cdot & \cdot & \cdots & \cdot \\ \cdot & \cdot & \cdot & \cdots & \cdot \\ \cdot & \cdot & \cdot & \cdots & \cdot \\ C_{n0} & C_{n1} & C_{n2} & \cdots & C_{nn} \\ \sigma_{10} & \sigma_{11} & \sigma_{12} & \cdots & \sigma_{1n} \\ \sigma_{20} & \sigma_{21} & \sigma_{22} & \cdots & \sigma_{2n} \\ \cdot & \cdot & \cdot & \cdots & \cdot \\ \cdot & \cdot & \cdot & \cdots & \cdot \\ \cdot & \cdot & \cdot & \cdots & \cdot \\ \sigma_{n0} & \sigma_{n1} & \sigma_{n2} & \cdots & \sigma_{nn} \end{bmatrix} \quad = \quad \begin{bmatrix} a_0 \\ a_1 \\ a_2 \\ \cdot \\ \cdot \\ \cdot \\ \cdot \\ \cdot \\ \cdot \\ \cdot \\ \cdot \\ \cdot \\ a_n \end{bmatrix} \qquad (6)$$

Measurment Vector — Basis Set — Characterization Vector

The basis set is the standard against which all other shapes of profile are compared. The measurment vector is obtained experimentally using (for a profile) the R-θ method. The characterization vector is derived from equation 6. The standard figures for compilation of the basis set are: circle, cardoid, lemiscate, equilateral triangle, square, pentagon, hexagon, etc.

Experimental

The image analyzer used consists of computer hardware and software connected to a video camera and printer.[10] The arrangement is shown in Figure 1.

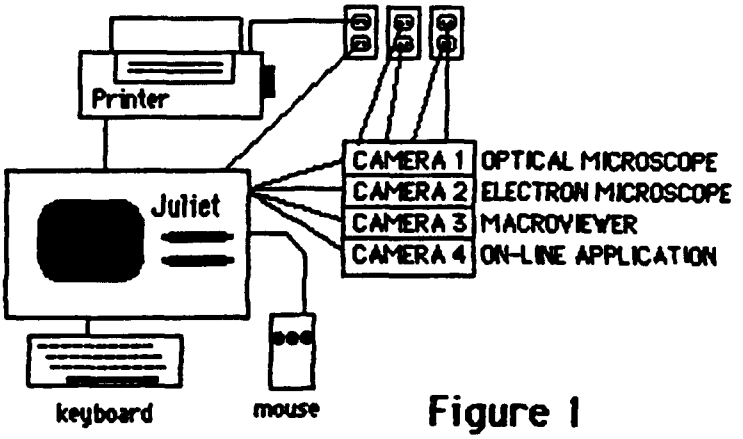

Figure 1
Outline of Image Analyzer

Results

Typical results for the size and shape of a sample of particles are shown in Figures 2 & 3 respectively.

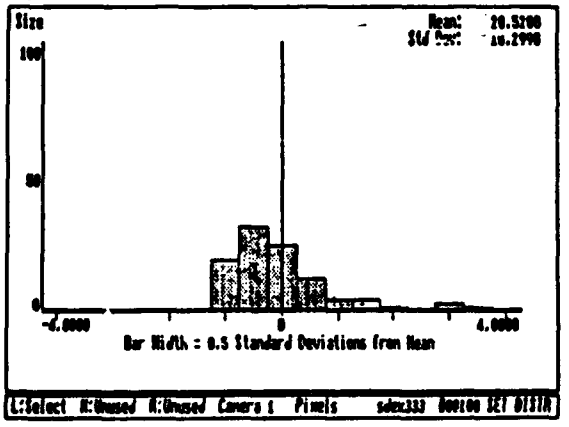

Figure 2

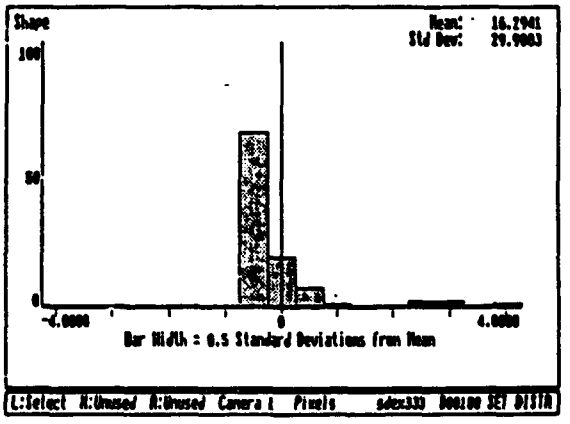

Figure 3

References

1. Beddow, J.K., Particulate Science and Technology, Chemical Publishing Co. New York, 1980.

2. Luerkens, D.W., "The R-Theta method derived from a variational principle.", Particulate Science and Technology, Vol. 4, No. 4, p. 353-361, 1986

3. Beddow, J. K., "Size, Shape and Texture Analysis in Solid/Liquid Systems." in Recent Advances in Solid-Liquid Separation, ed. H. Muralidhara, Batelle, 1986, pp. 37-61.

4. Luerkens, D.W., and Beddow, J.K., "Visions of the Future in Morphological Analysis", to be published in Powder Technology, 1988.

5. Luerkens, D.W. "Infinite Fibers and Threads", Particulate Science and Technology, Vol 5, No. 3, p. 261-270.

6. Luerkens, D.W., "Particle Surface Morphologies--Flakes", Particulate Science and Technology, Vol. 5, No. 3, p. 301-309, 1987.

7. Luerkens, D.W. "Particle Surface Morphologies - Finite Fibers, Part I, Mathematical Description." Particulate Science and Technology, Vol. 5, No. 2, p. 151-160.

8. Luerkens, D.W., "The Three Dimensional Particle" - Particulate Science and Technology, Vol. 4, No. 4, p. 371-378, 1986.

9. Luerkens, D.W., "The R-Theta Method Derived from a Variational Principle.", Particulate Science and Technology, Vol. 4, No. 4, p. 361-371, 1986

10. The Shapespeare Corporation, Juliet, A Technical Manual, Iowa City, Iowa, 1988

"Particle-Sizing Reference Materials from the National Bureau of Standards"

Thomas R. Lettieri
National Bureau of Standards
Gaithersburg, MD 20899

Abstract This paper summarizes the Standard Reference Materials available from the National Bureau of Standards for use in particle-sizing applications.

Introduction: The NBS/ASTM Particle SRMs Program

There are many areas of science and technology in which particulate material plays an important role; in most cases, some measure of the size of the particles is needed. Although there are many different kinds of instruments which can give the desired information about the particles, they all must be referenced to either a well-established physical model or to a well-characterized calibration artifact. Only with such standards can measurement uniformity and reproducibility be attained throughout the laboratory and, on a larger scale, throughout the country.

In order to promote uniformity in particle-size measurement, the National Bureau of Standards (NBS), under the guidance of an ASTM special committee, has developed a number of Standard Reference Materials (SRMs) for use in particle-sizing applications [1,2,3,4]. The particle-sizing SRMs certified by NBS can be grouped into two categories: broad-distribution glass beads and monosized polystyrene spheres. Given in the present paper is a summary of the particle-sizing SRMs currently available from NBS.

Broad-Distribution Glass-Bead SRMs

The broad-distribution glass-bead SRMs available from NBS are summarized in Table 1. As the Table indicates, the particles have a wide range of diameters, from 8 to 2160 μm. Photographs of particles from two of these SRMs, #1003 and #1019a, are given in Figs. 1 and 2, respectively. [As evidenced in the figures, the larger particles tend to be more spherical than the smaller ones.]

All of the glass-bead SRMs are certified using optical photomicroscopy, with a well-calibrated microscale used as the dimensional standard. With the purchase of each glass-bead SRM, the user gets a certificate of calibration which gives information about the distribution of particle diameters; a typical curve of volume distribution, for SRM 1003, is presented in Fig. 3. The certificate also discusses the application of the glass beads in the calibration of the effective opening of wire-cloth sieves.

Although the biggest application, by far, of the broad-distribution glass beads has been in the calibration of sieves, they have also found use in the calibration of electrical-sensing zone instruments ("Coulter counters"), optical-sensing zone instruments, forward light scattering instruments, sedimentation devices, and other instruments which measure broad particle-size distributions.

Table 1

NBS Broad-Distribution Glass Beads

SRM Number	Size, μm	Sieve Number	Wt./Unit
1003a	8-58	-	25 g
1004a	in prep.	-	-
1017a	100-310	140-50	84 g
1018a	225-780	60-25	74 g
1019a	760-2160	20-10	200 g

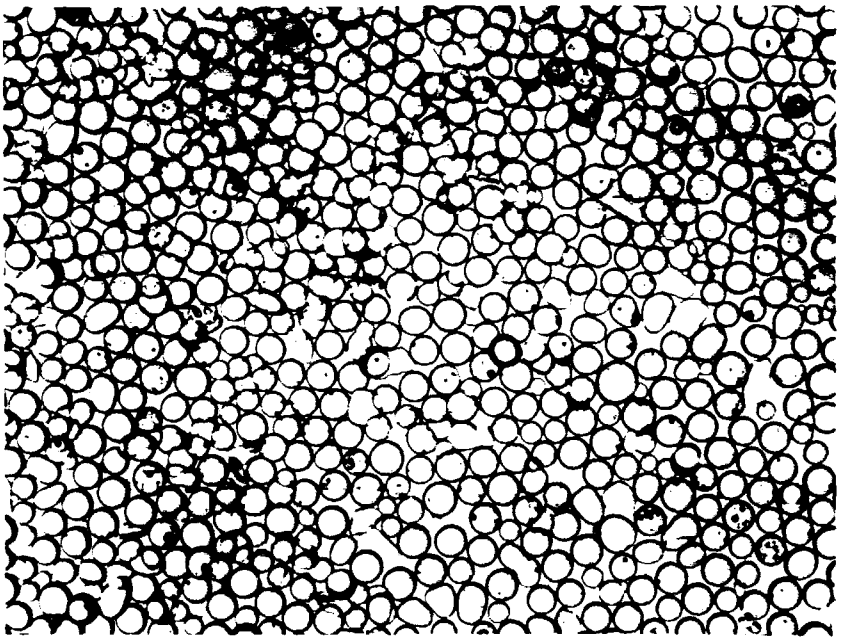

Fig. 1. Optical photomicrograph of SRM 1003 glass beads.

Fig. 2. Optical photomicrograph of SRM 1019a glass beads.

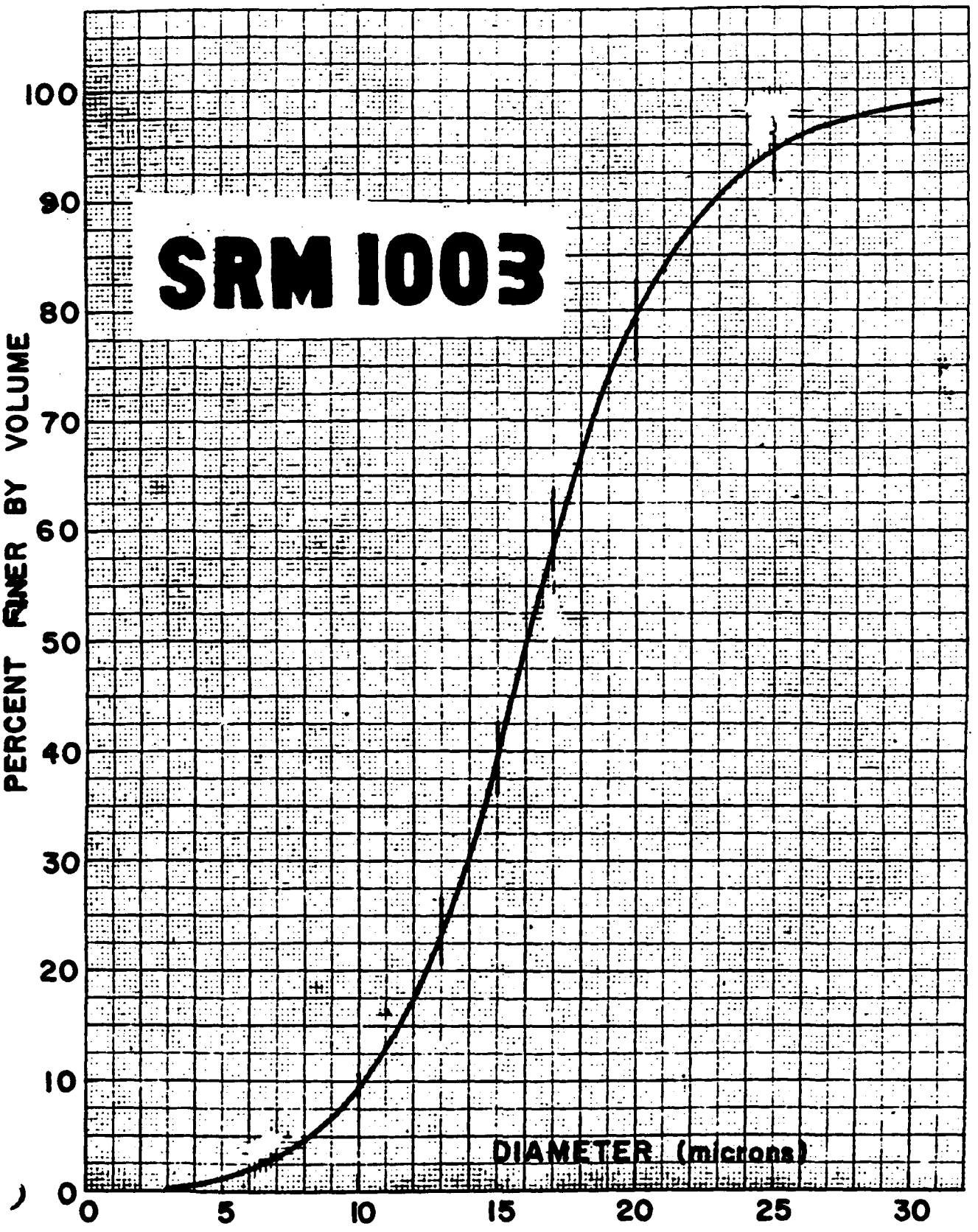

Fig. 3. Volume distribution for SRM 1003 glass beads.

Monosized Polystyrene-Sphere SRMs

The monosized polystyrene spheres currently available from NBS, which range from 0.3 μm to 30 μm in nominal diameter, are summarized in Table 2. In the near future, both 0.1 μm and 100 μm SRMs are expected to be certified. The polystyrene particles are highly spherical, have very narrow size distributions, and are accurately measured for mean diameter and, in some cases, for size-distribution width (Fig. 4). In contrast to the broad-distribution particles, these SRMs are intended to be "benchmark" standards at discrete, well-defined diameters. All but one of the monosized particle SRMs are sold in 5-ml plastic vials of particles in liquid suspension at about 0.5% weight concentration of particles (Fig. 5). The exception is SRM 1965 which is a microscope slide containing small patches of 10-μm polystyrene spheres made on the NASA space shuttle. The monosized-sphere SRMs also come with a certificate of calibration giving the certified diameter, as well as information about the use of the material.

Both optical and non-optical techniques were employed to certify the polystyrene-sphere SRMs, with the choice of technique determined by the mean size of the particles. The optical techniques used at NBS were optical array sizing, center distance finding (CDF), quasi-elastic light scattering (QELS), angular-intensity light scattering (AILS), and resonance light scattering (RLS). The non-optical methods available for particle-calibration purposes are transmission electron microscopy (TEM), metrology electron microscopy (MEM), and electrical-sensing zone. Details about these techniques, as applied to the certification of the monosized polystyrene spheres, are given elsewhere [1,2,3,4].

Applications for the monosized polystyrene spheres include the calibration of: optical and electron microscopes; light-scattering instruments; and other high-resolution devices which can measure very narrow size distributions.

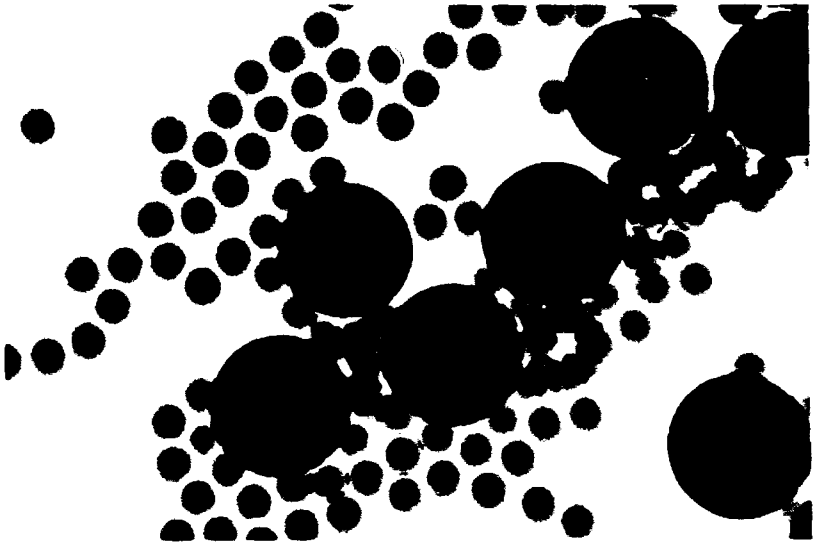

Fig. 4. Transmission electron micrograph of SRM 1690, 1-μm spheres (large circles) together with SRM 1691, 0.3-μm spheres (small circles).

Table 2

Monosized Polystyrene Spheres Currently Available from NBS

SRM #	Certif. Diam., μm	Uncert., μm	CV	Certif. Techniques	Comments
1691	0.269	± 0.007	< 2%	TEM, QELS	
1690	0.895	± 0.008	1%	AILS, array sizing	
1962	2.978	± 0.007	0.8%	CDF, (MEM)	
1960	9.89	± 0.04	0.9%	CDF, MEM, RLS	made in space
1965	9.94	± 0.04	0.9%	CDF	microsphere slide
1961	29.64	± 0.06	0.8%	CDF, MEM	made in space

Fig. 5. A vial of SRM 1690 microspheres and a calibration certificate.

Future Directions

Among a number of possibilities for future particle-sizing SRMs from NBS, two important candidates are a "particle-count" standard and a "particle-on-surface" standard. The former is envisioned as a mixture of two or more of the monosized polystyrene sphere SRMs, which is then certified for relative number of particle counts at each of the discrete diameters in the mixture. This type of SRM would have many applications, such as setting the vertical scale on a Coulter counter. A particle-on-surface SRM, on the other hand, would be applicable in the measurement of surface microcontamination in such areas as semiconductor processing, optical fabrication, and computer-disc memories. Other possibilities for future particle SRMs include opaque particles, aspheres, and cylinders.

Conclusion

The Standard Reference Materials certified by the National Bureau of Standards are intended to be used as primary calibration artifacts by manufacturers of particle-sizing instruments and by producers of powders and powder products. In general, the broad-distribution NBS glass beads can be used in everyday production applications, whereas the monosized NBS polystyrene spheres are not intended for everyday use, since the supplies of these materials are limited. For routine, production-line applications, the monosized microspheres sold by several commercial vendors are satisfactory.

References

[1] G. Mulholland, et. al., **J. Res. NBS 90**, 3 (1985).
[2] T. Lettieri and G. Hembree, **J. Coll. Int. Sci.** (to be published, 1988).
[3] T. Lettieri, et. al., **J. Coll. Int. Sci.** (to be published, 1988).
[4] T. Lettieri in **Optical Particle Sizing: Theory and Practice**, ed. by G. Gouesbet and G. Grehan (Plenum, New York, 1988).

Blank

PARTICLE SIZE MEASUREMENT IN POWDER TECHNOLOGY

Dr. Terry Allen and Dr. Reg Davies
Senior Consultants
E.I. du Pont de Nemours
Louviers 1357
Wilmington, DE 19898

INTRODUCTION

Powder Technology is an interdisciplinary science embracing many diverse industries, confectionery, cosmetic, pharmaceutical, chemical and metallurgical, and defense applications such as smoke grenades. Particle size is important in many powder handling operations such as storage, mixing, flow, grinding and packaging.

SAMPLING

Powders have an inherent tendency to segregate according to particle size and, to a lesser extent, particle density. In powder transport, vibration causes small particles to percolate under large ones and lift them to the surface. This phenomenon was the subject of a recent paper explaining why Brazil nuts are always on top in packets of mixed nuts (Rosato, et al., March 9, 1987, Phys. Rev. Letter).

When poured into a heap, the "fines" percolate into the center and the "coarse" roll down the outside. A 50:50 mixture of coarse and fine material may have 95% coarse on the outside of a heap and only 5% at the center.

The distribution of particles according to size, with a powder, is strongly related to the previous history of the powder and this makes obtaining a representative sample very difficult. Presently, the properties of tonnes of powder are predicted from measurements carried out on a few milligrams. Optimum conditions are attained if the following conditions are met.

GOLDEN RULE OF SAMPLING

1. A powder should always be sampled when in motion.

2. The whole of the stream of powder should be taken for many short increments of time in preference to part of the stream being taken for the whole of the time.

Examples are illustrated in a book by one of the authors (T. Allen, Particle Size Measurement, Edition 3, 1981, Methuen, NY). In general, optimum conditions are not obtained and the sampling errors can be considerable.

PARTICLE SIZE MEASUREMENT

There are scores of techniques available for particle size (and surface area) measurement and these have generated hundreds of commercially-available equipment. Ten criteria used in equipment selection are:

1. Capital costs versus running cost.
2. Speed of analysis.
3. Ease of operation.
4. Size range.
5. Versatility.
6. Reproducibility.
7. Accuracy, precision, resolution.
8. Servicing.
9. Data presentation.
10. Compatibility with product to be measured.

Size ranges are often classified as (1) submicron, (2) subsieve (1-100 microns), and (3) sieve (100+ microns) although there is considerable overlap. Subsieve powders may be measured by one of the following techniques:

1. Gravity sedimentation.
2. Microscopy (image analysis).
3. Field scanning.
4. Stream scanning.
5. Sieving (micromesh sieves).
6. Classification.

GRAVITY SEDIMENTATION

The standard gravity sedimentation technique is the Andreasen pipet. Approximately 4.5 g of powder is dispersed in 450 ml of liquid (usually water) and allowed to settle out of suspension. At preset times, e.g., 1, 2, 4, 8, 16, 32 and 64 minutes, 10 ml samples are withdrawn and the weight of powder (w) in the

extracted samples determined by drying and weighing. The settling times (t) and heights of fall (h) generate the sizes of the largest particles in the extracted samples and w is the weight undersize. The prime difficulty with the technique is making up a stable, disperse suspension. The method is time consuming, labor intensive and relies on skilled operation, but capital costs are low and versatility is high.

This technique has been largely replaced by x-ray sedimentation so that mass undersize (w) may be determined by x-ray attenuation. Analytical times are reduced by scanning the suspension to increase the rate of change of the ratio (h/t). The attenuation of an x-ray beam is related directly to the mass of particles in the beam, but no direct relationship holds for a light beam. Gravitational photosedimentation is widely used as a "fingerprint" method for comparison purposes. Several instruments are available for use with cuvets to extend the size range down to below one micron using a centrifugal field. Disc photocentrifuges used a line-start technique where the suspension is floated on top of a clear liquid.

FIELD SCANNING

Field scanning refers to techniques which directly determine the size distribution of an assembly of particles. The most popular of these are the ones using low-angle laser light scattering (LALLS) which are used in the 0.1 to 1800 micron size range. The Microtrac Small Particle Analyser, for example, will analyse from 0.1 o 42.2 microns (now increased to 60 microns) in 16 size channels and the standard analyser, from 0.7 to 700 microns in 20 classes.

The Armco Autometrics instrument uses ultrasonic attenuation to determine size distributions.

STREAM SCANNING

Stream scanning refers to analysers where the particles are sensed and sized, one by one, as they pass through a sensing zone. In the Coulter Counter, an aperture tube is immersed in an electrolyte containing the powder. The electrical reactance across the aperture is measured by two platinum electrodes on either side of the aperture. An external vacuum draws the suspension through the aperture and each particle generates a pulse according to its particle volume. The pulses are counted and stored and may be recovered in from 16 to 256,000 size channels. The size range for each aperture is from 1.5% to 45% of its diameter, and the total range of the technique is from 0.4 to 900 microns.

With a light source, a range of options are available. Light blockage instruments generate a pulse proportional to the

geometric shadow of the particle. HIAC/ROYCO manufacture a range of analyses operating using this principle. Some instruments collect forward-scattered white or laser light; in order to increase the collected light flux elliptical mirrors or lenses may be used.

Other instruments collect light scattered at 90 degrees to the beam direction. This has the advantage of generating a precise pulse height for each particle size, combined with the disadvantage of a strong dependence on refractive index.

The Brinkmann Model 2010 scans the sample with a laser beam using a rotating prism. The time spent on the particle is interpreted as particle size.

The Spectrex Prototron also uses a scanning laser, but uses forward light scattering for size determination.

The Lasentec Lab-tec scans with an infrared laser and picks up back-scattered radiation using a stereoscopic system. Particle size is measured by dwell time on the particle.

The Flow Vision Analyzer is designed for on-line monitoring of a flowing suspension. The light beam is fed to the process line through a fiber-optic cable and the light pick-up is fed to the detector through an optical cable. A visual display of the flowing suspension may be obtained using a camera and freeze-frame accessory.

CONCLUSIONS

The above comprises a limited description of a few of the instruments that operate in the 1- to 100-micron size range. The Field-Scanning and Stream-Scanning Instruments are more rapid than sedimentation but usually generate a more ambiguous size. The trend is to use these instruments in an on-line or rapid response mode to continually monitor processes.

PREDICTIONS OF A FATE OF A SMALL HETEROGENEOUS DROPLET BASED ON AN ABSORPTION PATTERN OF THE INCIDENT ELECTROMAGNETIC RADIATION

Marek A. Sitarski

Clarkson University, c/o U.S. DOE / METC, Morgantown, W.V. 26505

ABSTRACT

Dynamic behaviour of a small multiphase droplet exposed to electromagnetic fields, such as laser beams or a high temperature thermal radiation, attracts a considerable interest both from fundamental and applied points of view. Response of the particle to the external perturbation of a magnitude controlled in a wide range of orders provides a valuable information about dynamic properties of matter very far from the thermodynamic equilibrium. Recent advances in the laser technology and in the instrumentation for suspending of small particles in optical traps and in electrodynamic balances make possible an experimental verification of the predicted regimes and magnitudes of the response. Applications of this knowledge might also be essential for some of the current technologies. Propagation of laser beams and thermal radiation through a polluted atmosphere, controlled laser deposition of particles of advanced materials, combustion intensification by the radiation induced superfine atomization of colloidal droplets of modern fuels are some of the actual examples.

When the intense radiation field is incident upon a small heterogeneous droplet its fate depends primarily on the dissipation pattern of the electromagnetic energy inside the droplet. As compared with homogeneous droplets the radiation absorption inside multiphase droplets is especially nonuniform because of different absorptivities of the component phases and additional reflections/refractions at the inner interfaces. The resulting nonuniform surface temperature of the irradiated droplet accounts for the photophoretic force, and also formation of hot spots inside the droplet can cause its disintegration by explosive boiling of the liquid.

The current progress in computations of 3-dimensional absorption patterns inside heterogeneous droplets by use of the Mie scattering theory applied for multilayered spherical particles and of effective optical constants of concentrated colloids by use of the extended Bruggeman theory is presented. The algorithms and computer codes are developed for a monochromatic radiation beam and for the black body radiation.

The specific computations are performed for two- and three-phase colloid droplets of micronized coal and soot dispersed in water. The third phase is either a layer of surfactant at the water-gas interface or water vapor layer at the coal-water interface. The effect of intensity, size parameter and temperature of the incident thermal radiation on the processes of photophoresis, explosive boiling, and transient vaporization of the droplets is studied.

Blank

MICROCONTAMINATION CONTROL: ACHIEVING AND MEASURING ULTRA-CLEAN CONDITIONS

D. S. Ensor and R. P. Donovan

Research Triangle Institute
P.O. Box 12194
Research Triangle Park, NC 27709

The development of complex, dense silicon chips with feature dimensions of less than 1.5 μm has stimulated work on elimination of particles from manufacturing areas. Contaminating particles can render these chips nonfunctional by interfering with their surface geometry, by creating defects--either electrical shorts or voids--between layers deposited on the chip, and by introducing unwanted electrically active impurities into the chip bulk. To minimize or avoid these undesirable consequences, the fabrication of semiconductors is performed in clean rooms in which all air enters through high efficiency filters mounted in the ceiling (and often completely cover the ceiling) and exits through either floor return registers or side wall registers. This exhaust from the clean room is then typically recirculated back through the ceiling filters. The resulting flow pattern in the clean room is undirectional from ceiling to floor and is described as vertical laminar flow (VLF).

While filtering all entering and recirculating air effectively isolates the manufacturing area from the large concentration of particles that typically are found in outside ambient air, the concentration of particles in a clean room also depends on the activity and the particle sources within the clean room. The VLF design is thus an important feature that sweeps internally generated particles away from the work area and carries them directly to the ceiling filter.

State-of-the-art clean rooms at rest (no operations in progress; no personnel in the clean room) may have as few as 10 condensation nuclei particles per cubic foot of air. While particle size distributions in the outside ambient air follows a power law curve, recent data show that this relationship does not hold in a clean room at rest for particles less than 0.05 μm [Donovan, Locke, Osburn, and Caviness, 1985]. The observed flattening in the cumulative size distribution curve for particles less than 0.05 μm is

what is predicted from mathematically operating on a typical outside ambient air size distribution with a typical filter efficiency characteristic [Ensor, Donovan, and Locke, 1987].

Clean rooms in operation (i.e., not at rest) invariably exhibit short-term high concentration episodes called "bursts" in addition to a somewhat elevated stable background concentration. The origin of these "bursts" are not completely understood but can result from both human operator sources and equipment operation. Their existence recommends continuous monitoring at key positions in the clean room rather than aperiodic site sampling as a monitoring and control strategy.

Having particles in the clean room is of itself not sufficient to cause chip failure. The particles must deposit on the chips in vulnerable locations. The deposition of particles from the gas phase onto surfaces depends on mechanisms such as gravity, particle diffusion, and convection. The VLF design and thoughtful equipment layout minimize these mechanisms. Chip properties such as temperature and electrical charge also affect particle deposition [Donovan, Clayton, and Ensor, 1987].

Particles can also deposit on a chip during immersion in one of the many liquid baths to which it is exposed during manufacturing. While gravity is a much less important deposition mechanism in a liquid bath than in the air, other properties such as particle and chip hydrophobicity become important and need to be better understood.

Looming as the most important source of chip contamination at present, however, is the chip processing equipment itself. Particle emission by chip processing equipment, including the process chemistry, is now recognized as a chief source of chip failure, and suppliers of semiconductor processing equipment must now specify and control the particle concentration in the chip environment.

Donovan, R. P., A. C. Clayton, and D. S. Ensor. The Dependence of Particle Deposition Velocity on Surface Potential. In: 1987 Proceedings of the Annual Technical Meeting of the Institute of Environmental Sciences, pp. 473-478, 1987.

Donovan, R. P., B. R. Locke, C. M. Osburn, and A. L. Caviness. Ultrafine Aerosol Particles in Semiconductor Cleanrooms. J. Electrochem. Soc., 132(11), pp. 2730-2738, November 1985.

Ensor, D. S., R. P. Donovan, and B. R. Locke. Particle Size Distributions in Clean Rooms. J. Environ. Sci., 30(6), pp. 44-49, 1987.

PARTICULATE CONTROL RESEARCH AND DEVELOPMENT AT EPA

Dr. Norman Plaks
EPA
RTP, NC

ABSTRACT

Particulate control research and development at EPA is centered around the application of electrostatics in both electrostatic precipitation and in fabric filtration. The work in electrostatic precipitation is concerned with improving performance by separating the particle charging and collection functions to allow each to be optimized, thereby providing a significant increase in performance. Electrified fabric filtration places a charge upon the particles and then collects them on the filtration media, which is in an electric field. Electrification of the fabric filtration process results in both a reduced pressure drop and particle penetration. Other work in electrified fabric filtration improves collection of fibrous particles, such as asbestos, by first charging the fibers and subjecting them to an alternating current field at the filtration surface, which imparts a vibrational motion causing them to snag on the filter media. Other work is related to the development of mathematical engineering design models of the electrostatic precipitation and fabric filtration devices. Other areas of interest, which developed from the work on applied electrostatics, are in corona destruction of toxic air pollutants.

CONCLUSIONS AND RECOMMENDATIONS

During the past several years, a great deal of progress has been made in the multiple fields associated with fine particle technology. Perhaps one of the most important of these is the recognition of fine particle research as a significant discipline. Most of this progress has been driven by the semiconductor and clean room processing communities. Significant strides have also been made in the ceramic and composite fields and in filtration. However, there is still much that we need to learn and develop.

One of the major gaps in the state of the art is the problem of high aspect ratio particles. These morphologies pose specific problems in size distribution measurement. When the significant information requires measurements in more than one dimension, and in the same relative dimensions on each particle, all current methods fail. This problem is magnified by the difficulty of separating such particles from each other, particularly in the case of long tangled whiskers. Because of this, the additional problems of dispersing and orienting particles arise. Adding magnetic and electrical properties to such particles further magnifies the problem.

Another major concern is the measurement of physical properties of individual particles. The traditional problem to physicists and materials scientists has been growing crystals large enough to measure. This approach is not applicable for the information required for specific applications, and methods are needed for direct measurement of strengths, conductivities, heat capacities, etc. of individual particles.

The papers in the Particle Production Section identify numerous new techniques available for production of controlled size submicron particles of high purity. Further developmental effort is necessary to scale up these techniques to industrial production with high output. Submicron particles of narrow size distributions are needed for advanced ceramics, composites, pigments, and new areas such as high density magnetic recording media.

Particle sampling, measurement and characterization is essential in the areas of smoke dissemination testing, in industrial process monitoring, and in environmental control of industrial emissions in the atmosphere as well as for increasing the yields of microelectronics devices.

The diversity of the subject and applications of particles makes multidisciplinary technology transfer very valuable. The consensus of the participants at the Symposium was that such meetings are very valuable. We make the following specific

recommendations to promote technology transfer:

1. Plan and conduct similar meeting in the future at approximately two-year intervals.

2. Provide more advanced planning period to assure participation by experts.

3. Consider collaboration with other government agencies such as the National Institute for Standards and Technology, the Department of Energy, and the Environmental Protection Agency.

4. Streamline the format of the written contribution to facilitate compilation of proceedings.

Blank

APPENDIX - SYMPOSIUM PROGRAM

SPECIALTY SYMPOSIUM & WORKSHOP

PARTICLE PRODUCTION, CHARACTERIZATION, AND APPLICATIONS
"Current Issues and State-of-art in Fine Particle Technology"
May 16-18, 1988
Hunt Valley Marriott (near Baltimore, MD)

Sponsored by: Chemical Research, Development, and Engineering Center (CRDEC), U.S. Army, APG, MD

Symposium Coordinators:

Dr. Madhav B. (Arun) Ranade
Particle Technology, Inc.
P.O. Box 65420
Washington, D.C. 20035
(703) 538-6922

&

Erica R. Riley
CRDEC
Attn: SMCCR-RSP-B
APG, MD 21010
(301) 671-4294

PROGRAM:

Monday, May 16, 1988

9:00 a.m. - 10:00 a.m.: Registration

10:00 a.m. - 10:30 a.m.: Introductory Remarks - Erica R. Riley
Announcements - M.B. (Arun) Ranade

10:30 a.m. - 11:30 a.m.: Plenary Lecture - "Advances in Aerosol Filtration," Professor B.Y.H. Liu, University of Minnesota

11:30 a.m. - 11:45 a.m.: Discussion

11:45 a.m. - 1:00 p.m.: Lunch

1:00 p.m. - 2:30 p.m.: Technical Session: Particle Production I

"Particle Generation in Aerosol Reactors: A Review," Dr. David T. Shaw, State University of New York, Buffalo, NY

"Material Synthesis by Aerosol Processes," Dr. Sotiris E. Pratsinis, University of Cincinnati, Cincinnati, Ohio

2:30 p.m. - 3:00 p.m.: Break

3:00 p.m. - 4:30 p.m.: Particle Production I (continue)

"Lipid Tubule Microstructures: Formation, Metallization, and Application," Dr. Paul Schoen, Naval Research Laboratory, Washington, D.C.

"Novel Techniques for Particle Generation at CRDEC," Erica R. Riley, CRDEC, Edgewood, MD

"Dispersion and Dissemination of Dry Powders," Dr. M.B. (Arun) Ranade, Particle Technology, Inc., Washington, D.C.

4:30 p.m. - 5:00 p.m.: Discussion: Custom-Made Particles

Tuesday, May 17, 1988

8:30 a.m. - 9:00 a.m.: Registration

9:00 a.m. - 10:00 a.m.: Technical Session: Particle Production II

"Particle Preparation Using Aerosol Reactions," Dr. Richard E. Partch, Clarkson University, Potsdam, NY

"Colloidal Processes for Particle Production," Drs. Michael E. Mullins, Venugopal B. Menon, RTI, RTP, NC, and M.B. (Arun) Ranade, Particle Technology, Inc., Washington, D.C.

10:00 a.m. - 10:20 a.m.: Break

10:20 a.m. - 12:00 p.m.: Aerosol Characterization I

"Aerosol Sampling and Measurement," Dr. James W. Gentry, University of Maryland, College Park, MD

"Aerosol Sampling Studies," Drs. Dan Turner and Andrew R. McFarland, Texas A&M University, College Station, TX

"Optical Properties of Smoke Agglomeration," Drs. George Mulholland, Raymond Mountain, and Nelson Bryner, National Bureau of Standards (NBS), Gaithersburg, MD

12:00 p.m. - 1:15 p.m.: Lunch

1:15 p.m. - 2:30 p.m.: Technical Session: Particle Characterization and Application I

"Morphology of Profiles, Surfaces, and Three Dimensions," Dr. J.K. Beddow, University of Iowa, Iowa City, IA

"Predictions of a Fate of a Small Heterogeneous Droplet Based on an Absorption Pattern of the Incident Electromagnetic Radiation," Marek A. Sitarski, Clarkson University c/o U.S. DOE/METC, Morgantown, WV

"Mass Concentration Measurement by X-Ray Fluorescence," Dr. George Thomson, BRL, Aberdeen, MD

2:30 p.m. - 2:50 p.m.: Break

2:50 p.m. - 4:15 p.m.: Particle Characterization and Application II

"Light Scattering Inversion Methods for Concentration and Size Distribution," Dr. Janon F. Embury, CRDEC, Edgewood, MD

"Particle Control Research and Development at EPA," Dr. Norman Plaks, U.S. EPA, RTP, NC

4:15 p.m. - 5:00 p.m.: Discussion: Developments in Particle Characterization

Wednesday, May 18, 1988

8:30 a.m. - 9:00 a.m.: Registration

9:00 a.m. - 10:15 a.m.: Current Topics in Particle Technology

"Microcontamination Control: Achieving and Measuring Ultra-Clean Conditions," Dr. David S. Ensor and Robert P. Donovan, RTI, RTP, NC

"Particle-Sizing Reference Materials From the National Bureau of Standards," Dr. Thomas R. Lettieri, National Bureau of Standards, Gaithersburg, MD

10:15 a.m. - 10:35 a.m.: Break

10:35 a.m. - 12:00 a.m.: Current Topics in Particle Technology (continue)

"Recent Developments in Particle Characterization Techniques for Suspensions and Powders," Dr. Terry Allen, E.I. duPont, Newark, DE

"Particle Characteristics for Industrial Applications of Particle Technology," Dr. Reg Davies, E.I. duPont, Newark, DE

12:00 p.m. - 1:00 p.m.: Lunch

1:00 p.m. - Open : Discussion: Future Needs in Particle Technology for Defense and Industrial Applications